University of Siena

Department of Biotechnology, Chemistry and Pharmacy

PhD in Biochemistry and Molecular Biology

Ciclo XXXV

Development of image-based high content screening assays for testing monoclonal antibodies against *Neisseria gonorrhoeae* infecting human cells

PhD candidate: **Fabiola Vacca**

Thesis Supervisor: Prof. Rino Rappuoli

Academic year 2022-2023

Table of contents

List of abbreviations 4

Abstract 6

Introduction 7

1. Antibodies 7

1.1 Introduction 7

1.2 Structure and isotypes 7

1.3 Antigen-binding and FcR interactions 8

2. mAbs against antimicrobial resistant bacteria 9

2.1 How mAbs can tackle antimicrobial resistance (AMR) 9

2.2 mAbs against bacteria 10

2.3 Mechanisms of action of anti-bacterial mAbs 13

2.4 Approaches for discovery and production of mAbs 14

2.5 mAbs for vaccine discovery 14

3. *Neisseria gonorrhoeae* 16

3.1 Introduction 16

3.2 Epidemiology and transmission 16

3.3 Physiology and main virulence factors 18

3.4 Pathogenesis 21

3.4.1 Interactions with the mucosal epithelium 22

3.4.2 Interactions with the immune system 24

3.4.2.1 The innate immune system and phagocytic cells 24

3.4.2.2 Adaptive immune response 25

3.5 Therapeutic approaches and AMR 26

3.6 2C7 monoclonal antibody against N. gonorrhoeae 29

3.7 Vaccines and prophylaxis 30

3.8 Bexsero cross-protection studies 32

Background and aim of the project 35

Chapters 37

1. Generation of knock-in strains of *N. gonorrhoeae* expressing fluorescent protein for high-content imaging 37

Introduction 37

Results 38

Discussion 46

Experimental procedures **47**

Supplementary material **51**

2. Development of a novel visual opsono-phagocytosis screening assay for monoclonal antibodies against *Neisseria gonorrhoeae* 56

Introduction **56**

Results **57**

Discussion **72**

Additional data not included in the manuscript **74**

Experimental procedures **76**

Supplementary material **81**

3. New approaches to study *N. gonorrhoeae* colonization of epithelial cells 90

Introduction **90**

Results **90**

Discussion **97**

Experimental procedures **98**

Supplementary material **99**

4. Additional research activity: development of mAbs against SARS-COV-2 103

Conclusions and future perspectives 104

Publication list 106

References 107

List of abbreviations

ADCC	Antibody-dependent cell-mediated cytotoxicity
ADCP	Antibody-dependent cellular phagocytosis
AMR	Anti-microbial resistance
ASGP-R	Asialoglycoprotein-receptor
BRC	Baby rabbit complement
CFU	Colony forming unit
CR3	Complement receptor 3
CEACAM	Carcinoembryonic antigen-related cellular adhesion molecules
CDC	Complement-dependent cytotoxicity
CDC	Centers for Disease Control and Prevention
CDI	*Clostridium difficile* infection
CDR	Complementarity determining regions
dOMV	Denatured outer membrane vesicle
Egfp	Enhanced GFP
ECDC	European Centre for Disease Prevention and Control
ESCs	Extended-spectrum cephalosporins
Fab	Antigen-binding fragment
Fc	Fragment crystallizable
FcR	Fc receptors
FDA	Food and Drug Administration
GMMA	Generalized Modules for Membrane Antigens
Hep	Heptose
HSPGs	Heparan sulphate proteoglycans
Ig	Immunoglobulin
IL	Interleukin
Lbps	Lactoferrin binding proteins
lgtG	Glycosyltransferase G

LOS	Lipooligosaccharide
mAb	Monoclonal antibody
MAMPs	Microbial-associated molecular patterns
MDR	Multiple drug resistant
NspA	*N. gonorrhoeae* surface protein A
NET	Neutrophil extracellular trap
Opa	Opacity associated
OMV	Outer membrane vesicle
PA	Protective antigen
PID	Pelvic inflammatory disease
Por	Porin
PRRs	Pattern recognition receptors
Rmp	Reduction modifiable protein
Tfp	Type IV pili
Tbps	Transferrin binding proteins
TEM	Transmission Electron Microscopy
TLRs	Toll-like receptors
TNF	Tumour necrosis factor
SBA	Serum bactericidal assay
sfGFP	Superfolder GFP
vAIA	Visual adhesion-inhibition assay
STIs	Sexually transmitted infections
VRE	Vancomycin-resistant *Enterococcus* species
vOPA	Visual opsono-phagocytosis assay
WHO	World Health Organization
XDR	Extensively drug resistant

Abstract

BACKGROUND

Monoclonal antibodies (mAbs) represent a promising class of therapeutics against bacterial pathogens, including those which are developing antimicrobial resistance (AMR). Functional, high-throughput assays, which investigate the ability of mAbs to kill bacteria or protect the host, are currently lacking. The aim of this PhD thesis was to establish high-content and high-throughput methods to screen and characterize functional mAbs against *Neisseria gonorrhoeae*.

RESULTS

Two infection assays, named visual opsono-phagocytosis assay (vOPA) and visual adhesion inhibition assay (vAIA), were implemented in 96-well plates using the confocal microscope Opera Phenix. vOPA measures the ability of mAbs to promote phagocytosis of bacterial cells by THP-1-derived macrophages whereas vAIA explores bacterial adhesion to SV-HUC-1 epithelial cells and possible inhibition thereof. An image analysis pipeline was developed by exploiting the Harmony software associated with Opera Phenix. The pipeline relies on detection of fluorescent markers to identify bacteria and cells, counts the number of eukaryotic and prokaryotic cells in the field of view and discriminates internalized vs. external bacteria vs. bacteria associated with the host cell membrane. Screening of 96 human anti-*N. gonorrhoeae* mAbs, isolated from volunteers vaccinated with the anti-meningococcal vaccine Bexsero by means of a Reverse Vaccinology 2.0 approach, against the FA1090 strain revealed that one mAb with unknown target was able to exert high phagocytosis promoting activity, comparable to the positive control.

CONCLUSIONS

The confocal microscope Opera Phenix can accelerate the evaluation of antibody activity in host-pathogen interaction assays. Opera can quantify the phagocytic activity of macrophage-like cells and help the screening of an array of mAbs for their ability to promote this process. Furthermore, Opera can detect adhesion of bacteria onto epithelial cells and lastly, it can measure the fluorescence of FA1090 engineered to express GFP at the single-cell level and the fluorescence values obtained correlate with bacterial fitness.

Overall, this work represents the basis for further exploiting fluorescence microscopy in mAb discovery and development against bacterial pathogens of clinical relevance.

Introduction

1. Antibodies

1.1 Introduction

The antibody, also known as immunoglobulin, represents a critical component of the immune response, which has been exploited to study the immunity and the development of therapies[1,2]. Antibodies are proteins naturally generated by the immune system to defend the host from diseases, such as cancer or infections. They are synthesized exclusively by B lymphocytes[3], which, together with T lymphocytes, are crucial players in the adaptive branch of the immune system[4]. B lymphocytes can generate a huge and diverse repertoire of antibodies, each with its own amino acid sequence and different antigen-binding site[5]. Antibodies are the secreted form of the B-cell receptor, where one differs from the other for the C-terminus portion, which is a hydrophobic membrane-anchoring sequence in the receptor, and a hydrophilic sequence in the soluble form[6]. The first proof of the protective activity conferred by antibodies was passive 'serum therapy', that is, the use of sera isolated from animals with diseases (immunized animals) to confer protection to non-immunized humans[7]. Target specific antibodies able to bind bacterial toxins were first discovered by Behring and Kitasato in the early 1890s, treating diseases like diphtheria and tetanus[7]. Emil Adolf von Behring together with Erich Wernicke developed the first effective diphtheria antitoxin serum, obtained by immunizing a horse with *Corynebacterium diphtheriae*. The anti-infective substance in the serum was first named "Antitoxin," and later became antibody[8].

1.2 Structure and isotypes

The antibody is composed of two identical light chains, which can either be lambda (λ) or kappa (κ), and two identical heavy chains[9]. Each chain has a variable (V) region at its amino terminus, responsible for antigen binding, and a constant (C) region. The antibody includes two antigen-binding Fab (antigen-binding fragment) arms, which consist of the V region and the CH1 of the constant domain, linked to a single Fc (fragment crystallizable) domain[9] (**Fig. 1**). The Fab and the Fc are linked via the hinge region, which confers conformational flexibility to the antibody[9].The Fab fragment allows high antigen-specificity, while the Fc region can engage with different receptors and influence immune effector functions, persistence in circulation and transport across

cellular barriers[10]. Furthermore, it can be engineered to enhance and modify the antibody activity[11].

Both domains change rapidly throughout the immune response: Fab evolves to increase the affinity to the foreign antigen, while the Fc changes into five different isotypes to elicit different effector functions[12]. These isotypes are IgM, IgD, IgA, IgE and IgG. IgM is the first class of antibodies to appear during the primary immune response, whose affinity to the antigen is not yet mature, thus low, but with broad specificity[13]. It is expressed on the surface of mature B cells (prior-stimulation), co-expressed with IgD[14]. IgD can also be secreted in blood, mucosal secretions and can bind to basophils, inducing the release of antimicrobial factors[14]. IgA is the principal isotype in secretions, most importantly in the mucus of the epithelium of the intestinal and respiratory tracts[6]. IgE is found at very low levels in blood or extracellular fluid, can bind receptors on mast cells, triggering mast cells to release powerful chemical mediators[6]. Lastly, IgG is mostly found in serum and blood, and acts by activating the complement system and by opsonizing pathogens for engulfment[15]. The isotype is further divided into four subclasses in humans (i.e. IgG1, IgG2, IgG3, IgG4)[15].

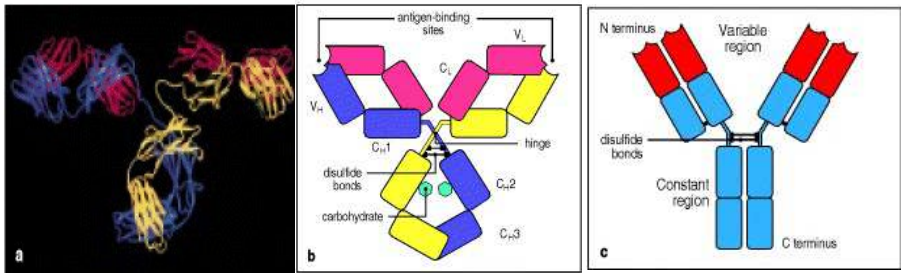

Figure 1. Structure of an antibody molecule. *Panel a shows an X-ray crystallographic structure of an IgG antibody. The two antigen-binding sites are at the tips of the arms, which are attached to the trunk of the antibody by the hinge region. Panel b illustrates the four-chain composition and the separate domains comprising each chain. Panel c shows a schematic representation of an antibody molecule[6]. Image taken from Janeway et al. 2001.*

1.3 Antigen-binding and FcR interactions

The two variable domains (Fv) of each chain build up the antigen-binding regions (paratopes), responsible for making physical contact with the antigenic determinant (epitope)[16]. This antigen binding site is made of six hypervariable loops (three from the light-chain V region and three from the heavy-chain V region) which are formed by the

complementarity determining regions (CDR)[17].The CDRs (CDR-1, -2, and-3).are separated by structurally conserved regions called framework regions (FR-1,-2,-3, and-4)[18].The length and composition of the CDR sequences are highly variable. This variability is the result of different mechanisms which take place during antibody development, such as the V(D)J genes recombination, the addition or deletion of nucleotides in junctions and the somatic hypermutations in the recombined genes[18]. These mechanisms are meant to generate a highly diverse number of antibodies from a limited number of antibody genes[18]. The specific interactions antibodies have for their antigen depend on the number and type of amino acids that form the CDRs loops, which determine the binding site surface topography; the affinity is dictated by non-covalent forces between the paratope and epitope [16]. Antigen binding does not only dictate the specificity of the antigen but can also influence the interaction of the antibody with the Fc receptor. Antigen binding of Fab portion of antibodies is linked to the engagement of Fc with Fc receptor. Antigen binding can allosterically promote Fc receptor recognition as it induces conformational changes in Fc domain and hinge regions[19]. The Fc can engage with different receptors, and the resulting intracellular signalling can lead to activating or inhibitory activity. Activating receptors include the FcγRI, which is a high affinity receptor that recognises monovalent antibodies, and FcγRIIa, IIc, FcγRIIIa and IIIb which have lower affinity and require avidity-based interactions. FcγRIIb, instead, is an inhibitory receptor[20].

2. mAbs against antimicrobial resistant bacteria

2.1 How mAbs can tackle antimicrobial resistance (AMR)

A major challenge in the field of medical microbiology and infectious diseases is antibiotic resistance[21]. Bacterial pathogens can develop mechanisms to withstand drug pressure and quickly develop resistance to new antibiotics[8]. In most cases, bacterial infections are treated empirically[22], before laboratory results, if performed, are known. Empirical treatment of the infection with antibiotics should be effective unless the causative pathogen is resistant to the administered drug. In that case, infection persists and, as a result, leads to an increase in hospital stay, morbidity and mortality[23]. The multi-drug resistant organisms of greater concern include oxacillin-resistant *Staphylococcus aureus*, vancomycin-resistant *Enterococcus* species (VRE), multidrug-resistant *Streptococcus pneumoniae*, and multidrug-resistant bacteria including *Pseudomonas* species, *Acinetobacter* species, *Klebsiella pneumoniae*, *Enterobacter* species[24]. There are multiple reasons behind the emergence of antimicrobial resistance

(AMR) in so many bacterial species: overuse and misuse of antimicrobials[8], caused by inappropriate selection and unrestricted access, and ineffective surveillance of AMR and clinical treatment failures[25]. To face this issue, resistance data are continuously monitored at a regional or national level, to verify whether empirical treatment for specific infectious diseases syndromes are still appropriate[26]. However, a defined antibiotic-resistance threshold above which empirical treatment recommendations should be adjusted for specific infections is still missing[26]. Molecular diagnostic approaches, including bioinformatics tools accompanied by other 'omics' technologies, can help on the surveillance, to predict infections and AMR and thus also aid in the development of novel treatment strategies[27].

When antibodies were found to be the molecules mediating protection in the sera, a new era of development of antibody therapy for diseases began. IgG, in particular the IgG1 subclass, has been exploited for the development of monoclonal antibodies (mAbs), which up to date are among the most effective therapeutic medications[20]. IgG efficacy in therapy relies on its high serum abundance, long half-life, safety and stability[28]. Unlike polyclonal antibodies, which are produced by a large number of B lymphocytes activated by numerous epitopes on one antigen, monoclonal antibodies are produced by a single lymphocyte clone and thus, recognize one single epitope[2]. Compared to polyclonal sera, mAbs are more specific, have less cross-reaction with host cells and resident flora [29,30]. In addition to minimal effects on bacteria in microbiota, mAbs have various characteristics which make them candidates to counteract AMR pathogens: high specificity, no susceptibility to existing resistance mechanisms, and synergy in working with the immune system to clear the bacterial pathogen[31].

2.2 mAbs against bacteria

Despite their success in treating cancer, viral infections and autoimmune diseases[8], and also non-malignant conditions, such as asthma or migraine[32], the United States Food and Drug Administration (FDA) has so far only approved three mAbs to treat bacteria, all of which work by targeting exotoxins, while many other candidates are in clinical trials (**Table 1**)[33]. Raxibacumab (Abthrax®) is a human IgG1 mAb that neutralizes the protective antigen (PA) component of the anthrax toxin complex, the main virulence factor of *Bacillus anthracis,* preventing toxin-mediated cell damage in inhaled anthrax infections[34]. Obiltoxaximab (Anthim®) is a chimeric IgG1 mAb derived from murine mAb 14B7 variant 1H, which also functions by neutralizing PA, showing therapeutic

advantages in all stages of inhaled anthrax and inhibiting bacterial dissemination[35]. Bezlotoxumab (Zinplava®) is a fully humanized IgG1 antibody capable of binding to two epitopes of the toxin B secreted by *C. difficile*, blocking the toxin from attaching to the host cell, preventing intestinal epithelial damage and colitis and reducing the risk of *C. difficile* infection (CDI) recurrence[36]. The difficulty in developing mAbs against bacteria has multiple reasons. For mAbs to be effective, they should target antigens which are surface exposed and expressed throughout the infection period, which are conserved among circulating bacterial strains and are antigenically distinct compared to epitopes on human proteins[31]. However, often bacteria can downregulate, abolish or modify the expression of epitopes, without compromising their virulence and fitness. Therefore, protein targets may be masked and hence be unavailable for antibody binding[31]. Moreover, bacteria have developed defense mechanisms against host immunoglobulins (e.g. production of antibody degrading proteinases) which can compromise the success of antibody-based therapy[37]. Furthermore, having one mAb with a single target may not be sufficient, as bacteria have multiple virulence factors, whose expression profiles vary while residing within the host [38]. Finally, despite obtaining good results *in vitro*, difficulties arise when results are translated to *in vivo* tests or human clinical trials. In fact, in some cases no correlation between *in vitro* and *in vivo* activity has been observed[39] and those mAbs which demonstrated an activity in mouse models of infections failed in Phase III clinical trials[40].

Table 1. Anti-bacterial monoclonal antibodies in clinical research[8].

Name	**DSTA4637S**	**AR-301**	**MEDI4893**	**ASN100**	**F598**
Disease	*S. aureus* pneumonia	*S. aureus* pneumonia	*S. aureus* pneumonia	*S. aureus* pneumonia	*S. aureus, N. gonorrhoeae*; *N. gonorrhoeae* urethritis
Target	Bacterial surface-Staph wall teichoic acid	Bacterial toxin-*S. aureus* alpha toxin	Bacterial toxin-*S. aureus* alpha toxin	Bacterial toxin-*S. aureus* alpha toxin/leukocidins	Poly-N-acetyl-D-glucosamine (PNAG)
Source	Human IgG1	Human IgG1	Human IgG1	Human IgG1	Human Fab

Format	Monoclonal AAC	Monoclonal	Monoclonal with extended half-life	Mixture of ASN-1 and ASN-2	Monoclonal
Developer	Genentech	Aridis Pharmaceuticals	Medimmune	Arsanis	Alopexx Pharmaceuticals, LLC
Status	Phase I	Phase III	Phase II	Phase II	Phase II
Last update	2020.01 Completed	2020.01 Recruiting2020.01 Recruiting	2019.10 Completed	2019.07 Terminated	2019.02 Terminated

Name	**514G3**	**MEDI3902**	**AR-105**	**KB001-A**	**KB001**
Disease	*S. aureus* bacteremia	*P. aeruginosa* pneumonia	*P. aeruginosa* pneumonia	*P. aeruginosa* pneumonia	*P. aeruginosa* pneumonia
Target	Bacterial surface-Staphylococcus protein A	Bacterial exopolysaccharide-Psl; secretion system-PcrV	Bacterial Exopolysaccharide-alginate	T3SS-PcrV	T3SS-PcrV
Source	Human IgG3	Human IgG1-Fab-ScFv	Human IgG1	PEGylated Fab	Human Fab
Format	Monoclonal	Bispecific	Monoclonal	Monoclonal	Monoclonal
Developer	XBiotech	Medimmune	Aridis Pharmaceuticals	Humanigen	Humanigen
Status	Phase II	Phase II	Phase II	Phase II	Phase II

Last update	2017.02 Completed	2019.12 Completed	2019.02 Completed	2015.01 Completed	2014.07 Completed

2.3 Mechanisms of action of anti-bacterial mAbs

The target of mAbs may be either exotoxins or structural cell surface components (proteins and exopolysaccharides)[37]. Through the Fab domain, the antibody binds specifically to the pathogen's antigens, blocking the antigen toxicity and inhibiting the interaction between the pathogen and host-cell receptors. To guarantee protective immunity the Fc portion of mAbs must interact with different receptors, which determine their effector functions[12]. In the process of bacterial clearance, mAbs can exert different modes of action: direct neutralization of toxins, inhibition of virulence factors, and stimulation of the host immune system[8] (**Fig. 2**). The stimulation of the immune system can take place in different ways. Through the Fc region, antigen-bound antibodies can bind to complement protein C1q, thus starting a series of proteolytic events known as complement cascade pathway. This leads to bacterial lysis, commonly known as complement-dependent cytotoxicity (CDC)[8]. Antibodies may bind to Fc receptors (FcRs) on immune cells, such as monocytes, macrophages and neutrophils, triggering antibody-dependent cellular phagocytosis (ADCP). For some bacteria, opsonophagocytic uptake and killing by neutrophils is a key component for host clearance[39]. Lastly, through antibody-dependent cell-mediated cytotoxicity (ADCC), mAbs can help eliminate infected cells displaying bacterial antigens on their surface[41]. In addition to the short-term properties, mAbs can also act via indirect mechanisms with effects lasting beyond the treatment itself, through ''vaccine-like effects''. Through the engagement of the host immune response, mAb treatment could lead to the stimulation of the endogenous humoral and cellular immune responses conferring protective immunity, similarly to vaccine approaches[41,42].

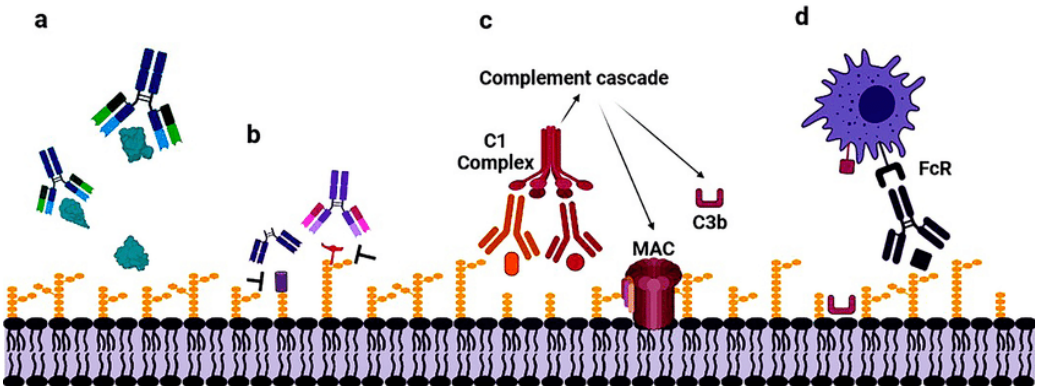

Figure 2. Modes of actions of anti-bacterial mAbs. *mAbs can (a) neutralize soluble toxins; (b) block virulence factors expressed on the bacterial surface; (c) lyse bacteria through the activation of the complement system; or (d) enhance phagocytosis of bacteria[8]. Image taken from Wang and Lu, 2022.*

2.4 Approaches for discovery and production of mAbs

Initially, mAbs were produced by clonal expansion of hybridomas[32]. Hybridomas were created by fusing spleen cells from an immunized mouse with human or mouse myeloma cells, taking advantage of their self-perpetuating activity[43]. After that, the hybridomas that produced the desired antibody reactivity were selected. As mouse proteins resulted to be immunogenic[43], they were not feasible to be used as therapeutic agents. This issue was solved by developing, first, chimeric mouse-human mAbs, followed by humanized (i.e., antibody structure containing less than 10% nonhuman sequences)[37] and then fully human recombinant mAbs. To clone and express fully human mAbs, new tools became available, such as phage display libraries, transgenic mice, mammalian expression cell lines[37], as well as the possibility to produce mAbs from human B lymphocytes isolated from subjects in convalescence or after vaccination[5]. Isolated B lymphocytes can be lysed, and through different rounds of RT-PCR amplification, the heavy and corresponding light chain gene transcripts of each immunoglobulin can be isolated. The resulting genes can be then cloned into eukaryotic expression vectors to produce human mAbs *in vitro*[5]. As it is possible to perform these reactions in multi-well plates, a huge number of Ig genes can be expressed. Once the functionality profile is obtained, it can be directly linked to the complete Ig heavy and Ig light chain gene sequence information which has been obtained as part of the cloning strategy. The expressed recombinant mAbs can then be tested for reactivity with diverse antigens[5].

2.5 mAbs for vaccine discovery

In addition to therapeutic applications, antibodies and their bound epitope can be templated and then evaluated, and the antigen-antibody interface can be explored. This can provide an innovative approach to identify protective antigens for the design of

vaccines capable of eliciting effective B-cell immunity[44]. Through structural biology tools, it is now possible to characterize the Fab complexed with the target antigen, also known as conformational epitope mapping studies[45]. The three-dimensional characterization can yield the atomic details of protective epitopes recognized by mAbs[45]. Monoclonal antibodies can be isolated from seropositive individuals and used to guide vaccine design in a reversal of the normal flow of vaccines to antibodies[46]. This approach is commonly referred to as Reverse Vaccinology 2.0 (**Fig. 3**). Reverse Vaccinology 2.0 is an evolution of the reverse vaccinology which exploits bioinformatics to find protective antigens[47]. This can be particularly useful for pathogens which are more refractory to vaccine design, and against which a vaccine is needed to respond to antimicrobial resistance[46].

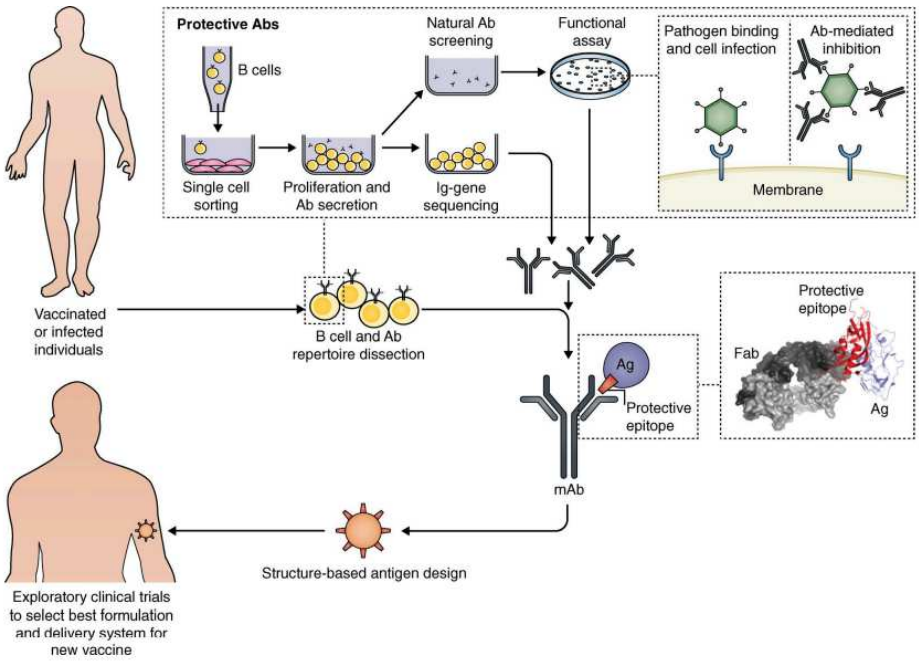

Figure 3. Schematic view of the Reverse Vaccinology 2.0 approach. *Single B cell sorting and culturing from vaccinated or infected subjects allow direct screening and selection of mAbs with desired functionality. Structural characterization of such mAbs bound to their target antigen allows for detailed definition of the protective epitope, which can then be engineered for presentation as an optimized immunogen. Image taken from Rappuoli et al. 2016.*

3. *Neisseria gonorrhoeae*

3.1 Introduction

Globally, emergence of AMR in sexually transmitted bacterial infections (STIs) is substantially compromising the effectiveness of treatment, becoming a critical health issue[25]. If these STIs are not detected and appropriately treated, infections result in significant morbidity, mortality and socioeconomic consequences[48]. Gonorrhea, the second most prevalent STI in the United States[49], could also become untreatable due to the high level of detected AMR cases[27]. *Neisseria gonorrhoeae* is the main causative agent of gonorrhea. It is a human pathogen that has been with man since antiquity, referred to by Hippocrates as 'strangury' (associated with 'the pleasures of Venus') until it was officially discovered in 1879 by Albert L. S. Neisser, after whom the genus is named[50]. In addition to the rapid rise of antibiotic resistance, two major problems complicate the treatment of gonorrhea. First, many patients (mostly women) are asymptomatic, remain untreated, developing complications and contributing to the spread of the disease. Second, infection does not result in long-term immunity to reinfection[51]. Vaccines or novel antimicrobials are therefore urgently needed but to date there are no viable novel approaches. The lack of solutions to many issues emphasizes the need for new knowledge about *N. gonorrhoeae* colonization and pathogenesis and innovative modes of treatment.

3.2 Epidemiology and transmission

The World Health Organization (WHO) estimated 82.4 million new cases of infected individuals in 2020, among adolescents and adults worldwide, with most cases in the WHO African Region and the Western Pacific Region[52]. The Centers for Disease Control and Prevention (CDC) stated that the rate of reported gonorrhea cases in the United States during 2015-2019 increased by 60.6% and 43,6% in men and women, respectively[53]. **Fig. 4** shows the distribution of the confirmed gonorrhea cases in 2018, from the most recent report of ECDC (European Centre for Disease Prevention and Control)[54].

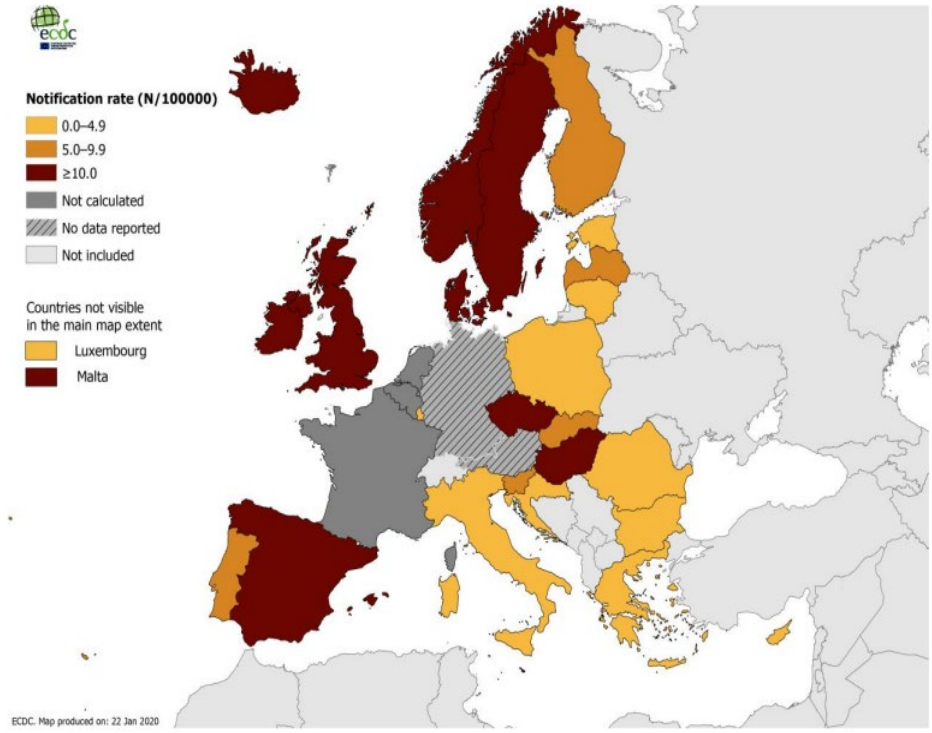

Figure 4. Distribution of confirmed gonorrhea cases per 100,000 population by country, EU/EEA,2018 [54]***.*** *Image taken from ECDC, Annual epidemiological report for 2018, 2020.*

N. gonorrhoeae mostly causes urethritis in men and cervicitis in women, being the urogenital epithelia of the cervix and urethra the main sites of infection. However, it is also able to infect rectal, pharynx, and conjunctival mucosa[55]. It typically spreads by sexual contact, although women can also transmit the pathogen to their child vertically during delivery[56]. A significant proportion of individuals become infected after single exposure, which highlights how easily the bacterium can be transmitted[57]. Among the current European guidelines, symptoms include: urethral discharge in men, mucopurulent cervicitis, dysuria, vaginal pruritus or abdominal pain in women[25]. These symptoms are the result of a strong inflammatory response, although asymptomatic infection occurs in 50–80% of infected women, and 1–40% of infected men[58]. The purulent exudate and resulting painful urination explain the symptoms in men, while in women remain unnoticed; inflammation does not occur in the same niche as urination and thus is less likely to be painful. Furthermore, in presence of symptoms, vaginal discharge may be mistaken for another disease, such as bacterial vaginosis or yeast infection[59]. This is highly problematic, since if not detected and treated promptly, the chance of developing complications dramatically increases[58]. In women in particular, *N. gonorrhoeae* will ascend from the cervix into the otherwise sterile uterus

or fallopian tubes in the upper genital tract, with the potential to cause pelvic inflammatory disease (PID). If left untreated, PID can cause scarring and dysfunction of the fallopian tubes, increasing the risk of ectopic pregnancies and infertility[60]. Moreover, babies born to infected mothers have a 30 to 45% increased risk for acute conjunctivitis, which could lead to blindness[61]. Other severe sequelae include ascending urethral infection in men, that results in inflammation of the testicle (epididymitis) and disseminated gonococcal infection with bacteremia in both sexes[57]. Furthermore, gonorrhea is often co-morbid with other STIs such as HIV, which increases the risk of transmission of this disease and has been reported to have immunologic and molecular interactions with the virus[62].

3.3 Physiology and main virulence factors

N. gonorrhoeae is an oxidase-positive gram-negative diplococcus, belonging to the betaproteobacteria phylogenetic group and the family Neisseriaceae [63]. The Neisseria genus currently consists of at least 23 species, of which about half are human-restricted species, some are animal-restricted and some both. In the genus, the only other opportunistic pathogen is *Neisseria meningitidis*, while other species (for example *Neisseria lactamica* and *Neisseria cinerea*) are commensals residing within the human nasopharynx[63].

Being an obligate human colonizer, *N. gonorrhoeae* cannot survive naturally outside its host[59]. It has a fastidious nature, which can be explained by the fact that, being adapted to live within its mucosal niches, it can metabolize a restricted number of carbon sources as it lost the capacity to synthesize nutrients readily available in the infected tissues [64]. Its genome size is approximately 2 Mb[65], much less compared to *Escherichia coli* genome, which is around 5 Mb[66], which also confirms its strict adaptation within its mucosal niche. From the oxidative metabolism of glucose, the gonococcus produces acid, but not maltose, lactose, sucrose or fructose. Unlike *N. meningitidis*, which is a polysaccharide-positive species, *N. gonorrhoeae* cannot produce a starch-like polysaccharide in the presence of sucrose[64]. On the surface, *N. gonorrhoeae* possesses crucial virulence factors, some of which function also as adhesins, as depicted in **Table 2.**

Type IV pili (Tfp) are retractable filamentous appendages, which are crucial for mediating initial cellular adherence, natural transformation competence, twitching mobility and immune evasion[67]. Several proteins are involved in the assembly of the pilus, including the main pilin subunit PilE, and PilC, a pilus-associated 110-kDa protein located at the tip of the pilus fiber[68]. In terms of pathogenesis, the pilus is an

essential factor for colonization, enhancing the capacity to interact with and adhere to host cells and tissues. Once the pilus has attached to the cell target, through a flagella-independent mode of motility called the ‘’twitching motility’’, it can retract through the bacterial cell wall, while the pilus tip remains attached to its target surface, and brings the bacteria in close contact with the host cell[69]. The pilus binds known receptors such as CD46, a glycoprotein expressed on the surface of every nucleated cell, and the complement regulatory protein 3 and I-domain containing integrins[70].

Opacity associated (Opa) adhesins are outer membrane proteins, whose name derives from the opacity they confer to bacterial colonies when viewed by oblique substage lighting[71]. *N. gonorrhoeae* encodes for 11 Opa proteins[71], whose main function is to mediate the interaction of bacteria with several host cell types, including epithelial cells on mucosal surfaces and various immune cells[71]. Furthermore, they promote bacterial aggregation within colonies[72], which could also explain the inherent resistance of opaque colonies to serum-mediated killing[73]. Each Opa also determines cell-tropism for *N. gonorrhoeae*. Depending upon which Opa protein is being expressed, bacteria can reside inside various cell types (e.g., within mucosal epithelial cells, endothelial cells, neutrophils or monocytes)[71]. They are commonly divided in 2 classes based on receptor engagement: the first, Opa50, binds to surface heparan sulfate proteoglycan (HSPG) receptors, and the second group, Opa51-60, binds to carcinoembryonic antigen-related cellular adhesion molecules (CEACAMs)[55]. Following interactions with CEACAM, gonococci come into closer contact with epithelial cells or phagocytes after Tfp-mediated adhesion. Furthermore, interactions between CEACAMs and Opa proteins can induce phagocytosis, triggering the engulfment of the bacteria into the epithelial cells and neutrophils[55]. Among the CEACAM family, CEACAM-5 is expressed on mucosal surfaces of the rectum, male penile urethra and female vagina and ectocervix while the female endocervix and uterus express CEACAM-1[64]. It may happen that during human infection, the *N. gonorrhoeae* cell surface lacks Opa proteins entirely (Opa-less), expresses one Opa variant only or expresses a combination of many *opa* alleles[59].

N. gonorrhoeae possesses a variety of lipooligosaccharides (LOS) which lack O-specific side chains and are known to bind the asyaloglycoprotein receptor (ASGP-R)[74]. Depending on the sialylation status of LOS, bacteria can show serum resistance or invade epithelial cells. LOS sialylation protects bacteria from complement-mediated killing and antimicrobial peptides[75]. During sexual transmission, bacterial sialidases, secreted by the cervicovaginal microbiota of women, first desialylate *N. gonorrhoeae* LOS to enable efficient transmission from women to men, as *N. gonorrhoeae* must be free of sialic acid to successfully bind and enter urethral epithelial cells[75]. Furthermore,

LOS contributes to the evasion of immune response, as the carbohydrate structures of LOS can mimic host molecules such as mammalian glycosphingolipids[76].

N. gonorrhoeae possesses the major outer-membrane porin protein, which is a nutrient channel and one of the most abundant gonococcal outer membrane proteins[77]. The *N. gonorrhoeae* porins PorB (i.e., P1.A and P1.B) are relatively conserved membrane-spanning proteins composed of trimers that form pleated barrels within the bacterial membrane. It binds complement factors C4b-binding protein and factor H[78]. Given the variation within the sequence and length of its surface-exposed loops expressed by different strains, PorB provides the basis for gonococcal serogroup and serovar typing schemes[77].

Table 2. *Neisseria gonorrhoeae* main virulence factors involved in adhesion [64].

Neisseria Adhesin	**Host Receptor**	**Host Receptor Location**
Pilus	CD46	CD46 is expressed on all nucleated cells
	Complement receptor 3 (CR3)	CR3 is expressed on epithelial cells of the female genital tract and phagocytic cells, including PMNs and macrophages.
Lipooligosaccharide (LOS)	Asialoglycoprotein-receptor (ASGP-R)	Urethral epithelial cells, spermatozoa
Opa_{HSPG}	Heparan sulphate proteoglycans	Expressed on most cell types, polarised to basolateral side of epithelia
Opa_{CCM}	CEACAM family of receptors	Differentially expressed on most cell types, including epithelia, endothelia and cells of haematopoietic origin. CEACAM-3 is only expressed by PMNs.
	CEACAM-1	
	CEACAM-3	
	CEACAM-5	
	CEACAM-6	

One of the reasons behind complications of the clinical outcome and eradication of the disease is the capacity of *N. gonorrhoeae* to display variation of surface antigens, virulence factors included. This variation can be due to two different mechanisms known as phase-variation or antigenic variation[77]. Phase variation affects gene expression, turning on or off the expression of an antigen, while antigenic variation modifies its sequence, the resulting chemical composition and, in some cases, its function. Antigenic variation stems from genetic recombination between sequences within the chromosome or following the integration of horizontally acquired DNA sequences. This is possible thanks to a RecA recombination system[79]. Pilin genes are a striking example of antigenic variation. Pilus results from the rearrangements between the gene encoding PilE and the silent pilin (*pilS*) locus[79]. Since sequences of the *pilE* and *pilS* genes vary between different strains, the number of potential pilin antigenic variants from intragenomic and horizontally acquired alleles is limitless[79]. PorB presents widespread antigenic heterogeneity within its surface loops, which has been exploited, through PCR and sequencing, to distinguish and classify different gonococcal strains in serovars[64]. Phase variation results from the presence of simple repeat sequences within the promoter or coding sequence of genes which induce slippage of DNA polymerase while replicating them (slipped-strand mispairing). Through this slippage, the resulting variation of repeats affects the promoter function and/or protein translation reading frame. The most affected components of phase-variation are the Opa proteins and components of the pilus (PilC1)[80]. The frequency of phase variation in *N. gonorrhoeae* is estimated to be approximately 10^{-3} per cell per generation[81]. Opa proteins undergo phase-variation. Each of the 11 Opa genes are constitutively transcribed[71] but protein expression undergoes phase variation at the translational level. Through changes in the number of CTCTT repeats in the leader peptide sequence of each of the 11 *opa* alleles in the chromosome, the expression of these genes is altered[59]. The expression of various sugar transferases involved in LOS biosynthesis also depends on phase-variation. Variable expression of glycosyl transferases leads to different composition of the variable α-chain LOS carbohydrates so that LOS can be modified to protect the bacteria from serum complement-dependent killing[79].

3.4 Pathogenesis

Pathogenesis of *N. gonorrhoeae* can be divided into different steps. First, the bacterium must adhere to the mucosal epithelial surface, competing with local microbiota. Then, it replicates in microcolonies, which are collections of bacteria formed by a few

diplococci. The gonococcus invades cells and translocates across the epithelial barrier to reach the subepithelial space. Within the subepithelial space, *N. gonorrhoeae* must persist within the tissues, while evading innate and adaptive immune responses. Rarely, the gonococcus leaves the site of initial infection, enters the bloodstream and causes disseminated gonococcal infection[59] (**Fig. 5**).

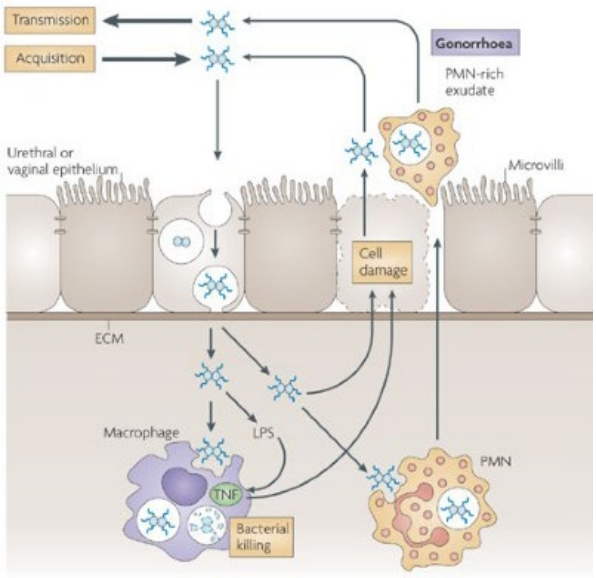

Figure 5. Stages in the pathogenesis of N. gonorrhoeae. *Neisseria gonorrhoeae establishes infection in the urogenital tracts by interacting with non-ciliated epithelial cells; this results in cellular invasion. Infection often leads to inflammation and polymorphonuclear leukocyte (PMN) influx. Engulfed N. gonorrhoeae are then secreted in together with PMN in an exudate. Both tumor necrosis factor (TNF) from phagocytes and gonococcal products, such as peptidoglycan and lipooligosaccharide (LOS), also cause toxic damage to ciliated epithelial cells of mucosal surfaces*[82].

3.4.1 Interactions with the mucosal epithelium

N. gonorrhoeae first adheres to mucosal surfaces using the type IV pilus, which binds to apically expressed receptors and then retracts to allow an intimate association of bacterial and host cell membranes. This is followed by a secondary association with the epithelial surface mediated by Opa proteins most of which bind to CEACAM. However, studies involving experimental infection in male volunteers have shown that inoculating subjects with gonococci lacking Opa expression still leads to infection,

suggesting that Opa may not be required for initial infection of urethral cells[83]. Surface factors LOS and porin also affect colonization[59]. Following adhesion, the gonococci start replicating, forming microcolonies and competing with the local microbiome to achieve a successful colonization. Furthermore, *N. gonorrhoeae* overcomes the attempt of the host to induce starvation by limiting its access to nutrients, as in case of iron sequestration. In the human body, free iron is quickly bound by one of two iron-binding proteins: transferrin and lactoferrin, lowering the level of free iron levels needed to support growth of *N. gonorrhoeae*. To access host iron stores, *N. gonorrhoeae* is capable of expressing two highly specific heterodimeric receptors that bind to transferrin (the transferrin binding proteins, Tbps) or lactoferrin (the lactoferrin binding proteins, Lbps) and physically remove iron to facilitate its access to the bacterium[64]. At the site of adherence to the cells, if invasion is successful, the bacteria move across the epithelium monolayer into the subepithelial space through a process commonly known as transcytosis. Throughout transcytosis, which requires endocytic recycling and vesicles, cells apply a host defense mechanism known as autophagy[55]. Transmission Electron Microscopy (TEM) studies have shown that when *N. gonorrhoeae* invades cells, many gonococci can be found in autophagosomes made of double-membrane autophagic structures[84]. In the early stages of invasion, most of the gonococci are impaired. However, in the late stages of invasion the gonococcus can inhibit autophagosome maturation and fusion with the lysosome and evade the autophagy pathway, maintaining the infection[84]. Transmigration from apical surface to the subepithelial space allows access to nutrients but eventually the bacteria must re-enter the urogenital lumen in order to infect another person. A small proportion of Opa proteins do not associate with CEACAMs but bind heparan sulphate proteoglycans (HSPGs), expressed on the basolateral side of the epithelial barrier[64]. This allows a subset of the infecting population to exit the infected tissue to allow transmission to another host[64]. As epithelial cells express pattern recognition receptors (PRRs), including Toll-like receptors (TLRs) that detect microbial-associated molecular patterns (MAMPs), the moment the cells encounter bacteria through PRRs, they will elicit a pro-inflammatory response[85]. How the pro-inflammatory response takes place dictates the difference between the symptomatic and asymptomatic infections in women and men, respectively. In women, *N. gonorrhoeae* colonizes and infects the epithelial cells of the endocervix. However, genital infections in women were not found to increase levels of the pro-inflammatory cytokines and chemokines, either locally or systemically[64]. This could be partly explained by the fact that women with *N. gonorrhoeae* infection tend to have higher vaginal pH, suggesting that low vaginal pH may protect this mucosa[64]. In the male urethra, gonococcus elicits the release of

interleukin-6 (IL-6), IL-8, tumour necrosis factor (TNF) and IL-1β, which recruit and activate leukocytes to combat the infection[86].

3.4.2 Interactions with the immune system

Infection by gonococcus is accompanied by an ineffective immune response, which seems to be the sum of different mechanisms. Firstly, this is due to the genital tissue properties as the female tract is an immune privileged site. Secondly, given its ability to alter surface epitopes, gonococci undergo selection for the most 'fit' variant within each potential niche of the human host[64]. Lastly, *N. gonorrhoeae* has evolved mechanisms to redundantly cause infection, modulate host innate and adaptive immune responses and persist within human tissues.

3.4.2.1 The innate immune system and phagocytic cells

The innate immune system plays a crucial role in pathogenesis, as *N. gonorrhoeae* does not express potent exotoxins and most of the damage results from activation and persistence of an inflammatory response at the site of colonization[59]. After invasion, gonococci stimulate local mucosal immune cells and initiate an inflammatory response, followed by the entrance of neutrophils and macrophages. Throughout this response, a portion of *N. gonorrhoeae* can survive in these phagocytic cells and persist[64]. In fact, symptomatic infection is typically characterized by a purulent discharge composed of bacteria and neutrophil granulocytes[55]. Furthermore, *N. gonorrhoeae* can also evade human (but not animal) complement-mediated killing. It can prevent membrane attack complex formation and it can shield itself from host recognition by expressing host molecules on the surface and by binding to complement regulatory proteins[59]. The main driver that dictates the interaction between gonococci and neutrophils are the Opa adhesins, which either bind to receptor CEACAM-3 or do not. CEACAM-3 is exclusively expressed by human neutrophils, and drives an opsonin-independent phagocytic engulfment and oxidative killing of Opa-expressing bacteria[87]. Most bacteria, (except those that engage CEACAM3, which are killed inside neutrophils) can survive and replicate inside and outside of neutrophils[59]. In fact, some gonococci can selectively express proteins that bind CEACAM1 but not CEACAM3[61]. There are various mechanisms that dictate survival between gonococci and phagocytic cells. Neutrophils, for example, can also release a meshwork of DNA and antimicrobial components, called NET (neutrophil extracellular trap), which first traps the pathogen to exert its bactericidal activity. *N. gonorrhoeae* can survive the NET, secreting

proteins that compromise its components (e.g. Nuc thermonuclease degrading the DNA)[88]. Even after phagocytosis, engulfed bacteria can survive intracellular lysosome by compromising its maturation[59]. It has been hypothesized that this is a survival mechanism of the pathogen, as *N. gonorrhoeae* aims to remain undetected by the immune system, using the cell as a Trojan horse, inside which it can survive and replicate [59]. Por B and IgA protease modify phagosome processing causing a delay in phagosome maturation and killing of engulfed gonococci. The porin first inserts into eukaryotic membranes to form ion-gated channels, triggering a transient rise in cytosolic Ca2+ levels[78]. This leads to lysosomal exocytosis and results in a redistribution of Lamp1 to the cell surface. This exposes Lamp-1 to IgA protease cleaving activity, which is the most efficient at neutral pH and much less efficient at pH 5.5, the pH of the lysosome lumen[78]. *N. gonorrhoeae* can also modulate macrophages phenotype and cell death[59]. Macrophages are highly plastic and in response to various signals, they may undergo classical M1 activation or alternative M2 activation. While the classical pro-inflammatory M1 phenotype promotes a Th1 response and possesses strong microbicidal and tumoricidal activity, the M2 promotes clearance of infection, dampens inflammation, tissue remodeling, tumor progression, and possesses immunoregulatory functions[89]. Macrophages interacting with *N. gonorrhoeae* have been reported to differentiate toward an M2 profile, inducing the release of anti-inflammatory cytokines[90]. Whether *N. gonorrhoeae* induces cell death in macrophages is not clear and there is debate in literature. *N. gonorrhoeae* has been shown to induce apoptosis in THP-1 cells, a monocyte-like cell line that can differentiate in macrophages[91], while Ritter et al. stated that *N gonorrhoeae* induces nonapoptotic cell death in human macrophages via pyroptosis[92].

3.4.2.2 Adaptive immune response

Most individuals infected by *N. gonorrhoeae* do not develop protective adaptive immune responses[93]. In fact, infection does not increase gonococcal-specific antibodies, whose titers are low and transient in infected patients[94], and redundant infections of the same strain do not elicit a memory response typically apparent upon re-exposure to the same antigens. This lack of immune response was observed also in female- mouse animal model infection, where infection does not result in local genital antibody responses or induction of adaptive type 1 or type 2 T helper cell responses[95]. Even though the urogenital tract is a poor immune-inductive site, even in immunogenic sites such as the rectum, which contain organized lymphoid follicles, *N. gonorrhoeae* does not elicit a better response[64]. As innate immune cells co-operate with adaptive

immune response, if the first are compromised, it can greatly affect the strength of response of the second. For example, macrophages polarized toward a M2-phenotype are less capable of activating T cells, as they inefficiently upregulate molecules involved in antigen presentation and T-cell activation, leading to a weak allogeneic T-cell stimulatory activity[90]. *N. gonorrhoe*ae exerts its suppressing activity also through antigen presenting cells. *N. gonorrhoeae* redirects dendritic cells to expose immunosuppressive properties and inhibits dendritic cell-induced proliferation of antigen-induced CD4+ T lymphocytes[93]. Through human cellular immune response*, N. gonorrhoeae* can also interact with and modulate directly T cells, suppressing Th1 and Th2 responses. *N. gonorrhoeae* induces secretion of cytokines which can specifically initiate a Th17 response (e.g., IL-23) while they don't release IL-12 which stimulates a Th1 response. Th17 T cells produce IL-17 is involved in the inflammatory response, enhancing the influx of neutrophils and the recruitment of other innate defense mechanisms[95]. Through specific Opa proteins, Opa52 particularly, gonococci bind to CEACAM-1 on primary $CD4^+$ T cells, downregulating their activation and proliferation in response to antigens[96]. This influences the human humoral immune response. Given the absence of CD4 + T cells that can direct antigen-specific B cells, this results in a non-specific B cell expansion with a poor antibody response. So et al. demonstrated that if primary human B cells are infected with *N. gonorrhoeae*, a subset of B cells starts to proliferate and to produce low-affinity, broadly reactive IgM antibodies[97]. *N. gonorrhoeae* drives the proliferation of these cells regardless of their antigen specificity, forming polyclonal antibodies which poorly interact with the infecting strain[97]. Furthermore, *N. gonorrhoeae* has developed ways to inhibit potentially protective antibodies. Outer membrane protein reduction modifiable protein (Rmp), despite being highly immunogenic, induces anti-Rmp antibodies that block the activity of bactericidal antibodies targeting gonococcal surface antigens[98]. Overall, *N. gonorrhoeae* suppresses adaptive immune responses, but Liu et al. demonstrated that reversal of the induced immunosuppression is possible and could enable the development of protective immunity[95]. Counter-manipulating this suppression to allow Th1-governed responses to emerge can allow the development of specific antibodies, establishment of memory, and accelerated clearance of infection[95].

3.5 Therapeutic approaches and AMR

An effective and long-lasting antimicrobial treatment is essential for prevention and control of *N. gonorrhoeae* infections. The increased emergence of multidrug resistance has heightened concern about the possibility of widespread untreatable gonorrhea. The

AMR phenomenon began since the mid-1930s, when sulfonamides were introduced and kept re-appearing following the introduction of a series of empirical antimicrobials, such as penicillin, tetracyclines, fluoroquinolones, macrolides (azithromycin), and third-generation cephalosporins (ceftriaxone or cefxime)[27] (**Fig. 6**). *N. gonorrhoeae* mechanisms of AMR span inactivation of drugs, mutation of antibiotic targets, enhancement of drug efflux and reduction of drug influx (for example, through decreased permeability of the PorB porin)[25]. Most genes conferring resistance are found in the chromosome, although the *blaTEM* gene and the *tetM* gene, which confer high-level resistance to penicillin and tetracyclines, are known to be plasmid-borne[59]. Behind the different factors driving AMR emergence, the unrestricted access to and over-prescription of antimicrobials has contributed to speed up the phenomenon[59]. Furthermore, *N. gonorrhoeae* is highly efficient in both DNA secretion and uptake, transferring partial or whole genetic material. In fact, it is naturally competent for uptake of neisserial-derived DNA during all stages of growth and actively secretes genomic DNA into the extracellular space through a type IV secretion system (T4SS)[99]. To aggravate things, despite its main specificity for neisserial genetic material, *N. gonorrhoeae* can internalize other genetic material at lower frequencies. This explains the remarkable frequency of both intra- and intergenomic recombination among and between gonococcal strains[64]. Eventually, the emerging resistance to monotherapeutic treatment led to the development of dual-therapy (SCs—ceftriaxone or cefxime and azithromycin) as first-line treatment for gonococcal infection. In 2010, the recommendation was to use a single intramuscular dose of ceftriaxone (250 mg) and a single oral dose of azithromycin (1g). 10 years later, in 2020, the CDC recommended to increase the dose of ceftriaxone to 500 mg[100]. Recent findings also demonstrated decreased susceptibility and/or AMR of *N. gonorrhoeae* to dual therapy[101]. The spread of ceftriaxone-resistant gonococcal strains has been confirmed in 2015 and, in 2018, the first strain resistant to ceftriaxone and azithromycin was isolated in the UK and Australia[102]. Globally, ciprofloxacin resistance is high, azithromycin resistance is increasing, and decreased susceptibility and resistance to ceftriaxone and cefixime continues to emerge[102]. Therefore, gonococcal strains started to exhibit multidrug resistance (MDR) or even extensively drug resistance (XDR) phenotypes. By definition, XDR gonococcal strains are strains resistant to ≥2 (MDR strains are resistant to 1) of the antibiotic classes currently recommended and ≥3 (MDR strains are resistant to ≥2) of the classes now less frequently used[103]. XDR strains, exhibiting high-level clinical resistance to all extended-spectrum cephalosporins (ESCs) combined with resistance to nearly all other available antimicrobials, were recently identified in Kyoto, Japan, Quimper, France, and Catalonia, Spain[103]. Fortunately, it seems that XDR strains

exhibit a lower fitness, and less capacity to spread further within local community. This was observed with the first XDR stain (H041) in Japan , after observing its spread in Kyoto and Osaka from 2010 to 2012[104].Today new therapeutic approaches are being evaluated, including antimicrobial drugs belonging to a different antibacterial family aside from the previously included ones, to whom the gonococcus has already developed a mechanism of resistance. Among those, three are in their late stage of development: solithromycin, zolifodacin, and gepotidacin[27].

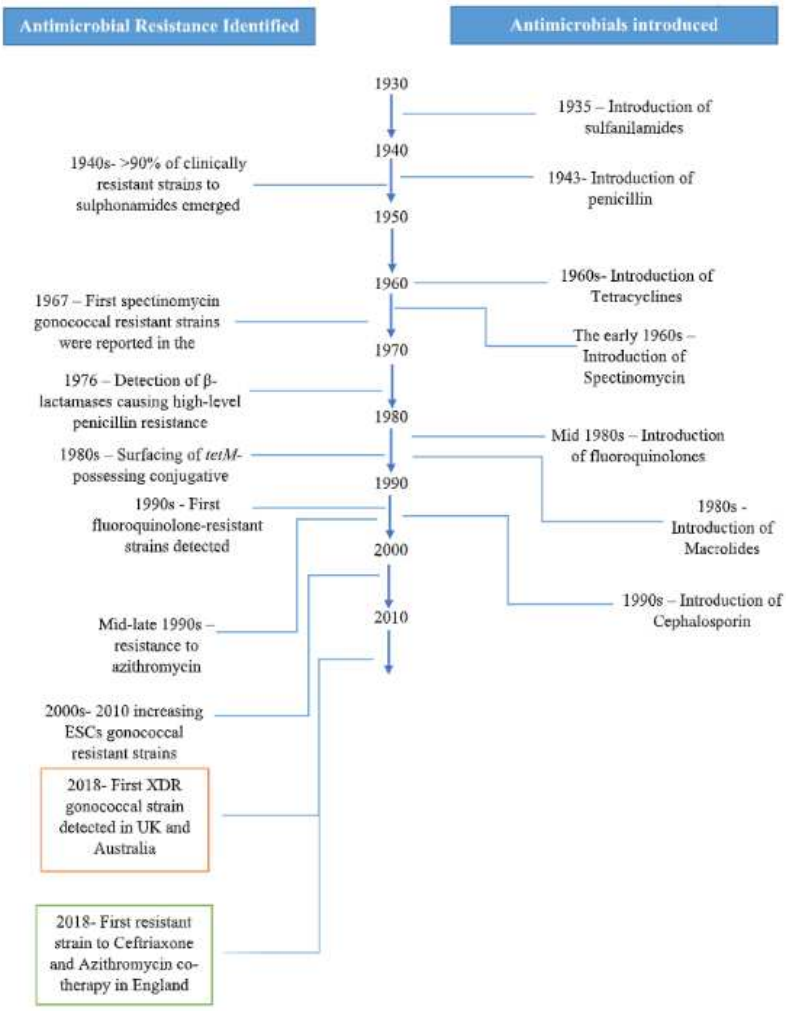

Figure 6. Timeline representing on the right the first introduction of antimicrobials and on the left the emergence of gonococci resistance to these therapeutic regimens[27].

In May 2012 the WHO published a global action plan concerning the spread and impact of AMR in *N. gonorrhoeae,* with the primary objective of regulating the spread of infections and minimize the eventual emergence of AMR[105]. Specifically, the

organization stated that "*the spread of resistant N. gonorrhoeae is not going to go away and will continue to affect increasing numbers of communities*"[105]. The organization highlights the need of solid guidelines for local health departments, to monitor the emergence of AMR, like how to determine the number of resistant gonococci as a proportion of all isolates tested. When the proportion of resistant strains obtained from the tested samples is at a level of 5% or more, or when any unexpected increase below 5% is observed in key populations with high rates of gonococcal infection (for instance in MSM or sex workers), the WHO recommends responding by changing national guidelines for STI treatment and management[105]. In October 2016 WHO published the Global Health Sector Strategy on STIs, which aims to solve the major public health concern caused by STI. To respond to the growing concern of the emergence of AMR in *N. gonorrhoeae* and increased incidence of gonococcal infections, it has set the objective of reducing the global incidence of gonorrhoeae by 90% by 2030[106].

3.6 2C7 monoclonal antibody against *N. gonorrhoeae*

mAb 2C7 is a candidate therapeutic mAb, which targets virulence factor LOS[76]. Gulati et al. generated various mAbs that reacted with LOS, obtained from splenic B-cells of mice immunised with outer membrane vesicles of *N. gonorrhoeae* strain WG, which were subsequently fused to murine myeloma cells to generate hybridomas. Among these mAbs, 2C7 (IgG3λ) was generated[76]. *N. gonorrhoeae* expresses multiple LOS forms due to phase-variation of LOS glycosyltransferase genes **(Fig.7)**. 2C7 binding requires expression of a lactose residue from heptose (Hep) II, addition of an α-linked Glc residue at the 3-position of HepII represents the first step in synthesis of the lactose extension from HepII and is mediated by the phase-variable LOS glycosyltransferase G (*lgtG*)[107]. Glycosyltransferases control glycan extensions from the LOS core heptoses (HepI and HepII), this may result in 4 different LOS mutant phenotypes with alternative glycan extensions: 2-Hex/G+, 3-Hex/G+, 4- Hex/G+, and 5-Hex/G+. 2C7 causes SBA of three of the HepI mutants *in vitro* (2-Hex/G+, 4-Hex/G+, and 5-Hex/G+). It does not promote direct killing by complement of the 3-Hex/G+ but induced opsonophagocytic killing of this glycotype in presence of neutrophils and complement. This is because mAb 2C7 deposited sufficient C3 on these bacteria for opsonophagocytic killing by human neutrophils[107]. 2C7 was engineered with an E430G Fc modification which, once 2C7 binds to the target, enhances hexamerization and Fc:Fc interaction[108]. This form is typically known as HexaBody technology[109]. Compared to mAb 2C7 with wild-type Fc, it increases complement activation, due to greater C1q engagement and C4 and C3 deposition. This translates into increased

bactericidal activity[108]. Furthermore, to exploit 2C7 *in vivo*, Parzych et al. developed a platform to deliver DNA-encoded mAbs in infected mice [110]. 2C7_E430G variant, once delivered in mice, demonstrated high potency even when mice were challenged 65 days after mAb administration[110].

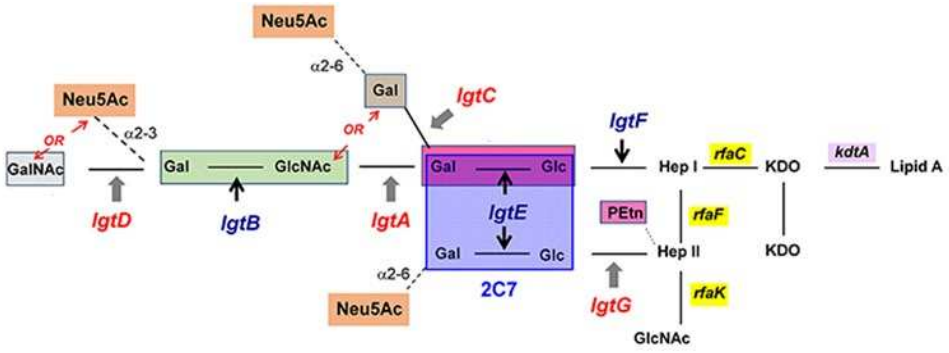

Figure 7. Structure of gonococcal LOS and 2C7 binding site. *LOS consists of three oligosaccharide (OS) chains. Phase variable genes involved in LOS biosynthesis include lgtA, C, D, and G and non-variable genes lgtF, lgtE, and B. LOS branching is terminated either by Neu5Ac (sialic acid) or otherwise extend(s) outward by adding hexose(s). LOS is attached to lipid A via two 2-keto-3-deoxy-mannooctulosonic acid (KDO) molecules. Two heptose residues branch from the OS chains. One OS chain elongates from the first heptose (Hep I) outward; two chains extend from the second heptose (Hep II). The blue square depicts the minimal structure for 2C7 binding[75]. Image taken from Gulati et al. 2019.*

3.7 Vaccines and prophylaxis

The high disease complications associated with gonococcal infections and the rapid evolution of antibiotic resistance in *N. gonorrhoeae* highlight the urgent need for a gonorrhea vaccine. Currently, research has focused on antigen discovery and the identification of protective immune responses, but no vaccine has been tested in clinical trials in over 30 years[111]. There have been past efforts to obtain a vaccine which could protect against the disease, but they failed[112]. There are various reasons for this: antigenic variation being displayed by the organism and the host's inability to generate a protective immune response, lack of immunological memory, lack of suitable animal models, absence of vaccine-targetable surface capsule in contrast to meningococcal vaccines, and no basis to establish correlates of protection[111,113]. These issues explain the poor investment in gonococcal vaccine development in the past 25 years[58].

However, interest in vaccine development against *N. gonorrhoeae* has been revived recently by the increased global interest in the use of vaccines to fight AMR bacteria**.** To measure vaccine candidate efficacy, current preclinical researchers determine the bactericidal or opsonophagocytic activity of antibodies, the blocking of target function, antibody surface binding, and infection with *N. gonorrhoeae* in a female murine genital tract infection model. Being a human pathogen, the gonococcus does not naturally infect any other animal, making the understanding of its lifestyle *in vivo* and eventually the testing of a vaccine candidate difficult[57]. An animal model of genital tract gonococcal infection has been established in female mice, and remains the only model in which the response of an intact mammalian immune system to genital gonococcal infection can be studied[95]. There are four current vaccine approaches (Table 3): (1) Meningococcal and gonococcal OMV vaccines that are intrinsically self-adjuvant; (2) purified protein subunit vaccines; (3) mixed OMV and protein subunit vaccines; and (4) immunotherapeutic vaccines that utilize adjuvants[57].

Table 3. Approaches for vaccines against *N. gonorrhoeae*[57].

Vaccine Approach	Vaccine Components/Antigens under Investigation [1]
Meningococcal and gonococcal OMVvaccines	VA-MENGOC-BC® MeNZB®: NZ 98/254 OMV (Omp85, FetA, PorA, PorB3, FbpA, RmpM, OpcA, and NspA) Formalin-inactivated whole cell microparticles
Purified protein subunit vaccines	AniA, Lst, OmpA, Opa, OpcA, PilC, PilQ, PorB, TbpB, TbpA, TdfJ, *Ngo*Φfil phage particles
Mixed OMV and protein subunit vaccines	Bexsero®: MeNZB OMV antigens with additional fHbp, NHBA, and NadA antigens
Immunotherapeutic vaccines	OMV vaccine with IL-12 adjuvant 2C7 LOS epitope mimic multi-antigenic peptide vaccine

OMVs are naturally secreted spherical vesicles formed by gram-negative bacteria (approximately 20-250 nm in diameter) and comprise the outer membrane and periplasmic luminal elements[100]. OMVs possess immunogenicity, as they contain most of the surface antigens in native conformation, adjuvant potential and the ability to be taken up by immune cells. These features make them attractive tools for the development of vaccines against pathogenic bacteria[100]. Unfortunately, they induce the strongest response to homologous strains from which they are derived, a limit which can be overcome with supplementation with other proteins to raise strong heterologous responses[57]. Another approach is based on the discovery of potential gonococcal vaccine antigens using bioinformatic tools. Zielke et al. performed proteomics-driven reverse vaccinology and managed to discover various potential vaccine antigens[113]. Homologs of BamA (NGO1801), LptD (NGO1715), and TamA (NGO1956), and two

uncharacterized proteins, NGO2054 and NGO2139, were highly conserved among different strains, surface exposed and secreted via naturally released membrane vesicles. After obtaining polyclonal rabbit sera against these antigens, they found that they elicited bactericidal antibodies that cross-reacted with diverse isolates. They observed that depletion of BamA caused loss of *N. gonorrhoeae* viability, suggesting it may be an essential target and a good candidate[113]. Immunotherapeutic vaccines use adjuvants to stimulate adaptive immune response to gonococcal infections[57]. Knowing that *N. gonorrhoeae* suppresses adaptive immune responses, including Th1 directed response, Liu et al. hypothesized that IL-12 (a T-cell stimulating factor, involved in the differentiation of naïve T cells into Th1 cells) could serve as an adjuvant for gonococcal OMV vaccines[95]. They performed immunization of OMVs, together with IL-12 encapsulated in microspheres, in the female mouse-animal model. This generated a Th1-driven, antibody-dependent, protective immune response that persists for at least several months and is effective against antigenically diverse strains of *N. gonorrhoeae*[95]. The monoclonal antibody 2C7 recognizes a conserved oligosaccharide structure of LOS[76] which could be used as a potential vaccine candidate. Since sugars are poor immunogens that induce T-cell independent responses, Gulati et al. configured 2C7 as a mimotope peptide, included in a tetrameric multiantigen peptide assembly (called TMCP2)[114]. They immunized mice with TMCP2 and an adjuvant (Toll-like receptor 4 and T_H1-promoting cytokine) and observed that immunization elicited bactericidal IgG and reduced colonization levels of gonococci in infected mice while accelerating clearance of infection[114].

3.8 Bexsero cross-protection studies

It seems that *N. meningitidis* OMV-based vaccines can show cross-protection against *N. gonorrhoeae*. A retrospective case-control study reported that vaccination with a serogroup B *N. meningitidis* outer membrane vesicle (OMV) vaccine can be associated with reduced rates of gonorrhea[115]. Specifically, this vaccine consists of OMVs from an endemic New Zealand strain (MeNZB). From 2004 to 2008, in response to an epidemic of *N. meningitidis* serogroup B, MeNZB was delivered to more than 1 million New Zealanders (81% of the New Zealand population aged younger than 20 years)[116]. The estimate vaccine effectiveness of MeNZB against gonorrhea was predicted to be 31% in a population that received 3 doses of the vaccine and was up to 20 years of age when vaccinated[115]. Furthermore, Le duc et al. demonstrated that, after vaccinating female mice with Bexsero, there was a significant reduction of the infection burden[106]. Bexsero induced antibodies that recognized different *N. gonorrhoeae* outer membrane

proteins, two of which (PilQ and NHBA) were also detected in sera of people vaccinated with Bexsero[111]. For the first time, a vaccine has been found to show some protection against gonorrhea, which could be, in part, explained by the fact that the vaccine can reprogram mucosal immunity[117]. Most importantly, it provided a proof of principle that could inform prospective vaccine development[115]. In fact, despite causing different diseases, *N. meningitidis* and *N. gonorrhoeae* are genetically and antigenically very similar, with 80–90% nucleotide identity across the genome and many proteins sharing high levels of identity (e.g. PorB shares 60–70% amino acid homology)[112,118]. Today, MeNZB is no longer available. However, it is contained in the broad-spectrum serogroup B vaccine Bexsero (4CMenB: 4 component Meningitidis B). The vaccine is composed of the New Zealand strain NZ98/254 OMV and three recombinant surface-exposed protein antigens. These antigens are the Neisseria adhesin A (NadA), the neisserial heparin binding antigen (NHBA) peptide 2 fused to accessory protein GNA1030 and fHbp variant 1.1 (subfamily B) fused to the antigen GNA2091[119]. The fusion with GNA proteins results in increased immunogenicity and serum bactericidal titers. The three components were verified by reverse vaccinology based on the complete genome sequence of reference MenB stain (MC58)[119]. The most abundant proteins in the OMVs are PorA, PorB, and OpcA, with the antigenically-diverse PorA being immunodominant and the main target of antibodies inducing serum bactericidal activity (SBA)[112].

Various studies have been performed to determine the homology of the vaccine components to *N. gonorrhoeae* antigens. NadA is absent in *N. gonorrhoeae* and fHbp, GNA1030, and GNA2091 are exposed on the surface. NHBA is believed to be the only recombinant antigen of 4CMenB that may induce protection against *N. gonorrhoeae*. However, functional antibodies are raised against other OMV components[112].Using bioinformatic analysis, a high level of amino acid sequence identity has been found between most of the major 4CMenB OMV proteins and *N. gonorrhoeae* homologs (**Table 4**) Furthermore, OMV-induced antibodies were found to be able to recognize gonococcal proteins[112].

Table 4. Bexsero vaccine components and their homology to gonococcal proteins[112].

OMV Protein Antigens				
NMB Locus[a]	Protein	Abundance in OMVs[b]	%ID to Ng FA1090[c]	%ID Between Ng Strains[d]
NMB2039[e]	PorB (porin, major OMP PIB)	42.54	67.3	88.6–100
NMB1429[e]	PorA (porin, serosubtype P1.4)	28.63	n/a	n/a
NMB1497	TonB-dependent receptor	4.60	96.1	98–100
NMB0382[e]	RmpM (OMP class 4)	3.08	93.4	99.6–100
NMB0964	TonB-dependent receptor	2.87	96.9	96.2–100
NMB1812	PilQ (Tfp assembly protein)	1.44	91.4	79.1–100
NMB0634[e]	FbpA (iron ABC transporter substrate-binding protein)	1.29	99.1	99.1–100
NMB1126/NMB1164	Putative lipoprotein NMB1126/1164	1.06	94.2	99.1–100
NMB1988[e]	FrpB (FetA, iron-regulated OMP)	0.96	94.3	94.6–100
NMB0461	Tbp1 (transferrin binding protein 1)	0.92	93.7	38.3–100
NMB0182[e]	OMP85	0.87	95	99.2–100
NMB1053[e]	OpcA (class 5 OMP)	0.75	43.8	98.9–100
NMB0088	OMP P1	0.54	94	98.9–100
NMB1540	LbpA (lactoferrin binding protein A)	0.46	n/a[f]	41.0–100
NMB0280	LptD (LPS assembly protein/organic solvent tolerance protein [OstA])	0.44	89.8	99.4–100
NMB1714	MtrE (outer membrane efflux protein)	0.29	96.4	95.3–100
NMB0109	LysM peptidoglycan-binding domain containing protein	0.26	88.7	97.3–100
NMB1333	hypothetical protein	0.24	96.3	97.3–100
NMB1567	FkpA (macrophage infectivity protein)	0.23	97.8	98.9–100
NMB0946	antioxidation AhpC TSA family glutaredoxin	0.20	98.5	99.6–100
NMB0375	MafA adhesin (mafA-1)	0.18	98.8	59.2–100
NMB0633[e]	NspA (OMP)	n/a	93.7	25.4–100

Recombinant Protein Antigens				
NMB Locus[a]	Protein	Variant (strain)[g]	%ID to Ng[c]	%ID Between Ng Strains[d]
NMB2132	Neisseria heparin binding antigen (NHBA)	peptide 2 (NZ98/254)	68.8	93.7–100
NMB1870	Factor H binding protein (fHbp)	peptide 8, variant 1.1 (MC58)	62.6[h]	98.9–100
NMB1994	Neisseria Adhesin A (NadA)	peptide 8, variant 2/3 (2996)	n/a	n/a
NMB1030	GNA1030 (NUbp)	n/a (2996)	92.6	98.8–100
NMB2091	GNA2091	n/a (2996)	95.6	99.5–100

Background and aim of the project

My PhD studies were part of a European Research Council (ERC) Advanced Project named vAMRes (Vaccines as a Remedy for Antimicrobial Resistant Bacterial Infections) whose aim was the discovery of mAbs against antimicrobial resistant bacterial species, including *N. gonorrhoeae*, with the final goal of developing new medications and support vaccine design. As explained in the Introduction section, the rationale behind our interest in *N. gonorrhoeae* relied in the increasing resistance of the bacterium to currently available antibiotics and in the lack of an effective vaccine. In addition, the reported partial protection conferred by the anti-meningococcal vaccine Bexsero against gonorrhea[112] justified the recruitment of vaccinated volunteers who donated their blood for the search of anti-*N. gonorrhoeae* mAbs.

Before I joined the Monoclonal Antibody Discovery Laboratory (MAD-Lab) at Fondazione Toscana Life Sciences, my colleagues had isolated Peripheral Blood Mononuclear Cells (PBMCs) from the blood of these volunteers and single cell sorted 4,609 Memory B Cells (MBCs) specific for the outer membrane vesicles (GMMA) contained in Bexsero. MBCs were then cultivated *in vitro* in the presence of appropriate stimuli (e.g. cytokines) to induce multiplication and secretion of mAbs in the culture supernatants. *N. gonorrhoeae*-specific mAbs were selected by means of Enzyme-Linked Immunosorbent Assays (ELISA) and further validated by the Luminex technology. The selected 553 candidates were cloned and expressed on the high-throughput format in 96-well plates and tested in Serum Bactericidal Assays (SBA) for the identification of mAbs that killed the bacterium in a complement-dependent manner. In addition to evaluating mAb potency in SBA, we sought to develop functional assays that could assess mAb activity in a host-pathogen interaction context. These additional assays were represented by the opsonophagocytosis and the adhesion inhibition assays and constituted the major topic of my research work described in this thesis.

Indeed, anti-bacterial antibodies may work by enhancing complement deposition for serum bactericidal activity but may also act through cell-mediated opsonophagocytic activity, or capacity to inhibit the interaction with epithelia. Therefore, it was important to evaluate whether Bexsero-induced antibodies could interact with the primary defense line of the immune system, such as macrophages, or prevent colonization of epithelial surfaces. Given the high number of mAbs expressed new tools which allowed screening of mAbs in a quicker and robust way were needed. In this work, I have mostly focused on the application of high-content and high-throughput confocal imaging to

the screening of mAbs against gonococcal strain FA1090. In details, in Chapter 1 I report the construction of constitutively fluorescent bacterial strains to be used in high-content microscopy. In Chapter 2 I describe the establishment of the visual opsono-phagocytosis assay (vOPA) to screen mAbs capable of enhancing the phagocytic activity of macrophages. In Chapter 3 I describe an approach I have explored to determine the adhesion of FA1090 to epithelial cells, based on the visual adhesion inhibition assay (vAIA). Lastly, a final Chapter reports my contribution to the development of mAbs against SARS-CoV-2, which enclosed a 6-month period carried out during the COVID-19 pandemic.

Chapters

1. Generation of knock-in strains of *N. gonorrhoeae* expressing fluorescent protein for high-content imaging

Introduction

In recent years, both academia and pharmaceutical industry have become increasingly interested in fluorescence microscopy, especially in a novel technique that is generally referred to as high-content screening (HCS). High-content screening combines high-resolution fluorescence microscopy with automated image analysis[120]. It is a high-throughput technology which exploits imaging to collect quantitative data from biological systems[121]. With this approach, it is now possible to study test compounds in disease-relevant cellular assays and visualize subcellular structures and monitor intracellular protein translocation[120]. Furthermore, in addition to visualizing the components, it is possible to apply appropriate image-analysis algorithms to quantify the distribution and brightness of the fluorophores used to label cells[120]. This might be useful in a context where the fluorescent protein, when expressed constitutively by cells and retained intracellularly, may have significant utility as a viability indicator[122].

Since the major goal of my thesis work consisted in the establishment of high-throughput screening assays using confocal microscopy, I first had to generate the tools which allowed subsequent object detection and image analysis. In this chapter, I will describe the creation of a knock-in strain of *N. gonorrhoeae* FA1090 expressing green fluorescent protein (GFP). I cloned a variant of GFP, called super-folder GFP (sfGFP)[123], in an integrative vector which I have used to transform FA1090. SfGFP is a more robustly folded version of GFP[123]. This version contains both 'enhanced GFP' and folding-enhanced mutations, which lead to improved folding kinetics, greater tolerance of circular permutation and greater resistance to chemical denaturants. This led to brighter *N. gonorrhoeae*, which was easily detectable by using the confocal microscope. After validating the successful transformation and expression of the protein, the fluorescent strains were characterized for their fitness in comparison to the wild-type and were used to determine whether sfGFP intensity could inform on the viability of bacteria in bactericidal assays performed by means of Opera Phenix.

Results

Cloning of superfolder GFP in integrative vector pGONO

To constitutively express GFP in FA1090, I used an integrative vector, named pGONO[124], where the cloned gene is under transcriptional control of the constitutively active tac promoter (Ptac) (**Fig. 8a, Supplementary Table 1**). The plasmid integrates into the *N. gonorrhoeae* genome by homologous recombination in a non-coding chromosomal region, between the two converging genes NGO0077 and NGO0078, encoding esterase and DNA polymerase respectively in FA1090. A variant of GFP, called super-folder GFP (sfGFP)[123], whose sequence was codon-optimised for expression in *N. gonorrhoeae* (**Supplementary data 1**), was obtained by gene synthesis and cloned into pGONO. Two key elements are required for *N. gonorrhoeae* to uptake DNA: one is the presence of DNA uptake sequences (DUS)[125] and the second is the linearization of the DNA fragment[126]. In this case, DUS regions were incorporated into the primers used in PCR (**Supplementary Table 2**) and the resulting amplification product was used to transform FA1090. Colonies selected on chloramphenicol were screened by PCR as shown in **Fig. 8b**. The first couple of primers (**Fig. 9a**) was used to amplify the region flanking NGO0077 and the end of the chloramphenicol resistance gene. The second couple of primers (**Fig. 9b**) was used to amplify the beginning of chloramphenicol resistance gene and the region flanking NGO0078. All colonies proved to have the sfGFP-containing fragment correctly inserted, and FA1090::sfGFP colony 1 was chosen for further characterization.

a)

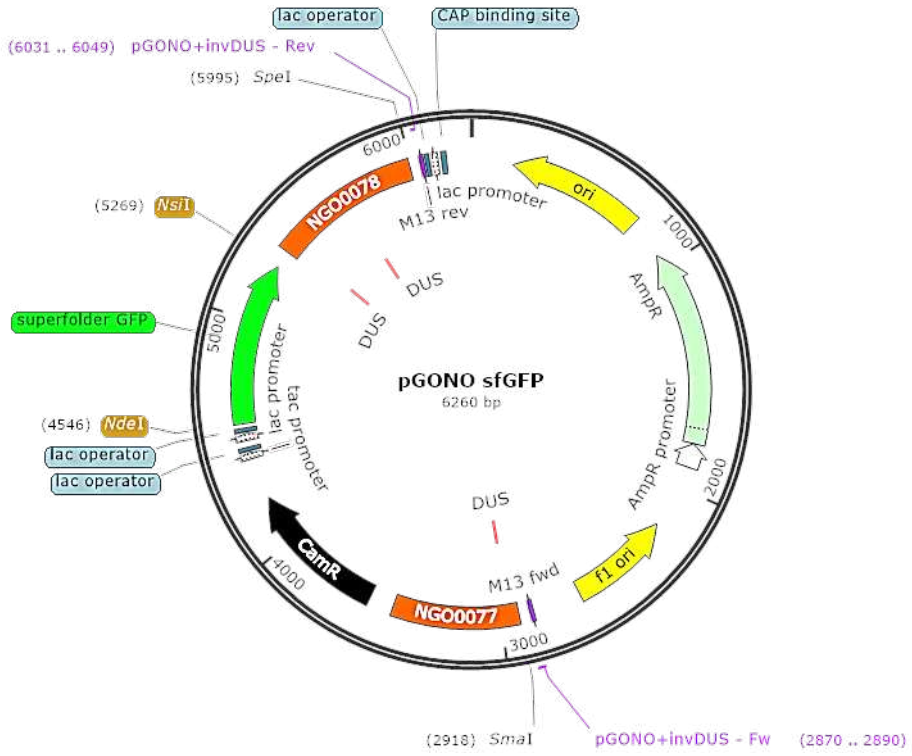

b)

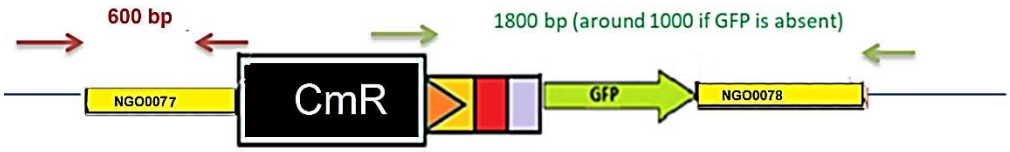

Figure 8. Map of pGONO-sfGFP. *a) sfGFP was cloned into the NsiI and NdeI restriction sites (in gold). The gene is placed under control of the Ptac promoter. CamR (chloramphenicol resistance gene) is depicted in black, AmpR (ampicillin resistance gene) in light blue, DUS (DNA-uptake sequence) in red. NGO0077 and NGO0078 (orange) are the homology regions which allow integration into the N. gonorrhoeae chromosome. b) PCR screening approach to determine the correct insertion of the construct into the genome. In red, amplification from FA1090 genome flanking NGO0077 until the beginning of CamR encoding gene. In green, amplification from the end of CamR until the FA1090 genome outside the recombination site NGO0078.*

a)

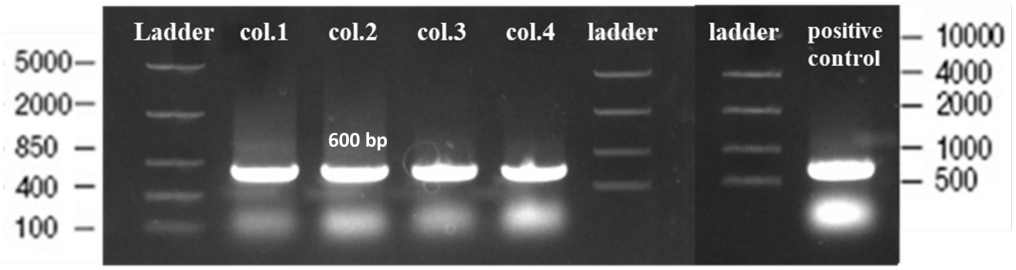

b)

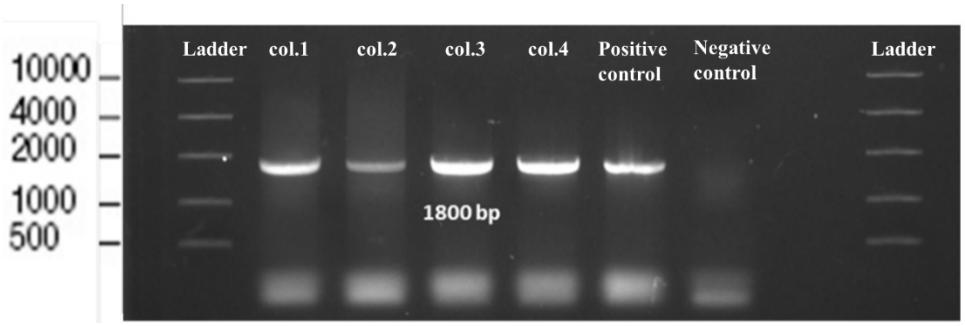

Figure 9. Results of colony PCR on FA1090::sfGFP transformants. *a) Amplification of 600 bp fragment from FA1090::sfGFP colony 1, 2, 3, 4. WHOF::dGFP was used as a positive control. b) Amplification of 1800 bp fragment from FA1090::sfGFP colony 1, 2, 3, 4. WHOF::dGFP was used as a positive control, FA1090 genome as a negative control.*

Expression of sfGFP does not compromise fitness of FA1090

To evaluate the impact of sfGFP expression on the fitness of FA1090, the growth rate of the wild type and of the recombinant strains were compared. As shown in **Fig. 10a**, the two strains grew similarly, and no significant difference was observed. CFU counts were also obtained at minutes 60, 120 and 180. **Fig. 10b** demonstrates that the number of CFU did not vary greatly between the two strains thus confirming that sfGFP expression in FA1090::sfGFP did not affect bacterial growth negatively.

In addition, as the sfGFP-expressing strain had to be used in SBA assays, susceptibility to complement-mediated killing in the presence of the control mAb 2C7[76] was measured. FA1090 and FA1090::sfGFP were incubated with different concentrations of 2C7 in the presence of 10% baby rabbit complement (BRC) (**Fig. 11**). 2C7 was equally effective against the two strains and no increased sensitivity to complement was noted for FA1090::sfGFP.

a)

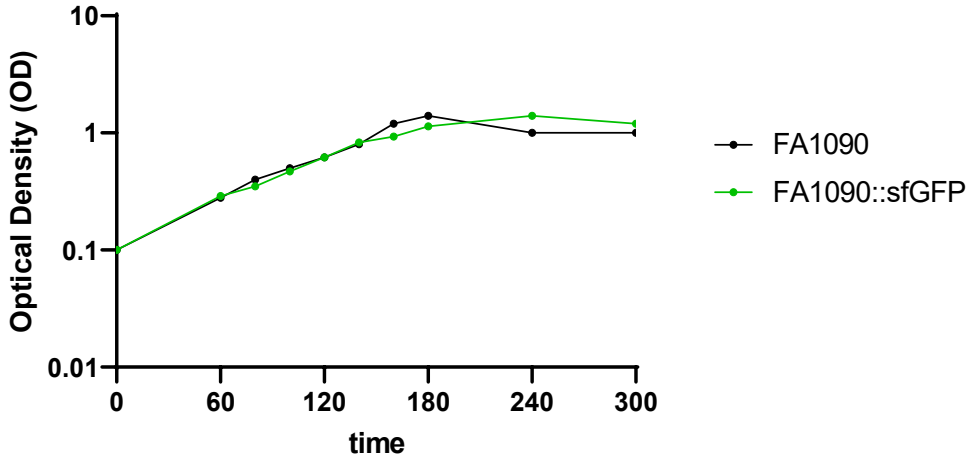

b)

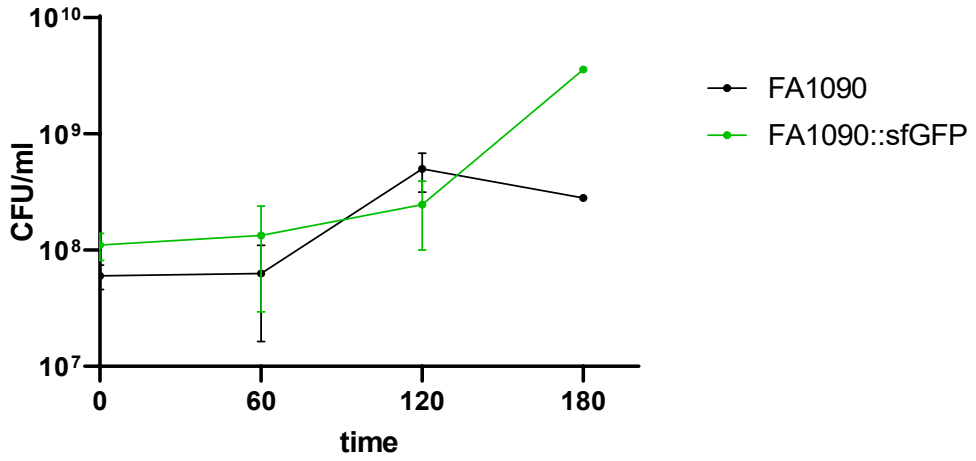

Figure 10. Comparison of FA1090 and FA1090::sfGFP fitness. *a) Growth curves of FA1090 and FA1090::sfGFP. The Y axis indicates the optical density at 600 nm (OD_{600}) and the X axis shows the time (minutes). b) CFU counts of FA1090 and FA1090::sfGFP during growth. Y axis indicates the CFU/ml and the X axis shows the time (minutes).*

c)

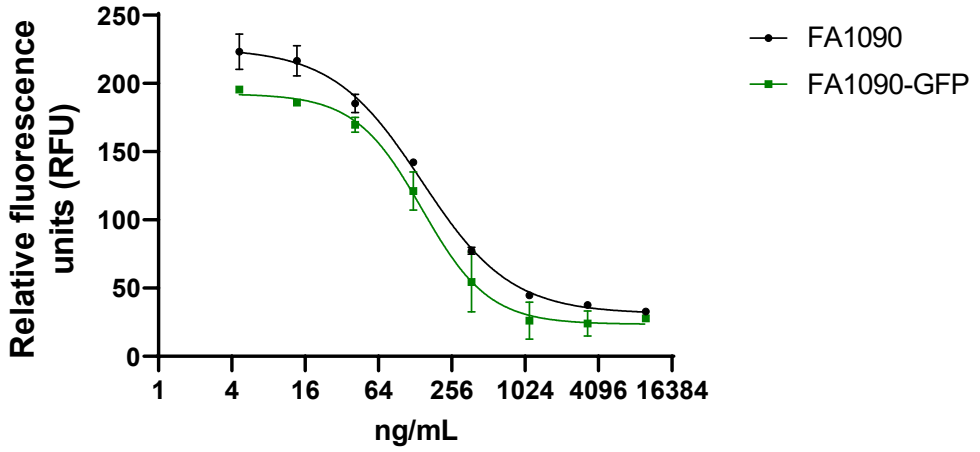

Figure 11. Comparison of FA1090 and FA1090::sfGFP in resazurin-based serum bactericidal assay. *Fluorescence of the resazurin metabolite resorufin was measured upon incubation of FA1090 and FA1090::sfGFP with different concentrations of 2C7 mAb in the presence of 10% BRC. Y axis depicts the relative fluorescence units (RFU), and the X axis depicts the different concentrations of mAb 2C7.*

Quantification of FA1090::sfGFP fluorescence in bactericidal assays and single-cell analysis using confocal microscopy

Given the ultimate objective of using FA1090::sfGFP in visual infection assays with mAbs and cells, it was crucial to determine whether fluorescence intensity of sfGFP could be measured by confocal microscopy and would be affected by treatment with complement. To this end, different percentages of baby rabbit complement (BRC) were tested and CFU were counted (**Fig. 12a**). Addition of 20% and 40% (v/v) active BRC caused bacterial death, as compared to heat-inactivated BRC, while 10% BRC determined 50% reduction in viable counts. The same experiment was carried out onto imaging plates, and the number of adherent bacteria and mean fluorescence intensity (MFI) of GFP were computed using confocal microscope Opera Phenix (**Fig. 12b, Supplementary Table 3**). Both the number of adherent bacteria and the MFI decreased upon addition of increasing amounts of BRC.

a)

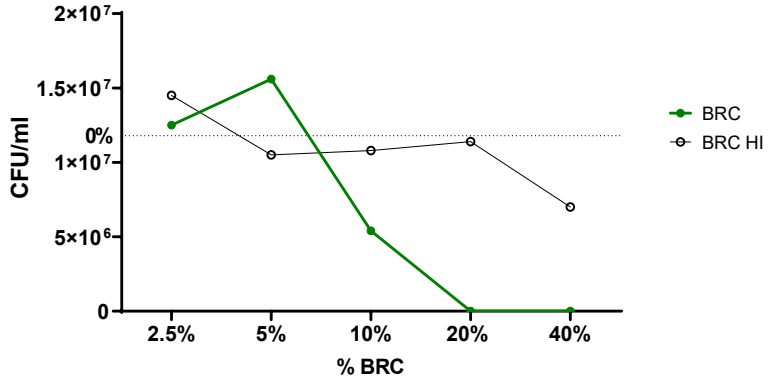

b)

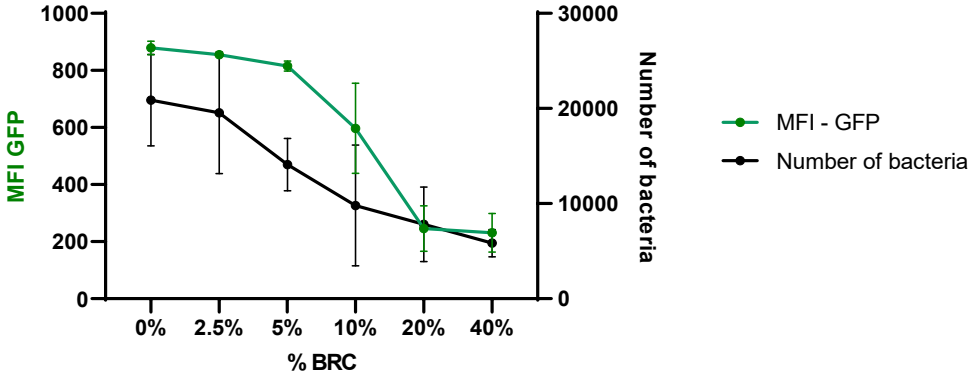

Figure 12. Sensitivity of FA1090::sfGFP to baby rabbit complement. *a) CFU counts upon incubation of FA1090::sfGFP with different amounts of BRC, indicated on the X axis. b) Mean Fluorescence Intensity (MFI) measured by confocal microscopy in the presence of increasing percentages of BRC. The right Y axis plots the number of bacteria counted by microscopy whereas the left Y axis plots the mean fluorescence intensity of sfGFP.*

In addition to measuring the MFI, which quantifies the fluorescence intensity of sfGFP in each well of the plate, Opera Phenix can detect bacteria at the single-cell level and quantify sfGFP intensity for each bacterium. The fluorescence intensity of each bacterial cell was calculated in the absence of BRC and on addition of 40% BRC, and the frequency distribution plotted (**Fig. 13**). While the 0% BRC population showed a normal distribution centered approximately at 900 MFI, the 40% BRC population was

shifted towards the lowest GFP intensity classes. Overall, these data indicated that the sfGFP signal could be used to monitor bacterial viability in microscopy-based assays.

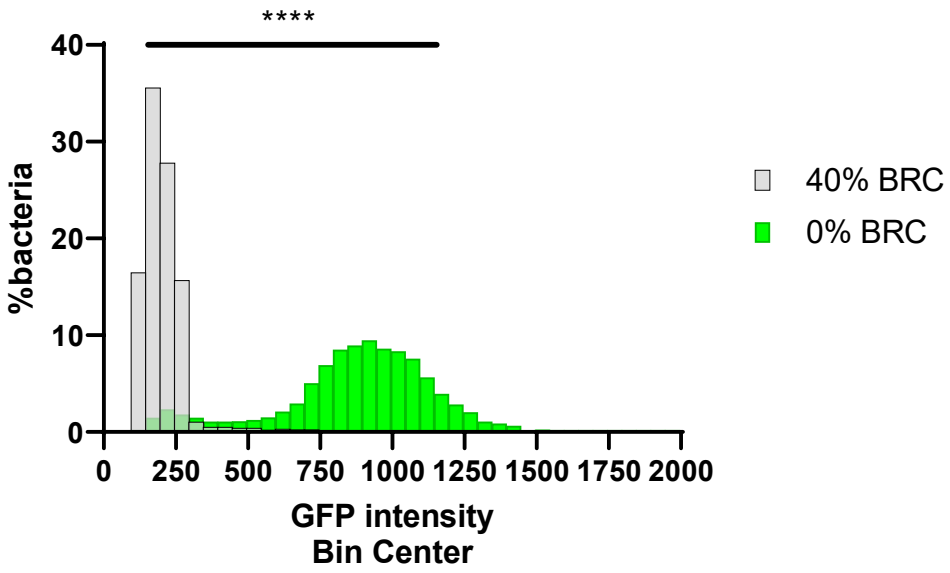

Figure 13. Frequency distribution of FA1090:sfGFP population in the absence of BRC and upon addition of 40% BRC. *The percentage of bacteria which fall into a specific range of GFP intensity is on the Y axis, while GFP signal is on the X axis. ****, $p < 0.0001$.*

The 0% BRC population was thus used to determine the different GFP intensity classes. First, the 25% and 75% percentile and median were quantified (**Table 5**). Results showed that the population ranged from a minimum of 126, and reached a maximum of 2147, while the median was 907. Based on the results in **Table 5**, in the absence of baby rabbit complement (0% BRC), it was possible to divide the frequency of distribution of GFP in four different groups (**Table 6**). Below the minimum (126), GFP intensity was very low and thus bacteria were considered as dead. Between 126 and the 25% percentile (756), GFP intensity was low, and bacteria were supposed to have compromised fitness. Bacteria included in the 25% and 75% (1050) percentile were considered as "normal population" and included most of the viable bacteria, with moderate GFP intensity. From the 75% percentile until the maximum value (2147), the GFP value was very high, and the population was considered viable.

Table 5. *Descriptive statistics of FA1090::sfGFP in the presence of 0% BRC.*

	0% BRC
Number of values	6456
Minimum	126.0
25% Percentile	756.3
Median	907.0
75% Percentile	1050
Maximum	2147

Table 6. *Identification of four different classes of bacteria based on GFP intensity values.*

GFP MFI values Range	**Group**	**GFP intensity**	**Biological significance assigned**
0-minimum	1	very low intensity of sfGFP	Dead bacteria
Minimum-25% percentile	2	low intensity of sfGFP	Low fitness
25% percentile-75% percentile	3	average intensity	Most representative viable bacteria
75% percentile-maximum	4	high intensity of sfGFP	Viable bacteria

The four groups were then plotted for all the tested BRC conditions (**Fig. 14**). At 40% and 20% BRC, group 1 was the most represented in the population, confirming the dead bacteria observed in **Fig. 12a**. At 10%, half of the population was represented by group 1 and the remaining half by group 3 (viable bacteria). At 5% and 2.5%, the most represented groups were group 3 and group 4, confirming that most of the bacteria in those populations were alive. In all conditions group 2 was equally present, which may represent a small subset of non-fit bacteria always present in the population. Overall, results were in line with data shown in **Fig 12a** and confirmed that sfGFP fluorescence can be used to determine the viability of bacteria.

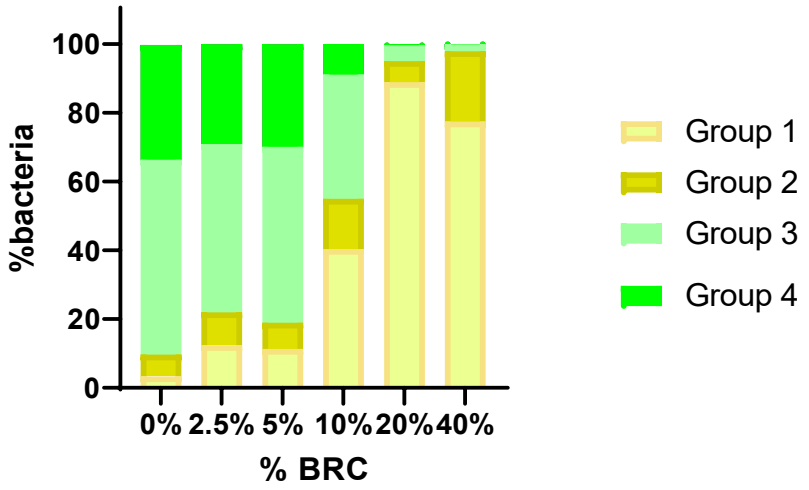

Figure 14. The four classes of sfGFP intensity are plotted for each concentration of BRC. *Group 1 (very low intensity of sfGFP), group 2 (low intensity of sfGFP), group 3 (average intensity), group 4 (high intensity of sfGFP) are differentially represented upon addition of different doses of BRC.*

Discussion

In this chapter I have reported the generation of a *N. gonorrhoeae* strain FA1090 which expresses constitutively the fluorescent protein GFP. This was obtained by transformation of naturally competent bacteria with an integrative plasmid containing the gene encoding for GFP. By homologous recombination, the gene was inserted into a non-coding region in the genome of FA1090. The correct recombination in the specific site of the genome was confirmed by colony PCR. Rather than using conventional eGFP, I used a version which carries mutations that enhance the folding of the protein, called superfolder GFP. The transformed strain is thereby called FA1090::sfGFP. Constitutively expressed fluorescent proteins have been used to track the growth of bacteria, by correlating bacterial density with the fluorescent signal[127]. Alternative approaches can be used to detect bacteria, such as fluorescent dyes[128] or immunostaining using pathogen specific antibodies. For instance, DAPI can label bacterial DNA. However, in infection settings where cells are also present, DAPI would indiscriminately stain cell nuclei as well, thus making bacterial detection difficult. By relying on the production of GFP by the bacterium, there is no need of using various staining or immunostaining approaches, thereby simplifying the logistics of the experiment, and allowing bacterial tracking in real time.

The ultimate aim of this work is to use FA1090::sfGFP in cell-based assays, which would allow easy detection of bacteria by means of the GFP signal. Interactions between bacteria and their cellular hosts have been studied with fluorescence-based techniques such as fluorescence microscopy and flow cytometry[129]. For this work, I have used the confocal microscope Opera Phenix. As FA1090::sfGFP is meant to be used in infection assays, I first checked that the protein would not compromise bacterial fitness. In this sense, both the growth curve and the susceptibility to serum bactericidal activity of antibody 2C7 were found to be the same as for the wild-type. Since fluorescence depends on active expression of the fluorescent protein by bacteria, I assumed that when dead, bacteria would stop expressing the protein and thus would stop being fluorescent. Therefore, I incubated bacteria with different amounts of baby rabbit complement and measured the mean fluorescence intensity for each condition. Increasing doses of BRC caused a drop in the mean fluorescent intensity, suggesting that the GFP signal could be a good proxy of bacterial viability. I also performed single-cell analysis of the live bacterial population by measuring the fluorescence emitted by each bacterium and categorized bacteria into different classes. Bacteria in favorable conditions were represented by a class with average intensity. However, at the deadliest dose of BRC, the class with the lowest intensity was mostly predominant. This is crucial especially in infection conditions, where bacteria infecting cells might reside intra-cellularly and might substantially differ from the extracellular population, and single-cell analysis, unlike batch measurements, would allow to distinguish the two populations residing in the same well.

Experimental procedures

Bacterial strains and culture conditions

N. gonorrhoeae strain FA1090 was used in this study and was cultured on gonococcal medium base liquid or agar (Difco™ GC Medium Base) plus Isovitalex (BD 211876). The strain was typically grown at 37°C and 5% CO_2 for approximately 15 hours. Transformants were selected on plates containing 2 µg/ml chloramphenicol. Chloramphenicol was used at 0.16 µg/ml in liquid media.

Cloning of sfGFP in pGONO

pGONO was a gift from GSK Research Center, Siena, Italy[124]. It was digested with NdeI and NsiI (New England BioLabs) for 2 hours at 37°C and digestion was

confirmed on 0.6 % agarose gel with FastRuler DNA Ladders (ThermoFisher Scientific). DNA was then precipitated with sodium acetate and ethanol.
The superfolder GFP sequence was codon-optimised for *N. gonorrhoeae* and was ordered as a synthetic gene on GeneArt (ThermoFisher). The gene was amplified with Phusion High-Fidelity DNA Polymerase (4 µl 5X Phusion HF, 0.4 µl dNTPs (10 µM), 1 µl SuperGFP-pGONO-F primer, 1 µl SuperGFP-pGONO-R primer, 3 µl template (10 ng/µl), 2 µl DMSO, 0.2 µL polymerase (2 U/µL),). PCR reaction was performed as follows: denaturation at 98°C/30 sec, 30 cycles composed of denaturation at 98°C/10 sec, annealing at 64°C/30 sec, extension at 72°C/30 sec and a final extension at 72°C/5 min.

The resulting amplified fragment was cloned in Zero Blunt TOPO vector (ThermoFisher) and transformed in chemically competent TOP10 *Escherichia coli* (ThermoFisher) cells according to the manufacturer's instructions. pTOPO-sfGFP was then digested with NdeI and NsiI for 2 hours at 37°C. Digestion was confirmed on 0.6 % agarose gel with FastRuler DNA Ladders (ThermoFisher Scientific). The resulting fragment was then extracted from gel using QIAquick Gel Extraction Kit (QIAGEN) and quantified. sfGFP was then ligated with pGONO using T4 DNA Ligase. The mixture (1µl pGONO (61 ng/µl), 7 µl sfGFP (20 ng/µl), 1 µl 10x DNA ligase buffer, 1 µl enzyme) was incubated overnight at 16°C. The ligation mixture was transformed in TOP10 *Escherichia coli* (ThermoFisher) cells. Colonies were screened by colony PCR using primers SuperGFP-pGONO-F and SuperGFP-pGONO-R. Positive clones were grown overnight in LB medium supplemented with ampicillin, plasmid DNA was extracted with QIAprep Spin Miniprep Kit (Qiagen) and sent to Eurofins for Sanger sequencing.

Preparation of pGONO-sfGFP for transformation

The DNA fragment to be used for transformation (which includes sfGFP, the chloramphenicol resistance gene and the two flanking integration sites) was either extracted from the plasmid by double restriction enzyme digestion or amplified by PCR using Kapa LongRange PCR polymerase (KAPA Biosystems). The plasmid was digested with restriction enzymes SmaI and SpeI (New England Biolabs). The PCR reaction took place in a final volume of 25 µl, and the mix contained 1µl plasmid template (112 ng/µl) 5 µl KAPA LongRange Buffer, 1.5 µl $MgCl_2$ (25 mM), 0.5 µl dNTPs (10 mM), 1 µl pGONO+invDUS – Fw (10 µM), 1 µl pGONO+invDUS – Rev (10 µM), 0.125 µl KAPA LongRange DNA Polymerase enzyme (5 U/µL). PCR reaction was performed as follows: denaturation at 95°C/3 min, 5 cycles composed of

denaturation at 95°C/30 sec, annealing at 50.3°C/30 sec, extension at 72°C/ 3 min and 30 cycles composed of denaturation at 95°C/30 sec, annealing at 71.9 °C/30 sec, extension at 72°C/3 min and a final extension at 72°C/3 min. Digestion and amplification were confirmed on 0.6 % agarose gel with FastRuler DNA Ladders (ThermoFisher Scientific). Products were then precipitated with sodium acetate and ethanol.

Transformation of FA1090

30 µl of linearised plasmid (20 ng/µl) or 10 µl of PCR product (90 ng/µl) was resuspended in TrisHCl (10 mM) and then mixed with FA1090 resuspended in PBS. As a negative control, FA1090 was mixed with PBS only. The mixture was spotted onto a GC agar plate + 1% isovitalex and left for 6h at 37°C, 5% CO_2. The spot was then streaked onto a GC agar plate + 1% isovitalex with 2 µg/ml chloramphenicol. After 24/48 hours colonies were re-streaked onto a GC agar plate + 1% isovitalex with 2 µg/ml chloramphenicol to prepare glycerol stocks and genomic DNA.

PCR from genomic DNA

Colonies grown on GC agar plates + 1% isovitalex were resuspended in 50 µl of PBS, incubated at 99°C for 10 minutes and centrifuged for 5 min. The supernatant containing genomic DNA was collected. Amplification of the target DNA fragment from FA1090::sfGFP genomic DNA was carried out by PCR using Kapa LongRange PCR polymerase (KAPA Biosystems). In a final volume of 25 µl, the PCR reaction mix contained 3 µl genomic DNA template, 5 µl KAPA LongRange Buffer, 1.5 µl $MgCl_2$ (25 mM), 0.5 µl dNTPs (10 mM), 1 µl ChlorampGONO-Ext-R (10 µM), 1 µl UP-FA1090-pGONO-F (10 µM), 0.125 µl KAPA LongRange DNA Polymerase enzyme (5 U/µL). PCR reaction was performed as follows: denaturation at 95°C/3 min, 30 cycles composed of denaturation at 95°C/30 sec, annealing at 59°C/30 sec, extension at 72°C/1 min and a final extension at 72°C/1 min. To amplify longer DNA fragment (1,800 bp) PCR was carried out with Phusion High-Fidelity DNA Polymerase (New England Biolabs) in a final volume of 20 µl. The mixture contained 3 µl genomic DNA template, 4 µl 5X Phusion HF, 0.4 µl dNTPs (10 Mm), 1 µl ChlorampGONO-Ext-F (10 µM), 1 µl UP-FA1090-pGONO-F (10 µM), 0.6 µl DMSO, 0.2 µl Phusion DNA polymerase. The PCR reaction was performed as follows: denaturation at 98°C/30 sec, 35 cycles composed of denaturation at 98°C/10 sec, annealing at 59°C/30 sec, extension at 72°C/1 min and 30 sec and a final extension at 72°C/5 min. Amplification

was confirmed on 1 % agarose gel with FastRuler DNA Ladders (ThermoFisher Scientific).

Growth curves and Colony Forming Units (CFU) counts

FA1090 and FA1090::sfGFP were grown in GC medium + 1% Isovitalex and GC medium + 1% Isovitalex + 2 µg/ml chloramphenicol respectively starting from Optical Density at 600 nm (OD_{600}) 0.1 at 37°C 5% CO_2. At 60, 120, 180, 240 and 300 minutes since the start of the culture the OD was measured. At minute 60, 120, 180, CFU counts were obtained after serial dilutions of the bacterial culture in PBS and plating on GC agar plates + 1% Isovitalex. After 24 hours, the colonies were counted.

Resazurin-based serum bactericidal assay (SBA)

FA1090::sfGFP was grown to mid-log phase and resuspended in Dulbecco's modification of PBS (PBSB). Reactions were performed by incubating bacteria in PBSB, 2% FBS and 0.1% glucose and in the presence of 10% v/v of Baby Rabbit Complement (BRC) (Cedarlane) and different concentrations of mAb 2C7 (5, 14, 41, 123, 370, 1110, 3330, 10000 ng/mL). The titre of the bacterial suspension was 1.8*10^7 CFU/ml. The reactions were incubated for 2 h at 37°C, 5% CO_2. 10 µl of resazurin was then added (0.025% w/v) and the reactions were incubated at 37°C, 5% CO_2 for 2 hours. The fluorescence signal was read using a Varioskan™ LUX multimode microplate reader at 560/590 nm excitation/emission wavelength (Thermo Fisher Scientific, Waltham, MA, USA).

Superfolder GFP fluorescence intensity to measure sensitivity to complement

FA1090::sfGFP was grown to mid-log phase and resuspended in Dulbecco's modification of PBS (PBSB) at final concentration of 1.8*10^7 CFU/ml. 50 µl of bacteria were plated onto ViewPlate-96 Black, Optically Clear Bottom, Tissue Culture Treated plates (Perkin Elmer) and left to adhere for 30 mins at 37°C, 5% CO_2. Different concentrations of BRC (40, 20, 10, 5, 2.5 % v/v) were prepared in PBSB, 2% FBS and 0.1% glucose and added to the bacteria. After 1h of incubation at 37°C, 5% CO_2, samples were fixed with 2% paraformaldehyde (PFA) and stained with DAPI.

96-well plates were imaged with the microscope Opera Phenix High-Content Screening System (PerkinElmer) using a 63x objective, numerical aperture 1.15, acquiring 23 fields of view per well, and 3 images on the vertical dimension to form a z-stack per each field of view. The image analysis pipeline was developed using Harmony Software of Perkin Elmer (Supplementary Table 2). Bacteria were detected by

analyzing the signal of DAPI (nucleoids), which allowed counting and identification of the population designated as “spots”, where each spot indicates the whole bacterial cell. For each spot, the maximum intensity of GFP was quantified and used for successive analysis.

Colony forming units (CFUs) bactericidal assay

FA1090::sfGFP was grown to mid-log phase and resuspended in Dulbecco’s modification of PBS (PBSB). Reactions were performed by incubating bacteria in PBSB, 2% FBS and 0.1% glucose and in the presence of different concentrations of BRC (40, 20, 10, 5, 2.5 % v/v). The titre of the bacterial suspension was 1.8* 10^7 CFU/ml. The reactions were incubated for 1 h at 37°C, 5% CO_2. CFU counts were obtained after serial dilutions of the bacteria in PBS and plating on GC agar plates + 1% Isovitalex. After 24 hours, the colonies were counted.

Data analysis

Statistical analysis, including descriptive statistics and unpaired nonparametric t-test (Mann-Whitney test), was performed with GraphPad Prism 8.

Supplementary material

Supplementary data 1. *Sequence of superfolderGFP (sfGFP) codon-optimised for expression in N. gonorrhoeae*.

ATGAGCAAAGGCGAAGAATTGTTCACCGGCGTCGTCCCGATCTTGGTCGA
ATTGGACGGCGACGTCAACGGCCACAAATTCAGCGTCCGCGGCGAAGGC
GAAGGCGACGCCACCAACGGCAAATTGACCTTGAAATTCATCTGCACCAC
CGGCAAATTGCCGGTCCCGTGGCCGACCTTGGTCACCACCTTGACCTACG
GCGTCCAATGCTTCAGCCGCTACCCGGACCACATGAAACGCCACGACTTC
TTCAAAAGCGCCATGCCGGAAGGCTACGTCCAAGAACGCACCATCAGCTT
CAAAGACGACGGCACCTACAAAACCCGCGCCGAAGTCAAATTCGAAGGC
GACACCTTGGTCAACCGCATCGAATTGAAAGGCATCGACTTCAAAGAAGA
CGGCAACATCTTGGGCCACAAATTGGAATACAACTTCAACAGCCACAACG
TCTACATCACCGCCGACAAACAAAAAAACGGCATCAAAGCCAACTTCAA
AATCCGCCACAACGTCGAAGACGGCAGCGTCCAATTGGCCGACCACTACC
AACAAAACACCCCGATCGGCGACGGCCCGGTCTTGTTGCCGGACAACCAC
TACTTGAGCACCCAAAGCGTCTTGAGCAAAGACCCGAACGAAAAACGCG
ACCACATGGTCTTGTTGGAATTCGTCACCGCCGCCGGCATCACCCACGGC
ATGGACGAATTGTACAAATAA

Supplementary Table 1. *List of plasmids used in this work.*

Name	Type	Features	Resistance	Source
pGONO	Integrative vector in *N. gonorrhoeae*	• Size: 5,500 bp • Cloning site (NdeI, NsiI) places the cloned gene under control of the promoter $P_{TAC.}$ • Integration site: non-coding chromosomal region, between the two converging genes NGO0077 and NGO0078, encoding esterase and DNA polymerase in FA1090	Cam^R (chloramphenicol resistance gene)	[124]

Supplementary Table 2. *List of primers used in this work.*

Name	Sequence (5'-3')	Features
SuperGFP-pGONO-F	ACAGGAAACACATATGAGCAAAGG	NdeI restriction site
SuperGFP-pGONO-R	AACGGGAGCGAATGCATTTATTTG	NsiI restriction site
UP-FA1090-pGONO-F	CCGCTGTTTCAGACGGCATTGGCT CGTATC	
DW-FA1090-pGONO-R	GCCGACCAAGTGCTGATTATCGA ATCCAAAGTCAG	
pGONO+invDUS – F	TATGCCGTCTGAAAGCCTTTCAGA CGGCATCAGTGAATTCGAATGGCC ATG	Inverted DUS sequence
pGONO+invDUS – R	AATGCCGTCTGAAAGGCTTTCAG ACGGCATAGCTATGACCATGATT ACG	Inverted DUS sequence
ChlorampGONO-Int-F	GAGTATTTCGACCACTATTTTGGCA ATACGC	
ChlorampGONO-Int-R	TCAGCAAGTCTTGTAATTCATCC	
ChlorampGONO-Ext-R	GCGTATTGCCAAAATAGTGGTC	
ChlorampGONO-Ext-F	TTGGATGAATTACAAGACTTGCTG	

Supplementary Table 3. *Image analysis pipeline for single-cell evaluation of GFP intensity built using software Harmony (Perkin Elmer).*

Building Block	**Input**	**Method**	**Output**
Calculate Image		Method:by formula Formula: A-300 A: DAPI Negative values: Set to Zero Undefined values: Set to local average	Calculated Image
Find Spots	Channel:Calculate Image ROI: none	Method:C Radius: <= 5,8 px Contrast:>0.17 Uncorrected Spot to Region Intensity> 1.3 Distance >= 1px Spot Peak Radius: 0 px Calculate spot properties: yes	Spots
Calculate Intensity Properties	Channel: eGFP Population:Spots Region:Spot	Method: Standard Mean: yes Maximum:yes Quantile Fraction: 50%	
Select population	Population: Spots	Method: Filter by property Intensity Spot eGFP max: 0>x>126 Spot area [px^2]: >20 Boolean Operations: F1 and F2	Group 1

Select population	Population: Spots	Method: Filter by property Intensity Spot eGFP max: 126>x>756.3 Spot area [px^2]: >20 Boolean Operations: F1 and F2	Group 2
Select population	Population: Spots	Method: Filter by property Intensity Spot eGFP mean: 756.3>x>907 Spot area [px^2]: >20 Boolean Operations: F1 and F2	Group 3
Select population	Population: Spots	Method: Filter by property Intensity Spot eGFP mean: 907>x>1050 Spot area [px^2]: >20 Boolean Operations: F1 and F2	Group 4

Define Results

Method: List of Outputs

Population: Spots

Number of Objects

Population: Group 1

Number of Objects

Population: Group 2

Number of Objects

Population: Group 3

Number of Objects

Population: Group 4

Number of Objects

2. Development of a novel visual opsono-phagocytosis screening assay for monoclonal antibodies against *Neisseria gonorrhoeae*

Note: this Chapter is part of a manuscript in preparation

Introduction

Monoclonal antibodies (mAbs) represent an important class of biological medications for cancer, autoimmune and, more recently, infectious diseases. They have achieved special relevance in response to the recent SARS-CoV-2 pandemic[130,131] and could be game-changers in tackling antibiotic-resistant bacterial infections[31]. Despite the difficulties in targeting bacterial pathogens, several mAb candidates are progressing through clinical development and more are being discovered, especially against Gram-negative antimicrobial resistant (AMR) species[132]. mAbs exert different modes of action when facing bacterial infections: they can trigger the complement cascade, thereby causing formation of the membrane attack complex (MAC) which induces cell lysis and death, they can induce agglutination of pathogens or of toxins or, in the presence of specialised immune cells like macrophages or neutrophils, they can enhance their intrinsic opsono-phagocytic activity[11]. In addition to promoting phagocytosis, antibodies can also restrict the survival of engulfed bacterial pathogens which may have developed mechanisms of phagosomal escape[133]. Opsono-phagocytosis consists in the engulfment of pathogens labelled with antibodies by phagocytic cells and represents an essential immune defence process against microbial infections[134]. Often considered as a major predictor of antibody protective efficacy[135], opsono-phagocytosis-promoting activity is an important feature for a mAb candidate for therapeutic use. In addition, understanding how antibodies elicited by a vaccine contribute to the opsono-phagocytic killing of the pathogen of interest could provide useful insights on correlates of protection[61].

While discovery and production of mAbs on the large scale is nowadays possible thanks to the progress in sorting and cloning technologies[136], evaluating their antibacterial activity in high-throughput platforms is still challenging. Standard assays, based on colony forming units (CFU) counting, to study phagocytosis of bacteria are available in the literature[137]. However, these methods are time-consuming and not compatible with a high-throughput screening (HTS) setting, when many compounds must be tested. HTS assays for assessing the opsono-phagocytosis promoting activity of mAbs rely mostly on the use of microplate readers[76,138] or flow cytometers[139,140]

which have been gradually replacing traditional CFU counts[141]. For instance, a fluorescence activated cell sorter (FACS)-based protocol to assess phagocytosis of *Staphylococcus aureus*, which measures the phagocytic ability of macrophages by detecting the internalisation of fluorescently labelled bacteria, has been reported[142]. Here we introduce an innovative methodology which relies on confocal fluorescence microscopy and combines single cell, high-throughput, and high-content screening in a dedicated image analysis pipeline. The new protocol was named visual opsono-phagocytosis assay (vOPA) (**Fig. 15a**). By exploiting fluorescent reporters, we achieved targeted labelling of different compartments of THP-1 cells and of the bacterial species used as a proof-of-concept (i.e. *Neisseria gonorrhoeae*), thus allowing single objects to be detected, segmented and incorporated into an image analysis pipeline.

Results

N. gonorrhoeae infecting macrophages can be visualised and quantified by fluorescence confocal microscopy

In the vOPA protocol herein described, THP-1 cells, an immortalised cell line with monocyte-like features, were selected as a cell model. THP-1 is a human leukaemia monocytic cell line that can be differentiated into macrophage-like cells (dTHP-1) and has previously been used to mimic human macrophage infection by *N. gonorrhoeae*[91]. We validated dTHP-1 as an appropriate model for the evaluation of antibody-mediated opsono-phagocytic activity by monitoring the presence of Fc receptors and of surface markers for macrophage differentiation via cytofluorometry. We demonstrated that upon differentiation, THP-1 cells showed increased expression of the macrophage differentiation marker CD11b and most of the cells retained the expression of CD64 (Cluster of differentiation 64) also known as FcγRI (Fc-gamma receptor 1) and CD32 (Cluster of differentiation 32) also known as FcγRII (Fc-gamma receptor 2) (**Supplementary Fig. 1**). While the total population of THP-1 cells expressed the Fc receptors, 60% of dTHP-1 showed positivity for the markers after differentiation.

Of note, both CD64 and CD32 allow cells to interact with IgG antibodies. We differentiated THP-1 cells directly on the imaging plate, where they adhered and were subsequently infected with *N. gonorrhoeae* strain FA1090, engineered to express GFP (FA1090::sfGFP). We used fluorescent staining to identify cell membranes, nuclei and

bacterial nucleoids (**Fig. 15b**) and quantified the phagocytosis process by means of images acquired with the confocal microscope Opera Phenix **(Fig. 15a).**
To determine which bacteria had been engulfed by cells, we performed immunostaining of the pathogens without permeabilizing the cells. Bacteria negative to the immunostaining were considered as internalised, whereas those labelled by the antibody were counted as external. The image analysis pipeline based on the "*Harmony High-Content Imaging and Analysis Sofware"* (Perkin Elmer) segmented and counted all bacteria present in images, then grouped them in three different populations: external, adherent to the cell surface and internal (please see **Supplementary Table 4** for the complete analysis pipeline). dTHP-1 cells were also counted and divided in two populations: infected and not-infected.

We first validated the efficiency and sensitivity of the described system by quantifying the number of bacteria and cells at different multiplicity of infections (MOIs) and times of infection (**Supplementary Fig. 2**) As expected, the total number of bacteria was impacted by the different MOIs, thereby proving that the assay is sensitive to different amounts of bacteria used to initially infect cells. As observed in Fig.3a, for all the tested MOIs, the number of "infecting bacteria" (i.e. the sum of internal and adherent bacteria) did not change significantly from 30 minutes up to 2 hours of infection, whilst it increased after 4 hours. Interestingly, the ratio of adherent/internal bacteria (2:1) was conserved in all conditions. **Supplementary Fig. 2** also shows the quantification of infected and non-infected cells. Different MOIs did not affect the number of segmented cells. However, as time of infection increased, the total number of cells decreased. This reduction was largely due to the non-infected cells decreasing with time while the number of infected cells did not drastically change from 30 minutes to 4 hours of infection. Based on these data, we concluded that it was possible to characterize different infection conditions using fluorescence microscopy and segmentation-based image analysis. The internal bacterial population represents bacteria which have been engulfed by cells, therefore their abundance is naturally dependent on the number of quantified infected cells. As a consequence, both populations (i.e. number of infected cells and number of internal bacteria) were taken into consideration to describe the phagocytosis process. Given the drastic changes in the number of non-infected adherent cells when time was extended beyond one hour, we decided to limit the infection time to 1 hour. In addition to the bacteria's number, generated images can be used to perform single-cell analysis of bacteria (**Supplementary Fig. 3**). Each bacteria cell can be individually analyzed by quantifying the fluorescence emitted by each bacterium. Given that with vOPA we can distinguish intracellular and extracellular bacterial

populations, the GFP intensity for each bacterium belonging to the internal and adherent populations was measured and the frequency distribution plotted (**Supplementary Fig. 3**). The two populations, in addition to a difference in the cell location, showed a difference in the intensity, where the internal bacteria peaked at lower GFP intensity values compared to the adherent ones.

a)

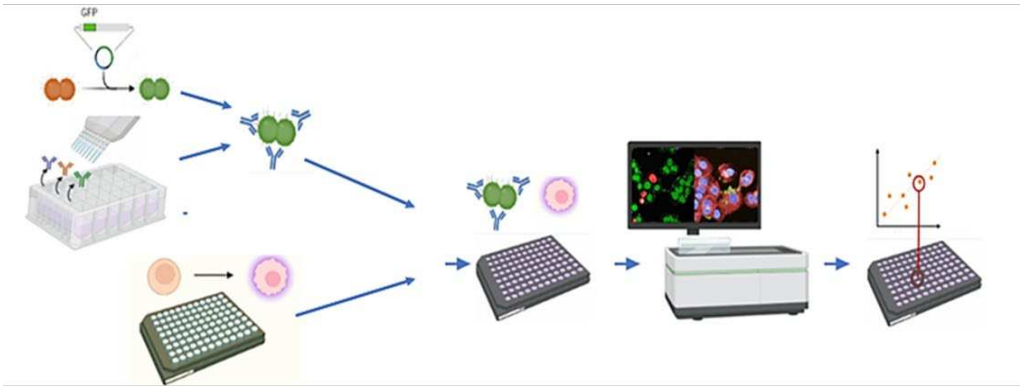

b)

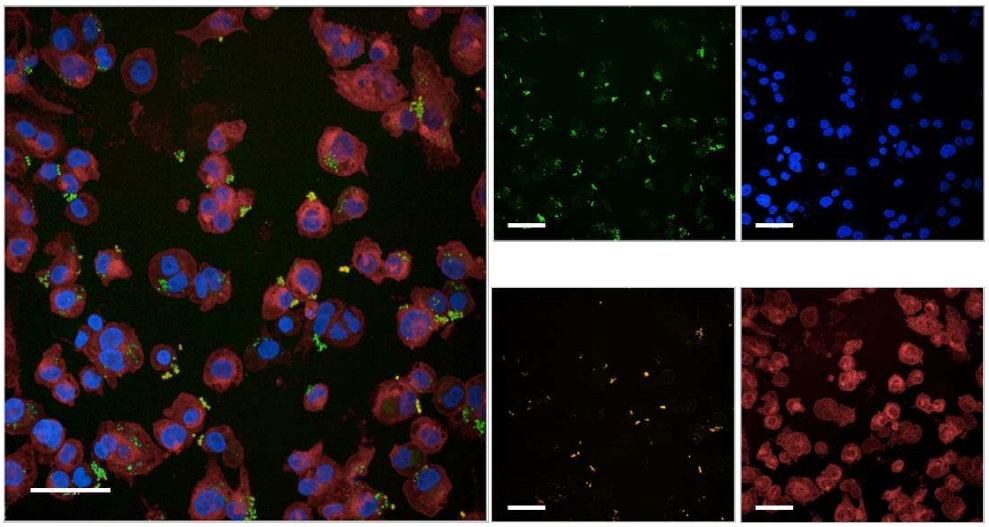

Figure 15. Workflow of vOPA and staining used to differentiate cells and bacteria. *a) Different steps used to perform vOPA. N. gonorrhoeae is engineered to express GFP and THP-1 are differentiated, seeded and imaged directly on the 96-well plate. mAbs are expressed in high-throughput format by Expi293 cells in 96-well plates and incubated with N. gonorrhoeae. The mixture is then transferred into a 96-well plate and used to infect pre-seeded THP-1 cells. After staining and fixation, images are acquired from each well with Opera Phenix and the image analysis process takes place. After performing data analysis, the most prominent candidates are selected. b) Four*

different colours used in vOPA: sfGFP expression by bacteria (green), DAPI (blue) to stain the nuclei and bacterial DNA, immunostaining (orange) to stain the bacteria outside the cells, and CellMask Deep Red (red) to stain cell membranes. Scale bar is 50 μm.

vOPA is a robust assay that can be used to measure the phagocytosis-promoting activity of monoclonal antibodies

We tested a mAb, referred to as 2C7, that is reported in the literature to be directed against the *N. gonorrhoeae* lipooligosaccharide (LOS)[76] and to promote phagocytosis of *N. gonorrhoeae* by neutrophils[76]. We assessed whether it could be used as a positive control in our assay. We compared samples containing 2C7 with two control conditions: one involved dTHP-1 cells and bacteria (no mAb), and a second condition with an unrelated mAb not able to bind to *N. gonorrhoeae*.

To optimise the infection conditions for this experiment, we tested two different MOIs and times of infection and exploited the quantification method described in the previous paragraph to compute the number of internal bacteria per infected cell in each experimental condition (**Fig.16**). **Fig. 16a** shows the input images for this quantification method for samples incubated with 2C7, with an unrelated mAb and for the no mAb condition. The phagocytosis-promoting activity of 2C7 at 10 μg/ml was confirmed (**Fig. 16b**) as it increased the number of internal bacteria per infected cell with respect to the controls. 2C7 was therefore considered as a positive control for the assay. The Z' factor[138] was derived as a measure of assay robustness (**Fig. 16b**), and is generally considered acceptable when is greater than 0.4. By computing the Z' factor, we observed that MOI 20 generated less separability between the conditions at both times of infection (Z'= 0.31 at 30 minutes, Z'= 0.03 at 1h). On the other hand, by using MOI 40 we observed more separability with higher Z' factors in both conditions (Z'= 0.40 at 30 minutes, Z'= 0.31 at 1h). Importantly, the background level of internalised bacteria per infected cell, measured with the no mAb and unrelated mAb controls, was higher at 1 h than at 30 minutes of infection. Therefore, we concluded that MOI 40 and 30 minutes of infection provided the best infection conditions for this assay with the highest Z' factor value (**Fig. 16b**). We named these infection conditions, staining protocol and image analysis pipeline as the visual opsono-phagocytosis assay (vOPA).

We then carried out vOPA with different concentrations of the 2C7 antibody in four experiments, two replicates each, each experiment performed on different days using different batches of dTHP-1. **Fig. 17a** shows representative images in presence of different concentrations of 2C7 , unrelated mAb and no mAb condition, where the

number of internal bacteria in the presence of 2C7 was significantly increased. We reported the normalised results in **Fig. 17b**, where 100% indicates the maximum value of the number of internal bacteria per infected cell for 2C7 at 10 μg/ml concentration, and 0% is the minimum value of the number of internal bacteria per infected cell considering the unrelated mAb condition at all of the concentrations tested. Despite the intrinsic variability associated with different batches of cells, we observed that the overall effect was conserved. Indeed, samples with 2C7 showed a dose-dependent increase in the number of internalised bacteria, while the unrelated mAb did not have any impact.

a)

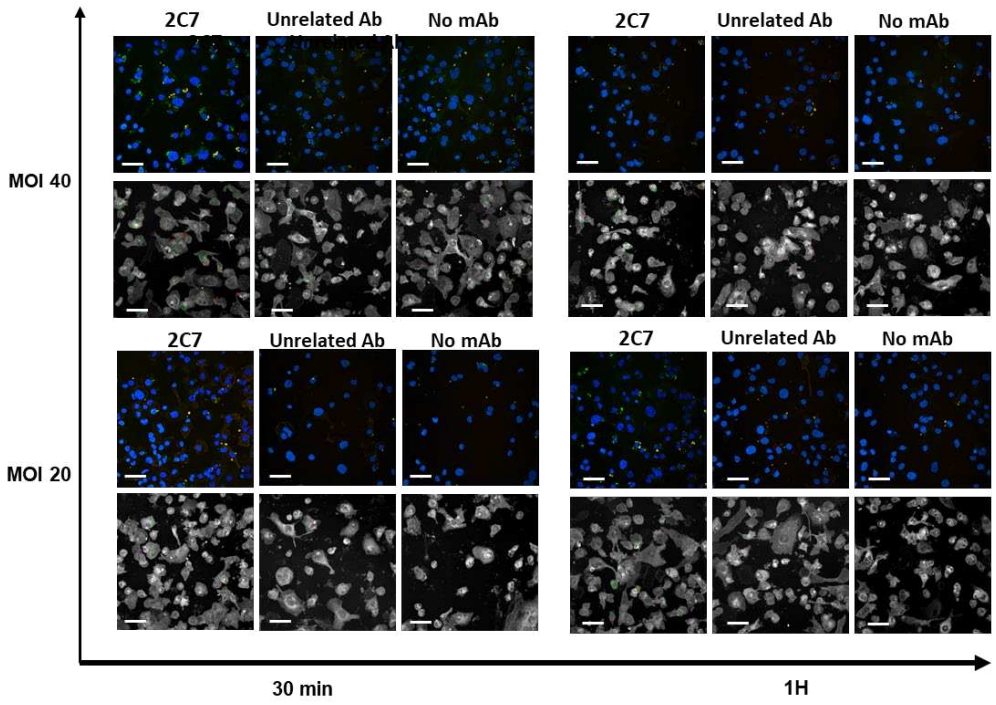

b)

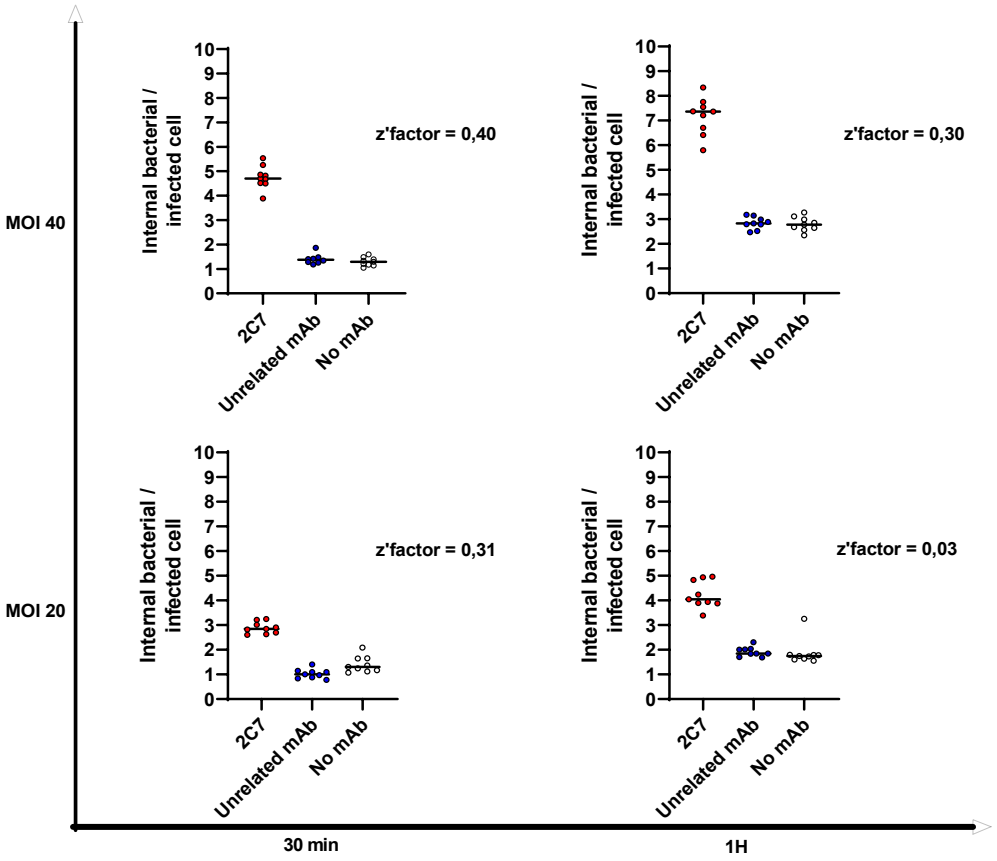

Figure 16. Evaluation of mAbs activity for two different MOIs and times of infections. *Panel a) shows images for each condition (MOI 20, 40 and time 30 min and 1H) and the staining used in the assay (except for CellMask, for better visual inspection) on the first row, and image analysis steps identifying internal bacteria in the second row. Images were taken upon incubation with 2C7 or with an unrelated mAb. The no mAb control is indicated. Scale bar is 50 µm. b) The figure shows the number of internal bacteria per infected cell in two MOIs (MOI 20 and MOI 40) and two times of infection (30 minutes and 1-hour conditions). 9 technical replicates of 2C7, unrelated mAb and no mAb samples were tested. 2C7 and the unrelated monoclonal (both at 10 µg/ml) were pre-incubated with N. gonorrhoeae. The Z' factor reported in the graphs was calculated by comparing the 2C7 and the unrelated mAb conditions.*

a)

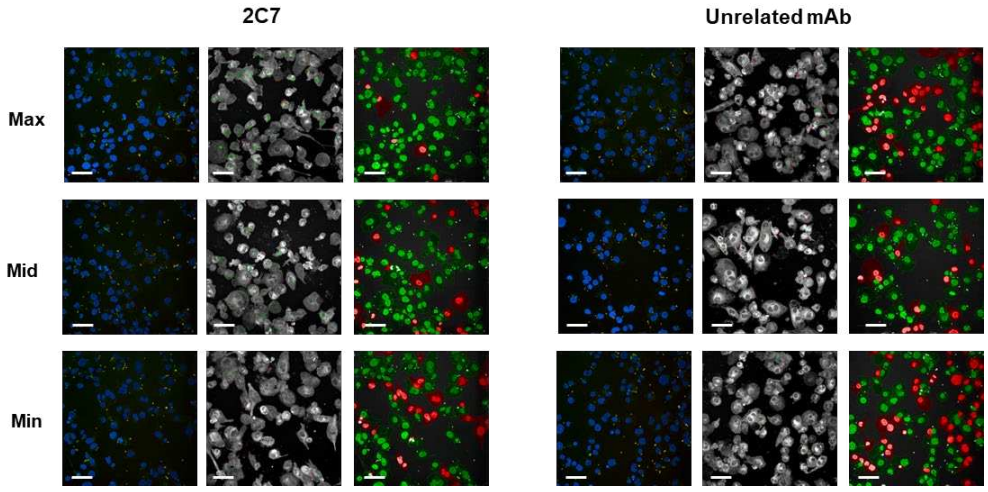

b)

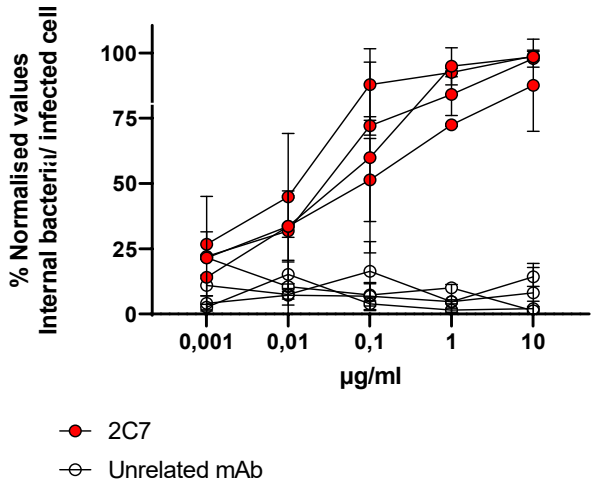

Figure 17. Validation of phagocytic activity promoted by 2C7 with vOPA. *a) Images acquired from samples incubated either with 2C7 (left) or with an unrelated mAb (right) tested at 10 µg/ml (maximum concentration, first row), 0.1 µg/ml (middle concentration, second row) and 0.001 µg/ml (minimum concentration, third row). For each condition, the first column depicts the staining used in the assay (except for CellMask, for better visual inspection). The following two columns show two steps of the whole image analysis pipeline: in the second column there is the image analysis step for the quantification of internal bacteria (green) and external bacteria (red) and*

the third column depicts the image analysis step which differentiates infected cells (green) and non-infected cells (red). Scale bar is 50 µm.

b) Four different experimental replicates of the dose-response activity of 2C7. The number of internal bacteria per infected cell for each condition was normalised using the maximum value measured at the highest concentration of 2C7 and was assigned 100%. The lowest value obtained with the unrelated mAb was considered as 0%. Dose-response curves of four biological replicates, each performed with two technical replicates, are shown. The y axis reports the normalised values of the internalised bacteria per infected cell, the x axis reports the concentrations of the tested antibody (µg/ml).

vOPA assay is validated by classical assay (cOPA)

To validate the new assay, we compared vOPA with a conventional OPA assay based on CFU counting[143] and here named classical OPA (cOPA) (**Fig. 18a**). We assessed the correlation between the two assays by measuring the total number of internalised bacteria per well upon incubation with different amounts of 2C7 or with an unrelated antibody (**Fig. 18b**). Since the classical assay lasts for 1 hour, vOPA was extended from 30 minutes to 1 hour for a more meaningful comparison. As **Fig. 18b** shows, the positive and negative controls displayed similar outcomes in the two types of assays with promotion of opsono-phagocytosis by 2C7 and no effect mediated by the unrelated antibody. Next, we measured the correlation between the two assays by computing the Pearson correlation coefficient for the 2C7 results (**Fig. 18c**). We observed an R squared value of 0.9611 with a p-value of 0.0006. Therefore, vOPA can measure the phagocytosis-promoting activity of mAbs in a consistent manner with respect to conventional CFU counting based procedures.

a)

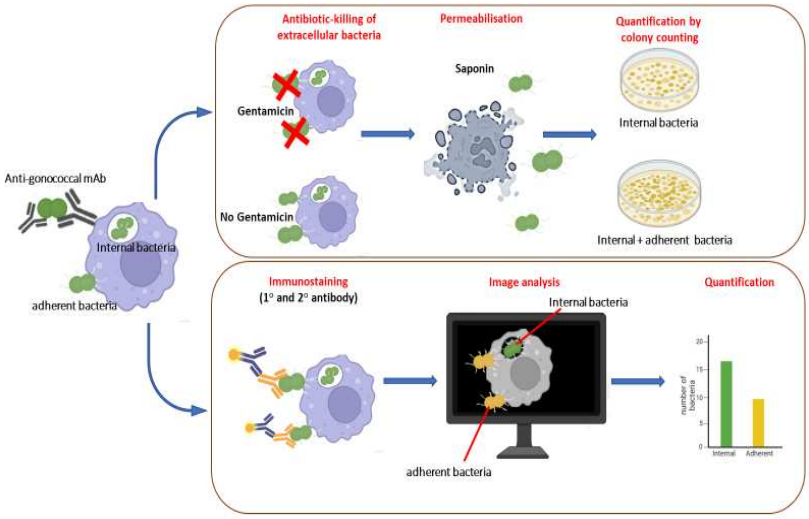

b)

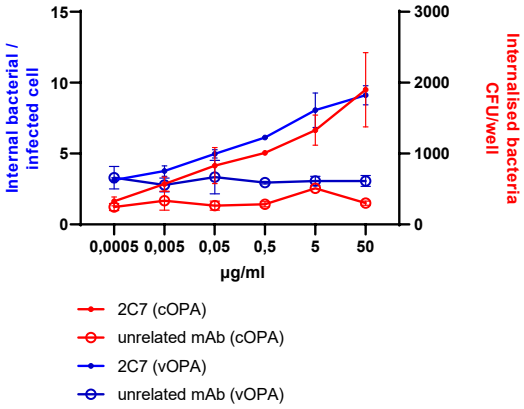

c)

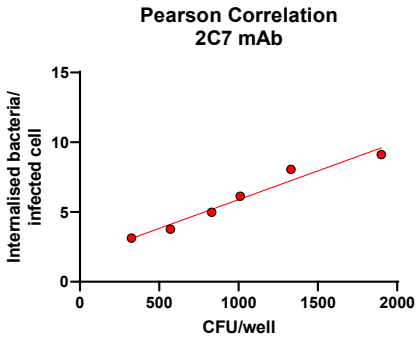

R squared	0.9611

P (two-tailed)	0.0006
P value summary	***

Figure 18. Comparison between cOPA and vOPA. *a) Graphical representation of the cOPA (top) and vOPA (bottom). When FA1090::sfGFP infect THP-1, two different populations appear: internal (engulfed) and adherent bacteria. To distinguish the internal from the adherent bacteria, the cOPA relies on gentamicin, an antibiotic which kills the extracellular bacteria. Cells are then permeabilized with saponin, and the internal bacteria are plated on agar and colonies counted. To obtain the number of adherent bacteria, permeabilization takes place without previous gentamicin treatment. vOPA relies on staining the adherent bacteria with primary and secondary antibody, which cannot cross the cell membrane and stain internal bacteria. After acquisition at the confocal microscope, image analysis can be used to quantify and distinguish the internal bacteria from the adherent ones. b) Comparison of results obtained with cOPA and vOPA using 2C7 and unrelated mAb. cOPA read-out is the number of internalised bacteria (CFU/well, right y axis), and vOPA read-out consists in the number of internal bacteria per infected cell (left y axis). The concentration of the tested antibody is shown on the x axis. c) Pearson correlation between vOPA and cOPA for 2C7 tested in serial 10-fold dilutions.*

Application of vOPA to high-throughput screening

In addition to the characterisation of the phagocytosis-promoting activity of 2C7 tested at different concentrations, we sought to apply vOPA to screening mAbs expressed in a high-throughput manner. In the latter case, the concentration of each monoclonal is usually not known before testing and can be subjected to variability. To mimic such a condition, we tested multiple replicates of a small-scale 2C7 expression experiment. Control conditions were included with unrelated mAb and no mAb samples. As **Fig. 19** shows, there was a good separability between 2C7 and the negative controls in the established infection conditions. Moreover, we calculated the Z' factor for all the quantitative metrics we could compute with our image analysis pipeline (**Table 7**). We observed that the number of internal bacteria per infected cell determined the highest Z' factor, thus prompting us to consider this as the best read-out that describes the phagocytic activity of cells mediated by mAbs. Finally, we computed the coefficient of variation (CV) for the number of internal bacteria per infected cell as a measurement of the deviation within the same experiment (intra-assay CV). It is generally recommended to be less than or equal to 20%[138,139]. We obtained a value of 5.10% and concluded that the intra-assay variability was acceptable.

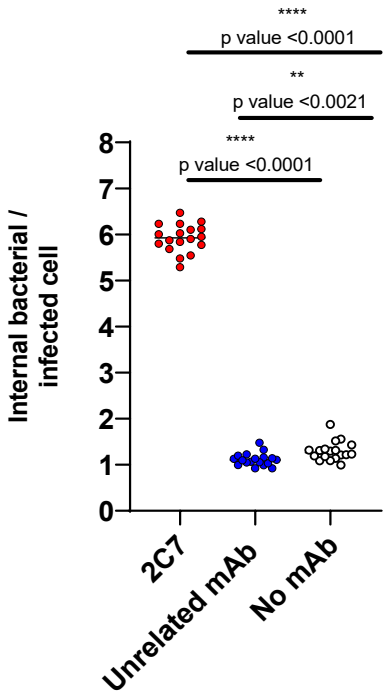

Figure 19. Application of vOPA for high-throughput screening*. Simulation of high throughput mAb expression. The number of internal bacteria per infected cell for each condition (2C7, unrelated mAb and no mAb samples) is reported on the y axis. 18 technical replicates for each condition were considered. On the graph we report the unpaired nonparametric t-test (Mann-Whitney test) p-value.*

Table 7. List of calculated Z' factors for each metric of the vOPA assay.

Read-out	Z' factor
Internal bacteria/ infected cell	0.726
Internal+adherent / infected cell	0.575
Total bacteria / infected cell	0,490
Internal bacteria/ total cell	0.725
Internal+adherent / total cell	0,620
Total bacteria /total cell	0.582

Anti *N. gonorrhoeae*-mAbs can be divided into three groups based on vOPA results

We then tested the possibility to employ vOPA as an efficient screening assay for the identification of mAbs promoting phagocytic activity for *N. gonorrhoeae*. Ninety-six

human anti-*N. gonorrhoeae* mAbs with unknown concentration, function or mode of action, derived from a screening described elsewhere (manuscript in preparation), were tested at one single dilution to select the positive hits. 2C7 was included as a positive control together with an unrelated antibody as the negative control. In order to use vOPA to select the mAbs with strong phagocytosis-promoting activity, we computed the fold-change of the number of internal bacteria per infected cell with respect to the negative control average value (**Fig. 20a**). We binned the fold-change values in four groups representing no-, low-, moderate- and high phagocytosis-promoting monoclonals. The corresponding thresholds were: 0-1 not-promoting, 1-2 low, 2-3 moderate, greater than 3 high phagocytosis-promoting activity. Out of 96 tested mAbs, one antibody showed high phagocytosis-promoting activity (red dot in **Fig. 20a). Fig**. **20b** shows the images of 2C7, a mAb from the high-phagocytosis promoting group, a mAb from the moderate-phagocytosis promoting group and the unrelated mAb.

a)

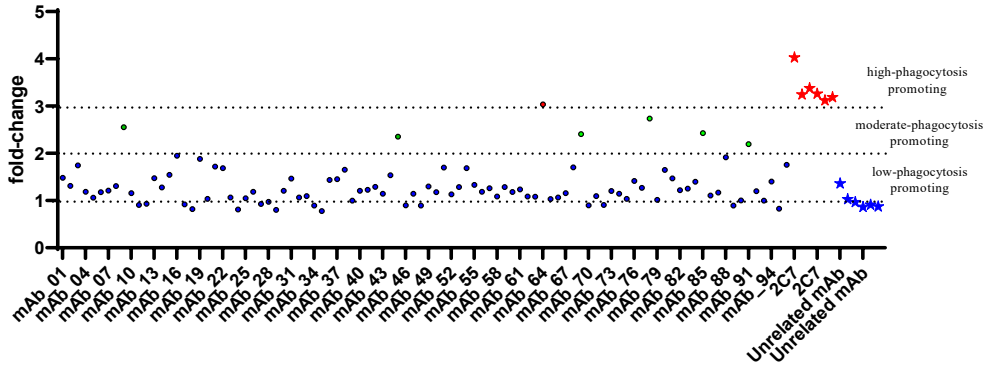

b)

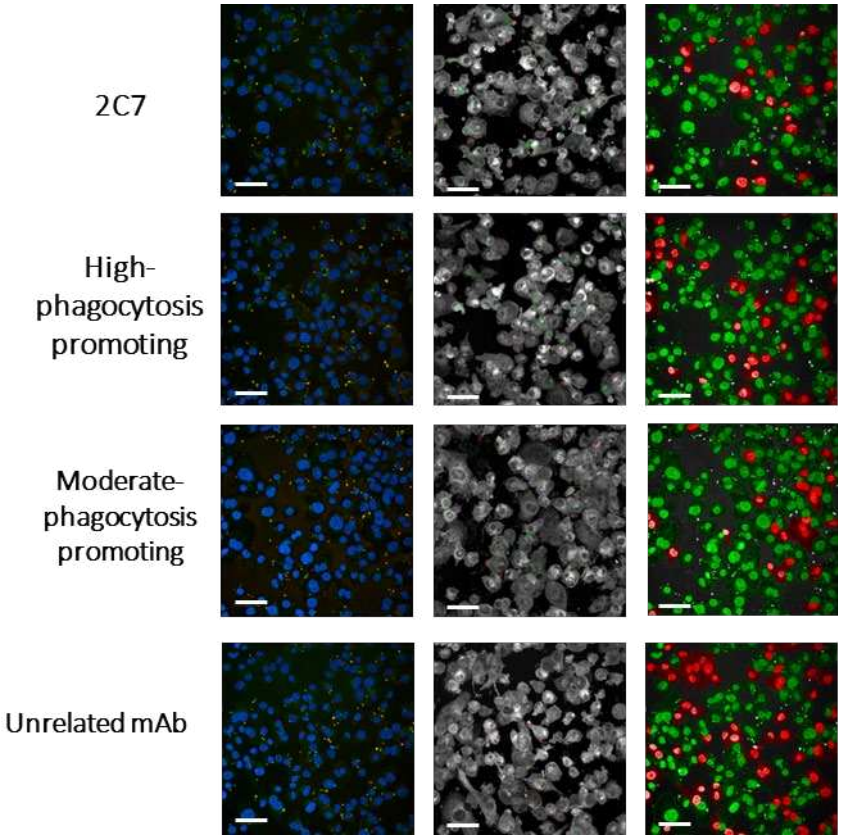

Figure 20. HTS screening of 96 mAbs using vOPA. *a) Screening of 96 anti-N. gonorrhoeae mAbs by vOPA. Each mAb was tested at one single dilution with no previous knowledge of the concentration. The fold-change in phagocytic activity with respect to the mean of the unrelated mAb is reported on the y-axis. Colours represent the four groups of phagocytosis-promoting activity into which mAbs were binned (white indicates no activity, blue means low activity, green is for moderate activity and red indicates high phagocytosis promoting activity). The positive (2C7) and the negative (unrelated mAb) controls are reported as stars. mAb_64 is depicted as a red dot, being the only mAb falling in the high phagocytosis promoting group. b) Images acquired from 2C7, high-phagocytosis promoting and moderate-phagocytosis promoting mAbs and negative control. The first column depicts the staining used in the assay (except for CellMask, for better visual inspection). The following two columns show two steps of the whole image analysis pipeline: the second column shows the image analysis step for the quantification of internal bacteria (green) and external bacteria (red) and third column depicts the image analysis step which differentiates infected cells (green) and non-infected cells (red). Scale bar is 50 μm.*

The most effective antibodies are not the ones that were expressed at higher concentration

The concentration of the 96 expressed mAbs was measured and found to range from 2 to 150 µg/ml, which is compatible with the small-scale expression system used. **Fig. 21** reports the correlation between mAb concentration and results of the vOPA experiment described above. The analysis revealed that the most effective antibodies were not necessarily the ones that were expressed at higher concentration. Most of the moderately and highly active monoclonals were tested at a concentration around 10 µg/ml. This demonstrated that the phagocytosis-promoting activity measured via vOPA was not driven by the antibody concentration but instead reflected intrinsic antibody efficacy. vOPA is therefore a very powerful assay for the high-throughput assessment of mAbs boosting the phagocytic activity of macrophages.

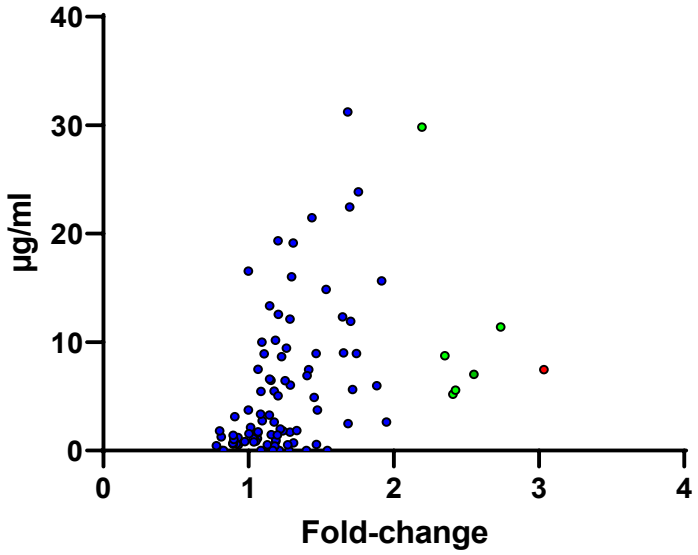

Figure 21. Comparison between fold-change of the phagocytic activity promoted by each mAb with respect to the negative control and the concentration of the corresponding mAb*. Concentrations are displayed on the y axis, while fold-change is reported on the x axis. The three colours represent the three groups of mAbs described in the text: blue means low activity, green is for moderate activity and red indicates high phagocytosis promoting activity.*

Dose-response curves confirm the potency of selected mAbs from vOPA HTS

From the panel of 96 mAbs, we selected two candidates. The first was the one promoting high levels of phagocytosis (the red dot in **Fig. 20a**) and the second was chosen from the moderate phagocytosis promoting group. The two mAbs were expressed and purified as recombinant proteins. We tested the monoclonals in a 10-fold dilution experiment starting from a concentration of 5 µg/ml (**Fig. 22**). We observed a dose-response behaviour for both mAbs, as the phagocytic activity decreased with decreasing concentrations of both antibodies. The two antibodies were confirmed to have different phagocytic potency as they promoted internalisation of different numbers of bacteria per infected cell at all concentrations tested. Furthermore, the activity of the high phagocytosis promoting mAb was comparable to the potency of 2C7, thus proposing it as an interesting candidate for further characterization.

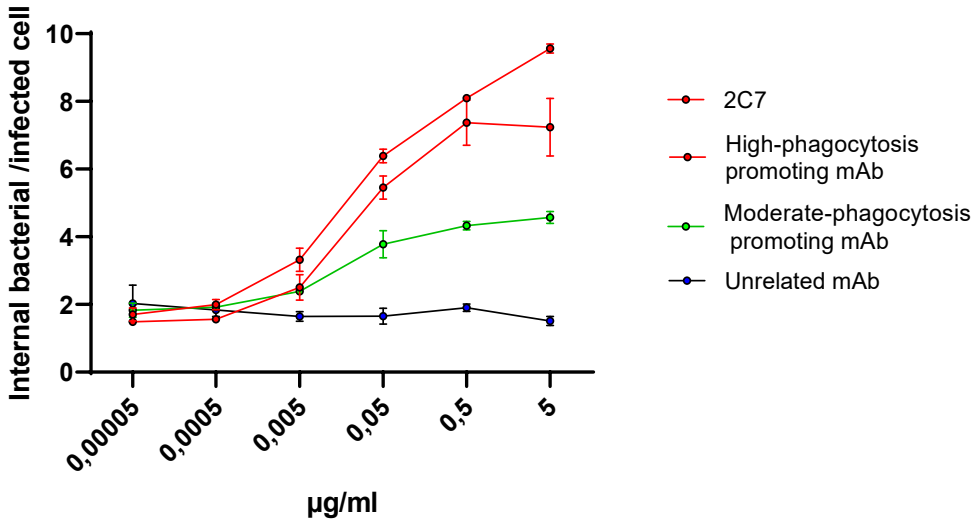

Figure 22. Dose-response activity of two recombinantly expressed monoclonal antibodies selected from the screening of 96 candidates*. One mAb is from the high phagocytosis promoting group (red), while the other is from the moderate phagocytosis promoting group (green). The positive control 2C7 and the negative controls represented by the unrelated mAb are depicted. mAb concentrations are indicated on the x axis, while the number of internal bacteria per infected cell is on the y axis.*

Discussion

In this work we reported the development and validation of an innovative assay that measures the opsonophagocytosis-promoting activity of mAbs against *N. gonorrhoeae* by means of confocal fluorescence microscopy (vOPA). The protocol was successfully optimised for application in the 96-well format and can be easily adapted to 384-well plates thus expanding the throughput.

The microscopy platform used here provided several advantages as compared to standard OPA experiments based on CFU counting. First, it allowed detection of fluorescently labelled single cells and single bacteria which could be quantified in different experimental settings. Secondly, a modular image analysis pipeline composed of several building blocks could be assembled and tailored to the scientific question we wanted to address, i.e. measuring bacterial engulfment by cells. Third, the output of the high-content analysis consisted in various metrics whose statistical significance was investigated by calculating the Z' factor and which resulted in the choice of the best parameter (number of internalised bacteria per infected cell) to describe the phagocytic activity of THP-1-derived macrophages. Of note, it was also possible to analyse bacteria at the single-cell level and quantify GFP intensity of each bacterium belonging to the adherent and internalised populations. The approach overcomes the limitations imposed by studies in batch such as those based on plate readers, where bacterial and cellular individualities cannot be explored. In this sense, the visual detection of host and pathogen by vOPA may contribute to further insights into their interplay. Importantly, the assay requires little hands-on time, involves addition of few reagents and can be automated to further increase processivity.

To mimic macrophage infection by *N. gonorrhoeae,* we chose THP-1 cells, an immortalised human leukaemia monocytic cell line that can be differentiated into macrophage-like cells and was extensively reported in the literature as a model for macrophage-like infection [145] and is optimal for reproducible results. The cell staining procedure employed here involved two dyes, DAPI and Cell Mask, whereas bacteria were genetically labelled by inserting the gene encoding sfGFP in their genome. This represents an important advantage since no additional staining steps are required for bacteria thereby simplifying the logistics. Since Opera can accommodate up to four detectors, rearrangements of the staining protocol may be required to visualise subcellular structures and increase the information extracted from the images. For example, the membrane staining (performed with CellMask Deep Red) can be

removed, and cell cytoplasm can be identified using Brightfield. This would make room for one extra color to detect subcellular structures.

We proved that there is a basal phagocytosis activity by dTHP-1 in the absence of mAbs. This is in line with dTHP-1 cells mimicking macrophages and their phagocytic activity. Normally bacteria express surface molecules (Opa proteins in case of *N. gonorrhoeae*) which act as natural opsonins[144] and explain the basal phagocytic activity of dTHP-1. Our infection conditions aimed to have the lowest basal phagocytosis activity by dTHP-1 to increase the sensitivity and appreciate the activity of any functional mAb.

The fate of bacteria after uptake by cells is an open question. One way to determine whether internal bacteria are alive or not is to count them over time, since one would expect viable bacteria to replicate and increase their numbers. However, we reported that longer times of infection led to a reduced number of adherent cells, suggesting a cytotoxic effect of the engulfed bacteria. Others have proven that *N. gonorrhoeae* induces apoptosis in THP-1 cells[137], in line with what we observed. Another way to determine the viability of engulfed bacteria is by viability staining or by co-localizing bacteria with early or late phagosomes. On one hand this may improve the descriptive power of vOPA while on the other it may increase the complexity of the assay by adding experimental and analytical steps. Importantly, the effect of addition of an exogenous source of complement to the experiment needs to be investigated.

Screening of a set of human anti-*N. gonorrhoeae* mAbs by vOPA resulted in the identification of one candidate with opsonophagocytosis-promoting activity similar to that of the 2C7 positive control, which was previously shown to enhance the phagocytic activity of neutrophils[76]. The test revealed that vOPA efficiently detects active mAbs independently of their concentration. In fact, the concentration of the positive hit was not among the top scoring ones but in the mid-range. We have shown that the assay is sensitive to different infection conditions, as it can quantify a different phagocytic activity of cells based on the number of input bacteria (MOIs) and time of infection.

Finally, since the assay relies on acquisition of high-quality images, appropriate storage and computational resources are required for efficient processing of raw data. In the experiments described here, each well produced 832 images which translated into a more than four-hour acquisition of 400 gigabytes and a 30-minute analysis time per plate.

In summary, an innovative opsonophagocytosis assay was developed by means of high-throughput microscopy. This is suitable for application to other cell types and bacterial species with minor adjustment of the experimental conditions and of the downstream analysis.

Additional data not included in the manuscript

Identification of target of mAb_64 using immunoblot and immunofluorescence

Among the 96 tested mAbs, mAb_64 was the one with the highest phagocytic activity, comparable to positive control 2C7. Its strong phagocytosis promoting activity made it an ideal candidate for antigen discovery. In order to identify the target recognized by the antibody, an immunoblot was performed, using denatured OMV (dOMV) or LOS from FA1090 (**Fig. 23**). Using an anti-porin mAb and a mAb recognising fHbp partner protein GNA 291 as controls, I demonstrated that mAb_64 did not recognize any molecule on the dOMV of FA1090 in the experimental conditions tested. When the experiment was repeated using an anti-LOS mAb as a control, mAb_64 failed to recognize LOS as well. Since Opa and pilus proteins are highly represented on the bacterial surface, I checked whether mAb_64 could bind FA1090 strains lacking either Opa (Opaless)[146] or PilE[147] (the main constituent of the pilus). By immunostaining (**Fig. 24**) I proved that mAb_64 retained the ability to bind FA1090 Opaless and FA1090 Δ*pilE*, indicating that neither the Opa nor the pilus are targets of the antibody. Therefore, the cognate antigen of mAb_64 was not identified.

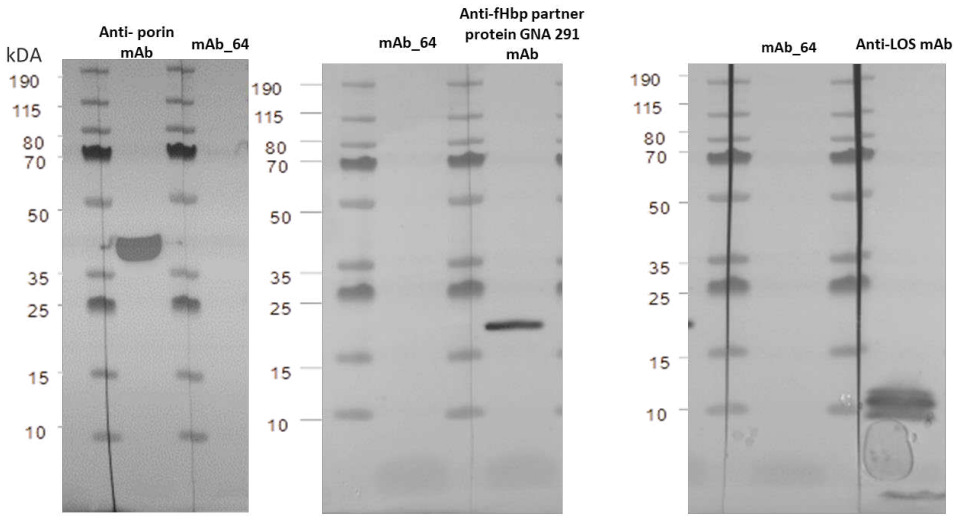

Figure 23. Immunoblot to identify the target of mAb_64. *From left to right: immunoblot of denatured outer membrane vesicles of FA1090 decorated with an anti-porin mAb as a control, immunoblot of denatured outer membrane vesicles of FA1090 decorated with the anti-fHbp partner protein GNA291 mAb, immunoblot of FA1090 LOS decorated with an anti-LOS mAb as a control. In all cases, incubation of the blots with mAb_64 did not result in any signal.*

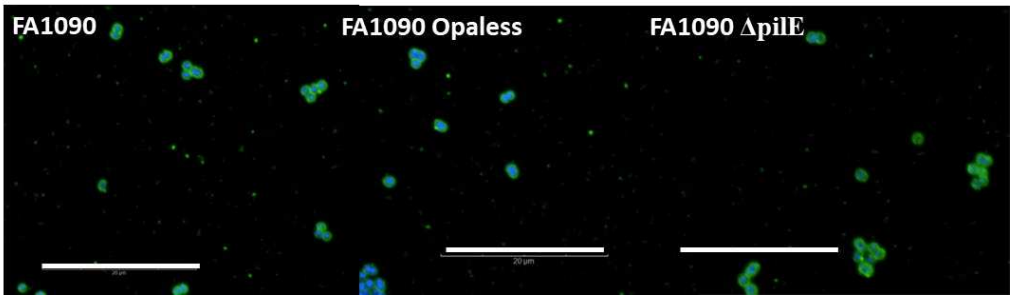

Figure 24. Immunostaining of N. gonorrhoeae with mAb_64. *From left to right: immunostaining of FA1090 wild-type (WT), FA1090 Opaless and FA1090 ΔpilE. DAPI stained bacterial DNA (blue) while mAb_64 recognized a surface exposed target (green). Images were acquired with Opera Phenix, 63x objective. Scale bar is 20 µm.*

Characterization of anti-*N. gonorrhoeae* serum-bactericidal mAbs

vOPA was also applied to characterize anti-gonococcal mAbs, isolated in the framework of the vAMRes project mentioned above, which exerted SBA activity. Some of these mAbs have known targets, such as LOS, porins or NspA (*N. gonorrhoeae* surface protein A), a highly conserved gonococcal antigen[148]. To determine whether there was a correlation between target and phagocytosis-promoting activity, all mAbs were tested at concentrations of 10-5 µg/ml, and results were normalized to the positive control 2C7 and to an unrelated mAb. As **Fig. 25** shows, mAbs with the highest activity (90-100%) recognized porins. All the anti-LOS mAbs, the anti-NspA mAb and most of the mAbs with unknown targets were characterized by lower activity in vOPA (less than 50%). Only 2 mAbs with unknown targets displayed a phagocytosis-promoting activity close to 80%.

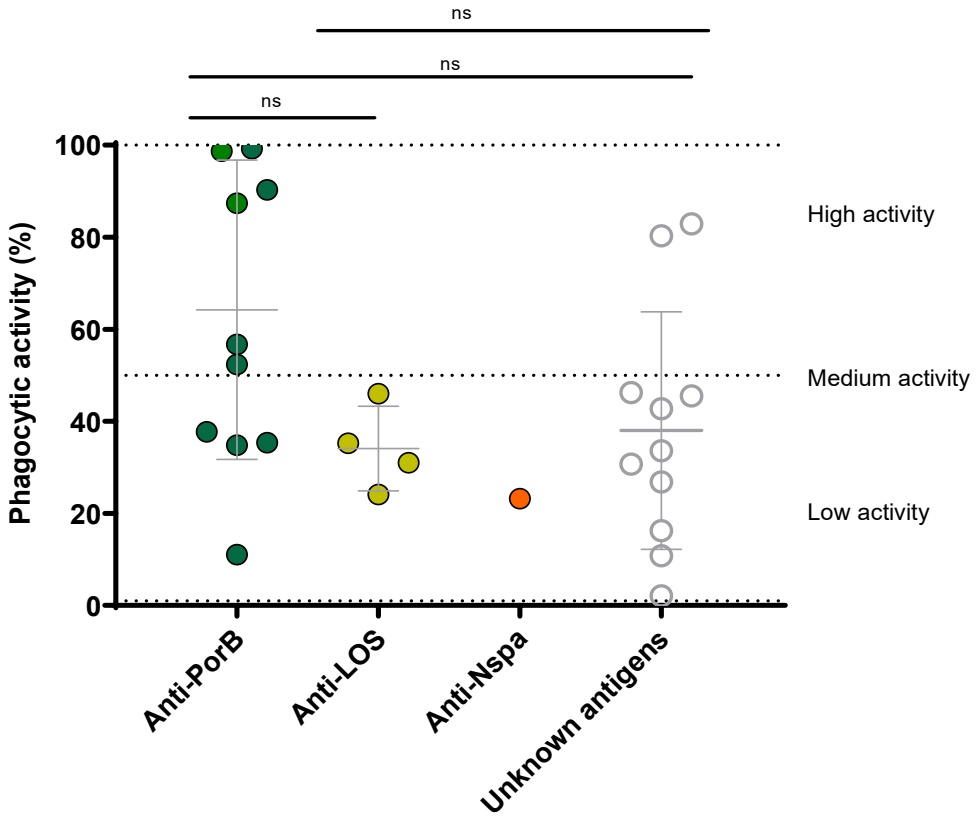

Figure 25. Phagocytic activity of four groups of mAbs (anti-porin B, anti-LOS and those which recognize unknown antigens). *Each value represents the opsonophagocytosis activity promoted by the mAb at the highest concentration tested (10-5 µg/ml) and was normalized to positive and negative controls represented by 2C7 and unrelated mAb (not shown). ns, not significant.*

Experimental procedures

Cell cultures

Human monocytic leukaemia cell line THP-1 (ATCC, Manassas, Virginia, USA) was cultured in RPMI1640 with Glutamax (Gibco 6187-010), 10% fetal bovine serum (Gibco 10500-064), 1 mM sodium pyruvate (Gibco 11360-070) and 10 mM Hepes (Gibco 15630-080) at 37°C and 5% CO_2. Cells were passaged three times per week and kept at a density below 1×10^6 per ml. Cells were stimulated for three days with 30 nM phorbol-12-myristate-13-acetate (PMA) in 96-well plates (Cell Carrier 96 Ultra, Black, Clear bottom TC treated, cyclic olefin, Perkin Elmer) at the density of 40,000 cells / well. Culture medium was then removed and replaced with RPMI without PMA for the following 48 h.

FACS analysis

Expression of IgG surface receptors and differentiation markers in THP-1 and differentiated THP-1 (dTHP-1) was tested by flow cytometry with the following reagents: CD64 PE-Cy7 1:200 and isotype mouse IgG1 k 1:50 (BD Pharmingen), CD32 BV711 1:30 and isotype mouse IgG2b k 1:30 (BD Pharmingen), CD11b BUV805 1:50 (BD Pharmingen), CD14 BV786 1:100 (BD Pharmingen). Cells were stained for CD45 BUV395 1:80 (BD Pharmingen). $2x10^5$ THP-1 cells per well were plated in a 96-well plate. Cells were stained for LIVE/DEAD™ Fixable Near-IR Dead Cell Stain Kit (Thermo Fisher) and after blocking with rabbit serum, 25 µl of mAbs and respective isotypes were added and incubated for 20 minutes on ice and in the dark. After washing, Cytofix/Cytoperm (BD) was added and kept for 20 minutes on ice, followed by PermWash 1X (BD). Intracellular stain of CD68 PE-CF594 1:200 (BD Pharmingen) and its respective isotype mouse IgG2b k isotype 1:3333 (BD Pharmingen) followed for 20 minutes. Washes were performed with PermWash 1X and PBS. Acquisition was done at Fortessa (BD biosciences).

Bacterial strains and culture conditions

N. gonorrhoeae strain FA1090, FA1090 Opaless[61] and FA1090ΔpilE[147] were used in this study and were cultured on gonococcal medium base liquid or agar (Difco™ GC Medium Base, BD 228950) plus Isovitalex (BD 211876). The strains were typically grown at 37°C and 5% CO_2 for approximately 15 hours. FA1090 was engineered to express a superfolder green fluorescent protein (sfGFP) (please see Chapter 1 of this thesis "Generation of knock-in strains of *N. gonorrhoeae* expressing fluorescent proteins for high-content imaging" for details) by integration of the encoding gene into the chromosome. The modified strain is called FA1090::sfGFP. Prior to cell infection, bacteria were suspended in gonococcal liquid medium containing Isovitalex and grown at 37°C to mid-logarithmic phase.

Expression of mAbs into cell culture supernatants

Expression vectors encoding for anti-*N. gonorrhoeae* antibody heavy and light chains were used as templates for transcriptionally active PCR (TAP) reaction[149]. The resulting linear DNA fragments were used for transient transfection of the Expi293F cell line (Thermo Fisher Scientific) with a heavy:light chain ratio equal to 1:2. The transfection process lasted for six days at 37°C with 8% CO_2 in shaking conditions according to the manufacturer's protocol (Thermo Fisher Scientific, US). Cell culture supernatants were harvested six days after transfection and clarified by centrifugation (4,500 x g, 15 min, 4°C). The reference antibody 2C7 was expressed in Expi 293 cells

as well. For medium-scale mAb expression and purification, expression vectors encoding for anti-*N. gonorrhoeae* antibody heavy and light chains were used for transient transfection of Expi293F cells in a total volume of 60 ml. Antibodies were purified by affinity chromatography on protein G columns using an AKTA-Go system (GE Healthcare Life Sciences) as described below.

Purification of mAbs by affinity chromatography

Filtered culture supernatants were purified with a 1 mL HiTrap Protein G HP column (GE Healthcare Life Sciences) previously equilibrated in Buffer A (0.02 M NaH_2PO_4 pH 7). The flow rate for all steps of the HiTrap Protein G HP column was 1 mL/min. Culture supernatants were applied to 1 mL HiTrap Protein G HP column. The column was equilibrated in Buffer A for at least 6 column volumes (CV) which was collected as the column wash. Each monoclonal antibody was eluted from the column by applying a step elution of 6 CV of Buffer B (0.1 M glycine-HCl, pH 2.7) and by collecting 1 mL elution fractions. Eluted fractions were analysed by non-reducing SDS-PAGE and fractions showing the presence of IgG were pooled together. Final pools were dialyzed in PBS buffer pH 7.4 using Slide-A-Lyzer G2 Dialysis Cassette 3,5K (Thermo Fisher Scientific) overnight at 4°C. The dialysis buffer used was at least 200 times the volume of the sample. Antibody concentration was determined by measuring the absorbance at 520 nm using Pierce BCA Protein Assay Kit (Thermo Fisher Scientific). All the purified antibodies were aliquoted and stored at -80°C.

Quantitative Enzyme Linked Immunosorbent Assay (ELISA)

mAb concentration in collected supernatants was measured by quantitative ELISA in 384-well plates. Plates were pre-coated with 2 µg/mL goat anti-human IgG (SouthernBiotech cat. N° 2040-01) and incubated at 4°C. Blocking was performed with BSA 1%-PBS1X for 1h at 37°C followed by the addition of mAb supernatants diluted in BSA 1%-PBS1X-Tween 0.05%, initially 1:20 and then 1:2 for the following dilution steps. Human IgG-UNLB (SouthernBiotech cat. N° 0150-01) at 10 µg/mL was used as a positive control. After 1h of incubation at 37°C, mAbs were washed away, a secondary goat anti-human IgG-Alkaline phosphatase (SouthernBiotech) antibody was added diluted 1:15,000 in PBS1X-BSA 1%+0,05% tween for 1h at 37°C. The alkaline phosphatase substrate p-Nitrophenyl Phosphate (PNPP) (Sigma-Aldrich) was added and the reaction was incubated for 30 min at RT before the luminescence signal was read using a Varioskan™ LUX multimode microplate reader (Thermo Fisher Scientific, Waltham, MA, USA).

vOPA assay

THP-1 cells were seeded and differentiated into 96-well plates as described above and after 5 days of differentiation were infected with FA1090::sfGFP grown to mid-logarithmic phase and pre-incubated with mAb supernatants diluted 1:5 in RPMI medium. After 30 minutes of pre-incubation, the mixture composed of mAbs and bacteria was added onto dTHP-1 at MOI 40. To synchronise the infection, the 96-well plates were centrifuged for 1 min at 200 xg. After 30 minutes of infection, each well was fixed with 2% paraformaldehyde (PFA) for 15 minutes, blocked with 1% (w/v) BSA. Extracellular FA1090::sfGFP bacteria were stained with primary antibody 2C7, at final concentration of 3 mg/ml , for 1h at RT, followed by secondary goat anti-Human IgG Alexa Fluor 568 (Thermo Fisher, A-21090) diluted 1:2,000 at RT for 30 minutes. CellMask™ Deep Red stain (Invitrogen) was used to stain the cell membrane, providing a means to delineate the cell boundary, and DAPI to stain cell nuclei and bacterial DNA.

Confocal microscopy and image analysis

96-well plates were imaged with the microscope Opera Phenix High-Content Screening System (PerkinElmer) using a 40x objective, numerical aperture 1.1, acquiring 16 fields of view per well, and 13 images on the vertical dimension to form a z-stack per each field of view. The image analysis pipeline (Supplementary Table 1) was developed using Harmony Software of Perkin Elmer. dTHP-1 cells were detected by analysing the combined signal of DAPI (nuclei) and CellMask (membrane), which allowed counting and identification of the two compartments. Bacteria were localised and segmented by combining the DAPI and GFP signals. Bacteria that overlapped with the cytoplasm of a cell were identified as infecting and distinguished as internalised if they were negative for the immunostaining and adherent if they were positive for the immunostaining. Ultimately, cells with infecting bacteria were considered as infected cells.

Immunostaining

FA1090::sfGFP, FA1090 Opaless[61] and FA1090ΔpilE[147] were grown to mid-log phase and resuspended in Dulbecco's modification of PBS (PBSB) at final OD of 0,1. 50 µl of bacteria were plated onto ViewPlate-96 Black, Optically Clear Bottom, Tissue Culture Treated plates (Perkin Elmer) and left to adhere for 30 mins at 37°C, 5% CO_2. Each well was fixed with 2% paraformaldehyde (PFA) for 15 minutes, blocked with 1% (w/v) BSA. Purified mAbs, at final concentration of 10 µg/ml, were added for 1h at RT,

followed by secondary goat anti-Human IgG Alexa Fluor 488 (Thermo Fisher, A-21090) diluted 1:2,000 at RT for 30 minutes. DAPI was used to stain bacteria nuclei.

Immunoblot

dOMVs or LOS from FA1090 were transferred to polyvinylidene difluoride membranes (Millipore, Billerica, MA) by electroblotting. Membranes were then blocked with PBS, 1% milk for 1 h at 37°C and probed with purified mAbs at 10 µg/mL, overnight at 4°C. Bands were visualized with anti-human IgG conjugated to alkaline phosphatase.

Gentamicin protection assay (classical OPA assay)

THP-1 cells were seeded in 96-well tissue culture plates at 40,000 cells /well and subjected to the differentiation protocol as described above. Infection was performed as described above. To quantify the number of internalised bacteria, extracellular bacteria were washed away three times with RPMI medium and gentamicin (100 µg/ml) was added for 30 minutes to kill adherent bacteria. Cells were lysed with 0.5% saponin for 5 minutes and dilutions of the suspension containing bacteria were plated on GC agar. The number of CFU was determined after 24–48 h incubation.

Data analysis

Statistical analysis, including Pearson correlation analysis and unpaired nonparametric t-test (Mann-Whitney test), was performed with GraphPad Prism 8.

Supplementary material

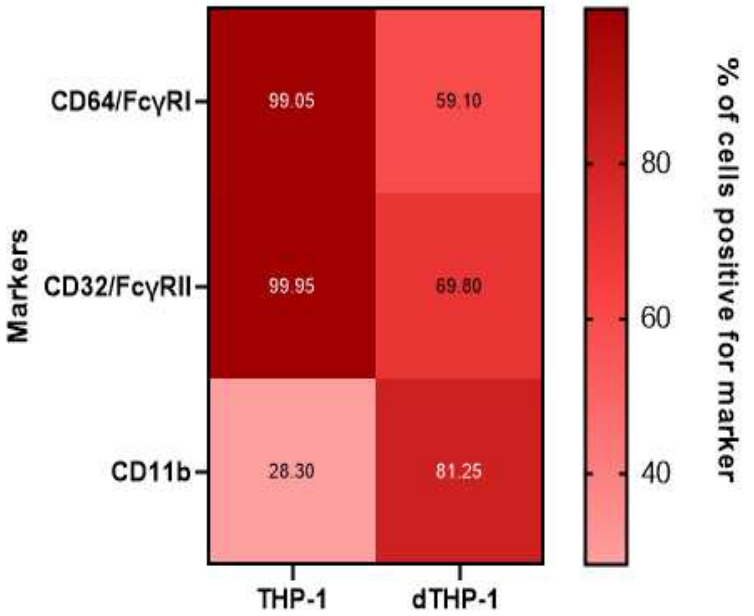

Supplementary Figure 1. Evaluation of the presence of markers CD64, CD32 and CD11b in THP-1 and dTHP-1 using flow cytometry. *Numbers in each square indicate the percentage of THP-1 cells positive for the marker. The red colour intensity increases with the percentage of cells positive for the marker.*

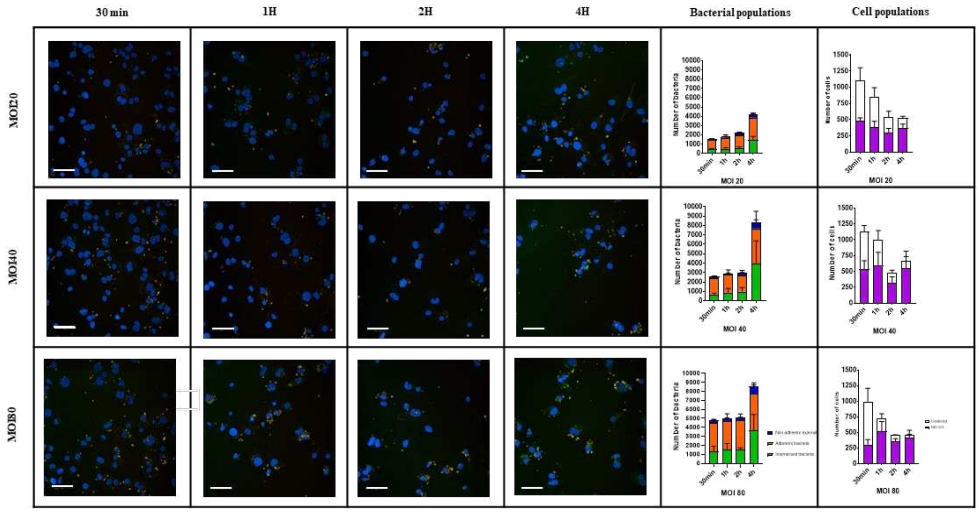

Supplementary Figure 2. Quantification of the number of bacteria and cells at different times of infection and with different MOIs*. The table displays different images for each condition used to obtain the data plotted in the last two columns.*

CellMask was removed for better visual inspection. Scale bar is 50 µm. The fourth column shows the three derived bacterial populations: internalised (green), adherent (orange), non-adherent external bacteria (blue). The fifth column shows the numbers of infected (purple) and uninfected cells (white). Graphs were compiled with data generated in 4 technical replicates and show average values and standard deviations.

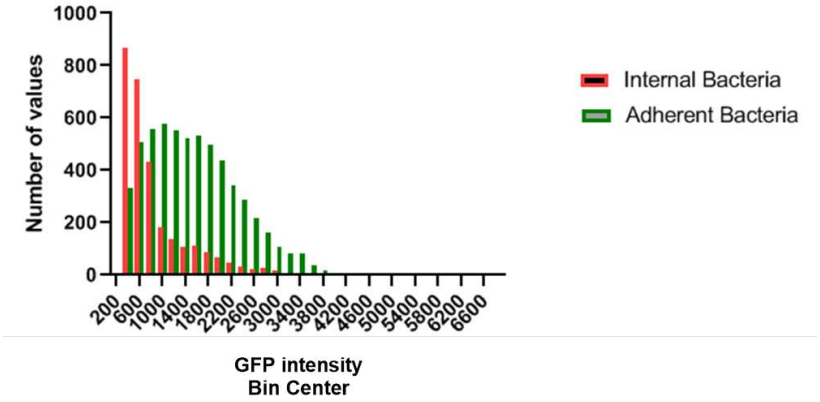

Supplementary Figure 3. Single-cell analysis of bacterial populations. *Red bars indicate the number of internal bacteria, while green bars indicate the number of adherent bacteria. The number of bacteria which fall into a specific range of GFP intensity (X axis) is reported on the Y axis.*

Supplementary Table 4. *Analysis pipelines for vOPA built using Harmony v4.9 (Perkin Elmer).*

Building Block	**Input**	**Method**	**Output**	**Property prefix**
Calculate Image		Method: by formula Formula: A-300 A: DAPI Negative values: Set to Zero Undefined values: Set to local	Calculated Image	

		average		
Find nuclei	Channel: Calculated image ROI: none	Method: C Common threshold: 0.41 Area:>30 um^2 Splitting coefficient: 7.0 Individual threshold: 0.39 Contrast:>0.11	Nuclei	
Find Cytoplasm	Channel: CellMask Deep Red Nuclei: Nuclei	Method: D Individual threshold: 0,29		
Find Spots	Channel: EGFP ROI: none	Method: C Radius: <= 5,8 px Contrast:>0.17 Uncorrected Spot to Region Intensity> 1.3 Distance >= 1px Spot Peak Radius: 0 px Calculate spot properties: yes	Spots	
Calculate Intensity Properties	Channel: DAPI Population: Spots Region: Spot	Method: Standard Mean: yes Maximum: yes Quantile		Intensity Spot DAPI

		Fraction: 50%		
Select population	Population: Spots	Method: Filter by property Intensity Spot DAPI mean: >300 Spot area [px^2]: >20 Boolean Operations: F1 and F2	Spots selected	
Select region	Population: Nuclei Region: Cell	Method: Resize region [um/px] Outer border: -5 px Restrictive population: none Inner border: INF px	Cell resized	
Select population	Population: Spot selected	Method: Select by Mask Region: Spot Mask population: Nuclei Mask Region: Cell Resized Select by: Overlap>50% Use inverted	Bacteria non-cytoplasm	

		Mask:yes		
Select population	Population: Spot selected	Method: Select by Mask Region: Spot Mask population: Nuclei Mask Region: Cell Resized Select by:Overlap>50% Use inverted Mask: no	Bacteria cytoplasm	
Calculate Intensity Properties	Channel: Alexa 568 Population: Spot selected Region: Spot	Method: Standard Mean: yes Sum: yes Maximum: yes Quantile Fraction: 50%		Intensity spot Alexa 568
Select population	Population: Spot selected	Method: Filter by property Intensity Spot Alexa 568 Mean:>500	Bacteria 568	
Select population	Population: Bacteria cytoplasm	Method: Select by Mask Region: Spot Mask population: Bacteria 568	Adherent Bacteria	

		Mask region: Spot Select by: Overlap > 50% Use Inverted Mask: no		
Select population	Population: Bacteria cytoplasm	Method: Select by Mask Region: Spot Mask population: Bacteria 568 Mask region: Spot Select by: Overlap > 50% Use Inverted Mask: yes	Internal Bacteria	
Select population	Population: Bacteria non-cytoplasm	Method: Select by Mask Region: Spot Mask population: Bacteria 568 Mask region: Spot Select by: Overlap > 50% Use Inverted Mask: no	Non-adherent External Bacteria	
Calculate position properties	Population: Nuclei Region:	Method: Cross-Population		Cell_with_bacteria

	Cell resized	Population B: Spots Selected Region B: Spot Overlap: yes		
Calculate position properties	Population: Nuclei Region: Cell resized	Method: Cross-Population Population B: Internal bacteria Region B: Spot Overlap: yes		Cell_with_ internal_bacteria
Select population	Population: Nuclei	Method: Filter by Property Cell_with_ bacteria:>0	Infected cells	
Select population	Population: Nuclei	Method: Filter by Property Cell_with_ internal_ bacteria:>0	Infected cells with internalized bacteria	

Define Results

Method: List of Outputs

Population: Spots selected

Number of Objects

Population: Bacteria cytoplasm

Number of Objects

Population: Adherent bacteria

Number of Objects

Population: Internal bacteria

Number of Objects

Population: Non-adherent External Bacteria

Number of Objects

Population: Nuclei

Number of Objects

Population: Infected cells

Number of Objects

Population: Infected cells with internalised bacteria

Number of Objects

Method: Formula Output

Formula: (a/b)*100

a: Internal Bacteria – number of objects

b: Spot Selected – number of objects

Output name: % Internal bacteria

Formula: (a/b)*100

a: Adherent Bacteria – number of objects

b: Spot Selected – number of objects

Output name: % Adherent bacteria

Formula: (a+b)/c

a: Adherent Bacteria – number of objects

b: Internal Bacteria – number of objects

c: Infected Cells – number of objects

Output name: Bacteria per Infected cell

Formula: a/b

a: Internal Bacteria – number of objects

b: Infected Cells – number of objects

Formula: (a/b)*100

a: Infected Cells – number of objects

b: Nuclei – number of objects

Output name: % Infected cells

Formula: (a/b)*100

a: Infected Cells with internalised bacteria – number of objects

b: Nuclei – number of objects

Output name: % Infected cells with internalised bacteria

3. New approaches to study *N. gonorrhoeae* colonization of epithelial cells

Introduction

N. gonorrhoeae requires surface proteins/receptors (Opa proteins, porin, Type IV pili, LOS) to adhere to and invade epithelial cells[59]. Among these, Type IV pilus and Opa are considered essential for the colonization of the mucosal epithelium of the genital tract[59].

The three recombinant protein antigens in the 4CMenB vaccine against *N. meningitidis* are important for bacterial virulence and two of them are specifically involved in host-pathogen interaction. Of these, NHBA facilitates binding to epithelial cells, while NadA mediates binding to and invasion of human epithelial cells[119]. Therefore, antibodies elicited by the vaccine could play a role in inhibiting the interaction of *N. meningitidis* with epithelia at the infection site. Given the cross-protection studies from gonorrhea infection in a cohort of people vaccinated with 4CMenB in New Zealand[115] and the high similarity between *N. meningitidis* and *N. gonorrhoeae* in the proteins which compose the vaccine[150], antibodies elicited by Bexsero (containing 4CMenB) may also play a role in inhibiting adhesion of gonococcus to epithelial cells. This is the reason why I tried to optimize an assay (visual adhesion inhibition assay or vAIA) to quantify *N. gonorrhoeae* adhesion to epithelial cells and then determine whether mAbs or a polyclonal serum could interfere with this interaction.

Results

To model the first step of infection (adhesion) of FA1090 to epithelial cells and evaluate whether mAbs could inhibit or reduce this interaction, a visual adhesion inhibition assay (vAIA) was designed. This assay is based on the use of the confocal microscope Opera Phenix and exploits image analysis to quantify the number of adherent bacteria in a 2-dimensional model of infection. The cells used for the model are called SV-HUC-1, which are a transformed urethral cell line grown to reach confluence and mimic a monolayer. FA1090::sfGFP (described in Chapter 1) can be identified through sfGFP expression, while cells are stained for their membrane (CellMask Deep Red) and nuclei (DAPI) (**Fig. 26**). The image-analysis pipeline developed using Harmony (**Supplementary Table 5** and **Fig. 27**) relies on the

quantification of the number of adherent bacteria and of the percentage of cell confluence, that is, the area occupied by cells in the specific field of view.

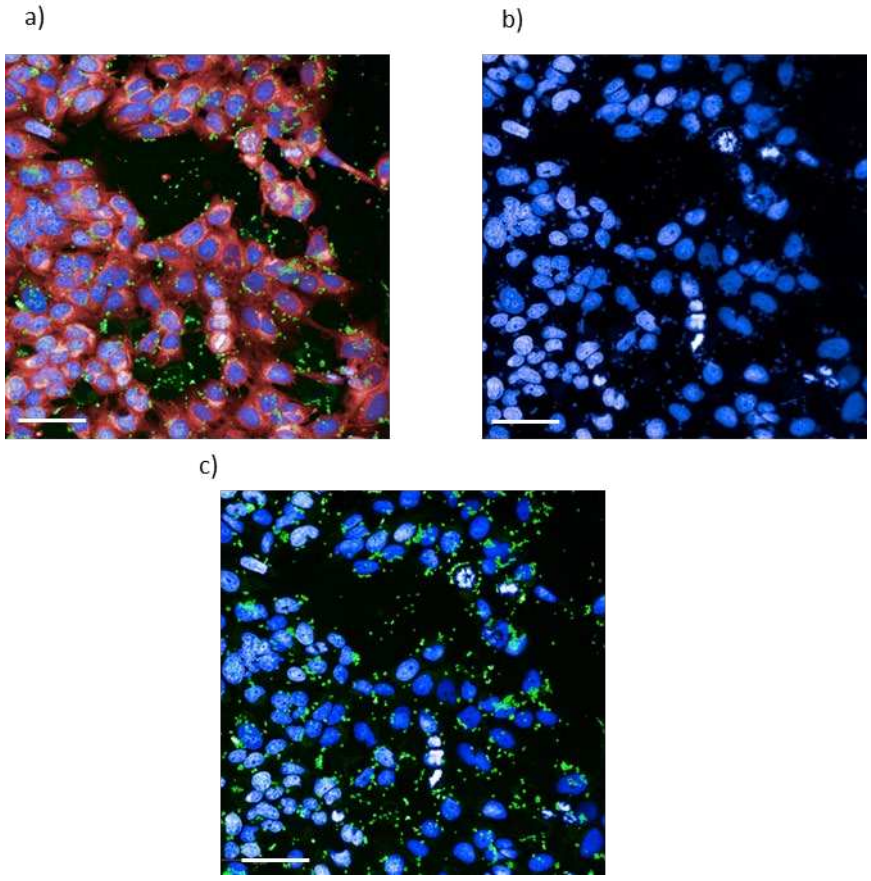

Figure 26. Three different colors used in vAIA. *sfGFP expression by bacteria (green), DAPI (blue) to stain cell nuclei and bacterial DNA and CellMask Deep Red (red) to stain cell membranes. Panel a) shows the whole staining, b) DAPI staining of cell nuclei and bacterial DNA. Panel c) shows the GFP emission of bacteria overlapping the DAPI signal of bacterial DNA. Scale bar is 50 μm.*

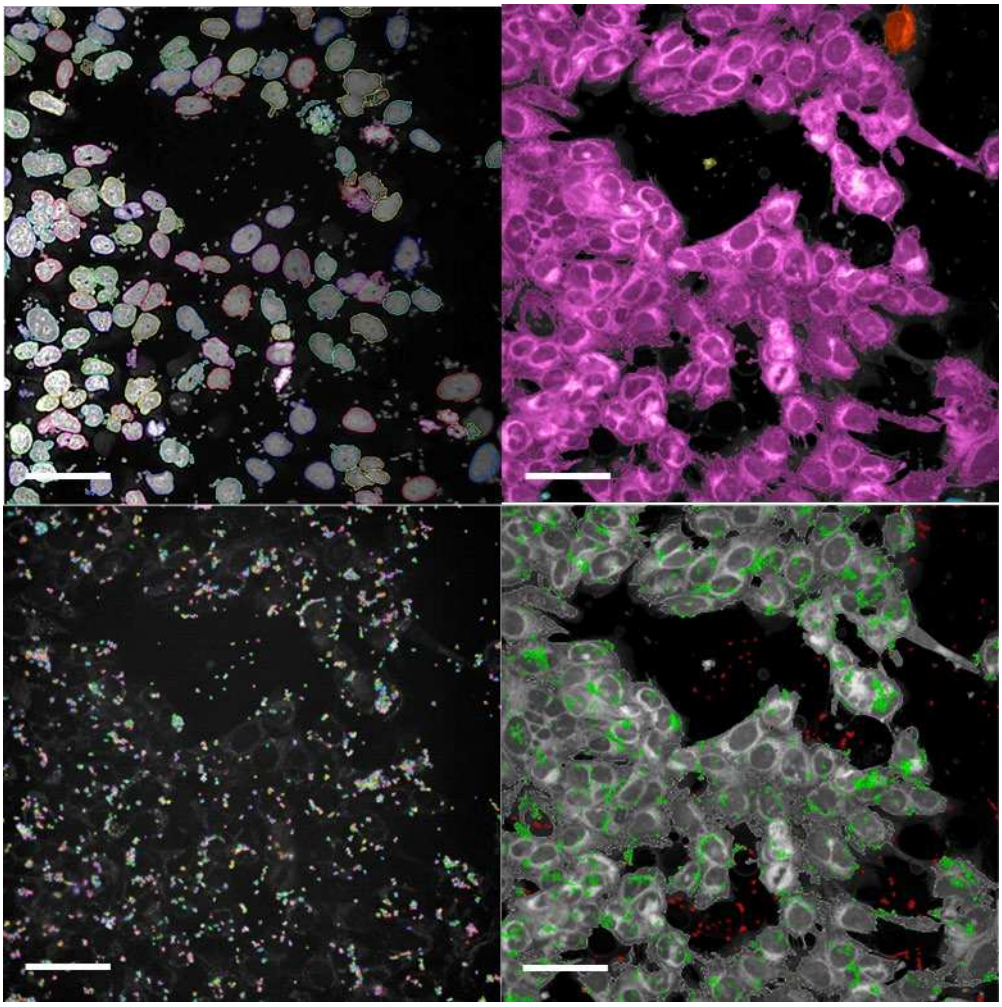

Figure 27. Image analysis steps to quantify the number of adherent bacteria on SV-HUC-1 cells. *The image on top left shows the identification of cell nuclei using DAPI signal. On top right CellMask Deep Red identifies cells. The image on bottom left illustrates the identification and quantification of the "spots", i.e. the bacterial population, using sfGFP signal. On bottom right adherent bacteria (green) can be discriminated from non-adhering bacteria (red) by means of immunostaining. Scale bar is 50 µm.*

Since the number of adherent bacteria is strictly dependent on the area occupied by cells, a crucial point was to adjust the assay conditions to obtain a reproducible percentage of cell confluence. Two crucial factors were identified: the time required for cells to reach confluence after plating an initial number of 35,000 cells per well onto the 96-wells plate, and the material that constitutes the bottom of the well. As **Fig. 28a** shows, three days of cell growth on cyclin olefin bottom leads to a higher and less variable cell confluence compared to two days of growth on the same plate material.

However, the best result was achieved with 3 days of growth on plastic bottom plates (**Fig. 28b**).

a)

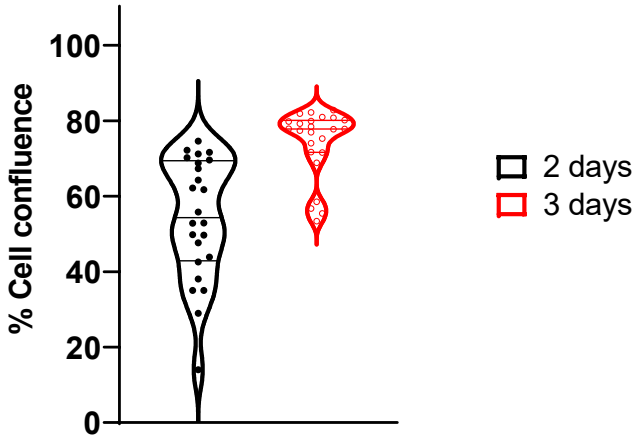

b)

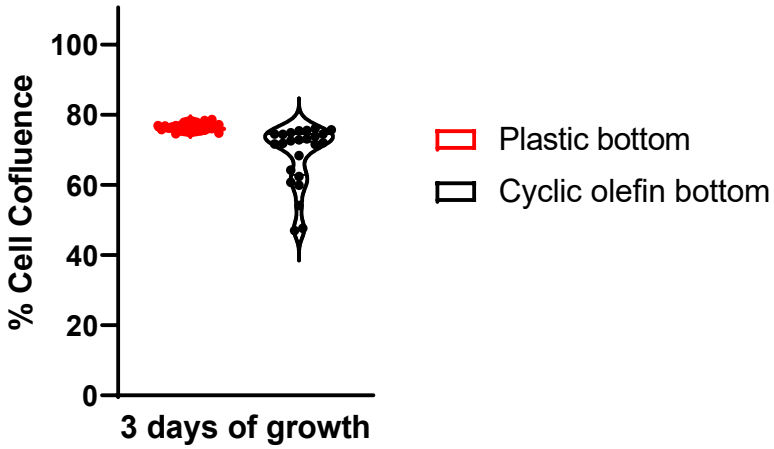

Figure 28. Violin plots used to represent the percentage of cell confluence according to different incubation times and plate material. *a) Cells plated on cyclin olefin bottom plates for 2 and 3 days. Cells come from the same batch. b) Cells plated either on cyclin olefin or on plastic bottom plates for 3 days.*

Once cell culture conditions were defined, FA1090::sfGFP was used to infect the cells for 1 hour with different input OD_{600} (**Fig. 29**), starting from OD 0.012 until OD 0.1.

Results showed that the number of adherent bacteria increased with increasing ODs. However, a linear correlation was maintained until OD 0.05, while at OD 0.1 the number of adherent bacteria seemed to reach a plateau. Therefore, the assay conditions can be controlled until OD 0.05. **Fig. 29** shows the biological reproducibility between two experiments performed on different days. **Fig. 30** confirms the technical reproducibility within the same experiment.

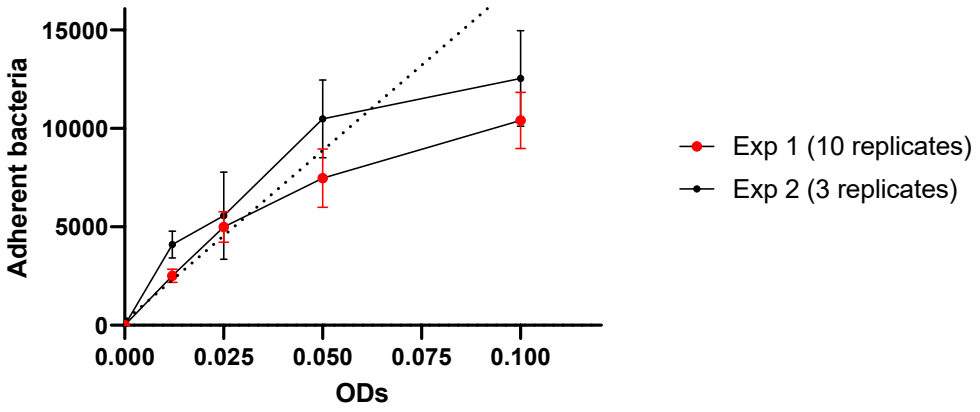

Figure 29. Correlation analysis between bacterial input OD (X axis) and number of adherent bacteria (Y axis). *The dotted line shows the theoretical linear correlation between the two values. The graph shows mean values and standard deviations of at least 3 technical replicates for each experiment.*

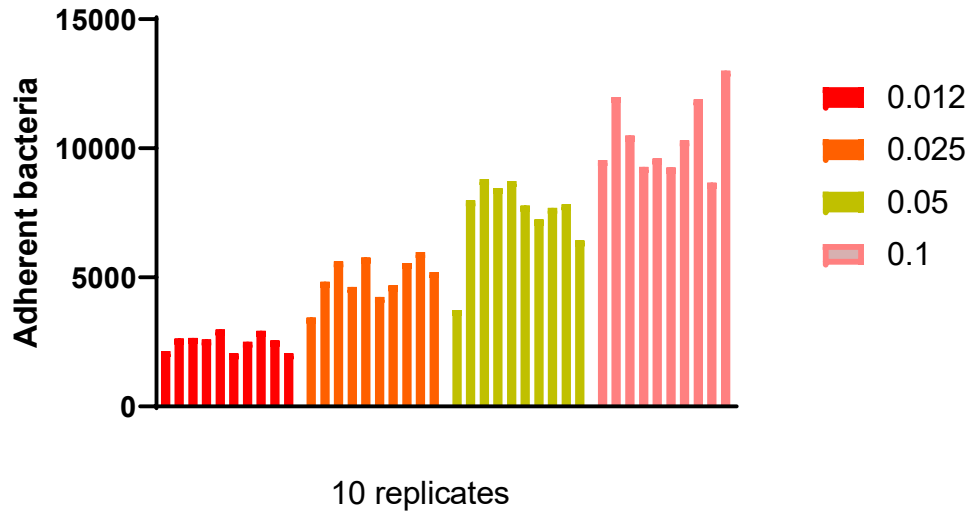

Figure 30. Analysis of the technical reproducibility of vAIA with 10 replicates for each OD. *The graph shows on the Y axis the number of adherent bacteria counted for*

each condition. The tested ODs are 0.012 (red), 0.025 (orange), 0.05 (yellow), 0.1 (pink).

To determine whether vAIA could be used for mAbs testing, the ability of an anti-gonococcus polyclonal serum to inhibit the adhesion of bacteria was evaluated. The serum was obtained from mice immunized with GMMA (Generalized Modules for Membrane Antigens) from FA1090 and was used in different dilutions to pre-incubate FA1090 before infecting SV-HUC-1 cells. The serum obtained from mice immunized with alum was used as a negative control. **Fig. 31a** shows inhibition of bacterial adhesion by the anti-FA1090 GMMA serum. Indeed, the number of adherent bacteria decreased upon addition of increasing concentrations of serum. However, when the experiment was repeated (**Fig. 31 b, c**), the effect was variable or not detectable and overall hardly reproducible.

Since treatment with polyclonal serum did not result in satisfying data, anti-gonococcus phagocytosis-promoting mAb 2C7, which recognizes LOS, and mAb_64 with unknown target were tested together with an unrelated mAb and the no mAb condition at concentration of 10 μg/ml for inhibition of adhesion (**Fig. 32**). Unfortunately, also in this case, no effect was observed.

a)

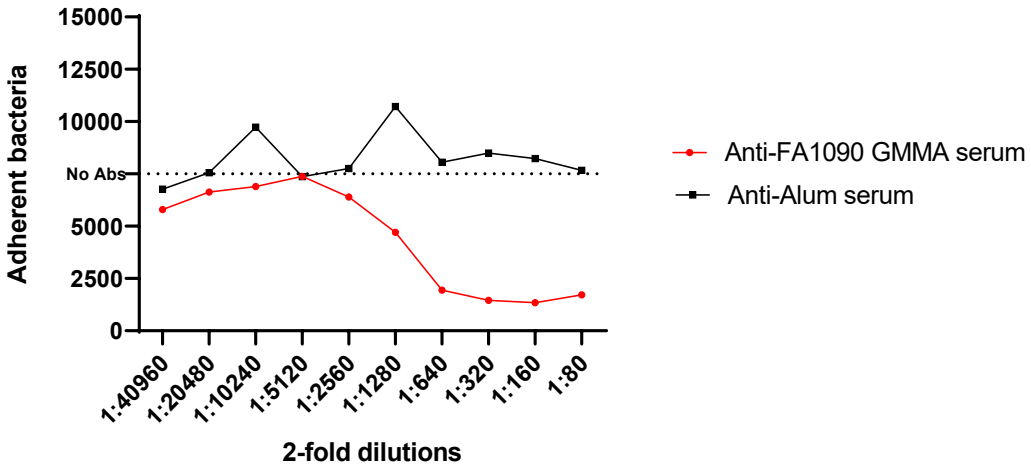

b)

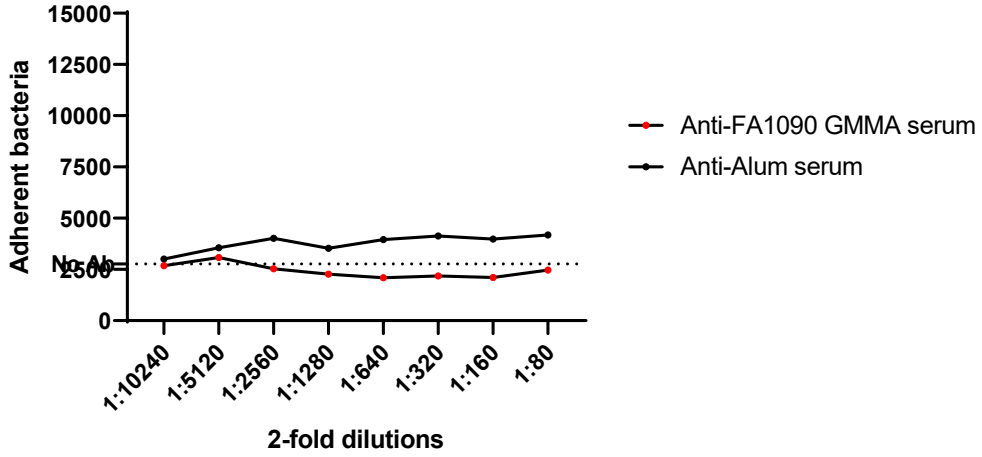

c)

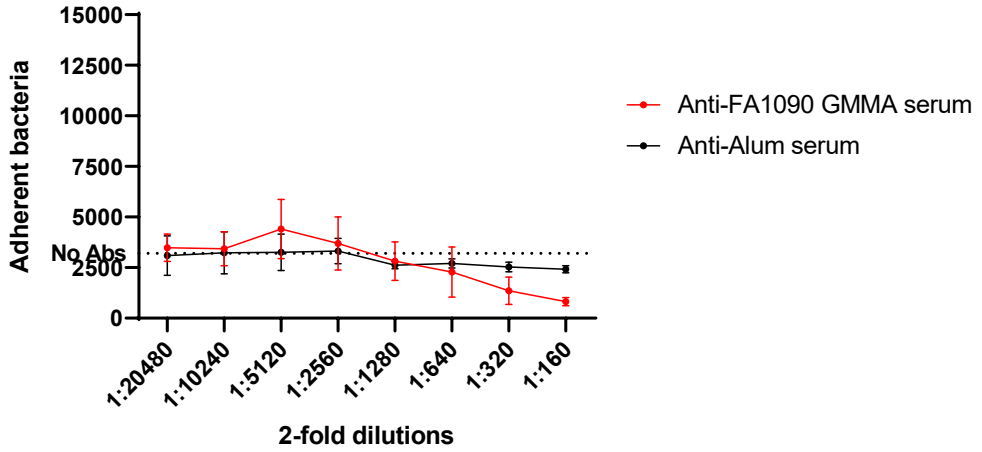

Figure 31. Quantification of adherent bacteria in the presence of the anti-FA1090 GMMA serum and anti-alum serum. *Panels a, b and c show results obtained in three different experiments, performed on different days.*

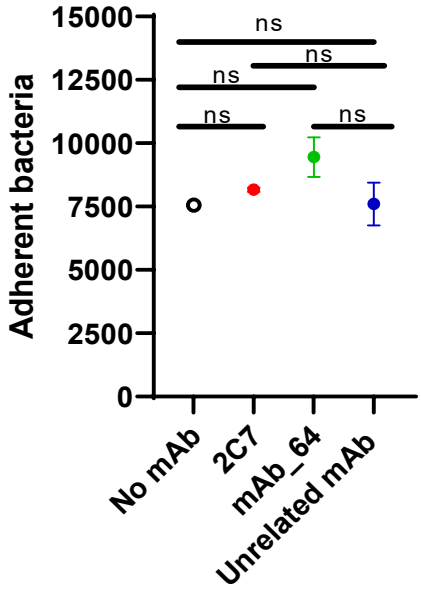

Figure 32. Quantification of adherent bacteria in the presence of anti-gonococcal phagocytosis-promoting mAbs 2C7 and mAb_64. *mAbs were tested at 10 µg/ml and compared with an unrelated mAb and with the no mAb condition. The Y axis reports the number of adherent bacteria. ns, not significant.*

Discussion

In this Chapter I described the visual adhesion inhibition assay, an assay which is meant to measure the ability of mAbs and polyclonal sera to reduce the adhesion of *N. gonorrhoeae* onto urethral epithelial cells SV-HUC-1. The assay was carried out on imaging plates, with bacteria expressing GFP (FA1090::sfGFP) constitutively and cells stained for nuclei and membranes. Once infection was performed, images were acquired using Opera Phenix. The image analysis pipeline applied here quantified the number of bacteria adhering to the cell membrane. Being SV-HUC-1 adherent cells, once plated they grew for three days while forming junctions, which allowed cells to be attached one to the other. For image analysis purposes, rather than quantifying the number of cells (nuclei) I quantified the confluence, that is, the area occupied by cells. In addition, I optimized the plating conditions to achieve the same confluence of cells, to ensure reproducibility of results. Adhering bacteria were counted based on the GFP signal which colocalized with the CellMask Deep red signal, which stained the membrane. If an antibody that binds to bacterial surface factors involved in adhesion interfered with the binding of the bacteria to the host cells, this would translate into a reduced number of adherent bacteria. This assay presented two limitations: the first

consisted in the lack of an effective positive control to validate the assay and the second was related to the limitations associated with the immortalized cell line used as a model. In the first case, a polyclonal serum was supposed to act as a positive control to validate vAIA. Although treatment with serum reduced the number of adherent bacteria, results were inconsistent and not reproducible. This could be ascribed to the antigen and phase variability of bacterial surface structures involved in adhesion. Two mAbs, 2C7 and mAb_64, who showed the highest phagocytosis promoting activity in vOPA, were tested but showed no effect in vAIA. Given the absence of a robust positive control, I cannot exclude that the assay conditions were not sufficiently reliable to test mAbs and conclude they have no efficacy in reducing adhesion. Secondly, using an immortalized cell line may not be sufficient to mimic the site of infection. Cells are not polarized, thus may lack surface components necessary for proficient interaction with bacteria. Future efforts should be directed towards investigating other cellular or multicellular models (organoids for example) and find appropriate positive controls for the inhibition of bacterial adhesion to the cell surface.

Experimental procedures

Cell cultures

Simian Virus Human Urethral cell line SV-HUC-1 (ATCC, Manassas, Virginia, USA) were cultured in F-12K Medium (Kaighn's Modification of Ham's F-12 Medium) (ATCC), 10% fetal bovine serum (Gibco) at 37°C and 5% CO_2. Cells were passaged three times per week and kept at a density below 1×10^6 cells per ml. Cells were plated in Greiner CELLSTAR® 96-well plates, flat bottom black polystyrene wells with micro-clear bottom (Sigma-Aldrich) at the density of 35,000 cells / well and left for three days at 37°C and 5% CO_2.

Bacterial strains and culture conditions

N. gonorrhoeae strain FA1090 was used in this study and was cultured on gonococcal medium base liquid or agar (Difco™ GC Medium Base) plus Isovitalex (BD Biosciences). The strain was typically grown at 37°C and 5% CO_2 for approximately 15 hours. The strain was engineered to express a superfolder green fluorescent protein (sfGFP) by integration of the encoding gene into the chromosome. The modified strain is called FA1090::sfGFP. The gene was inserted in the genome using an integrative vector (please see Chapter 1 of this thesis "Generation of knock-in strains of *N. gonorrhoeae* expressing fluorescent proteins for high-content imaging" for details).

Prior to cell infection, bacteria were suspended in gonococcal liquid medium containing Isovitalex and grown at 37°C to mid-logarithmic phase.

Visual Adhesion Inhibition Assay (vAIA)

SVHUC-1 cells were seeded into 96-well plates as described above and after 3 days of growth were infected with FA1090::sfGFP. FA1090::sfGFP was grown to mid-logarithmic phase and pre-incubated with sera/mAbs with a final OD of 0.05 in RPMI medium. Serum obtained from mice immunized with GMMA (Generalized Modules for Membrane Antigens) from FA1090 was used in different dilutions to pre-incubate FA1090 before infecting SVHUC-1. Serum obtained from mice immunized with alum was used as negative control. Both were gifts from GSK Research center, Siena. After 30 minutes of pre-incubation, the mixture composed of mAbs and bacteria was added onto SVHUC-1. To synchronise the infection, the 96-well plates were centrifuged for 1 min at 200 xg. After 1 hour of infection, each well was washed 3 times with PBS and fixed with 2% paraformaldehyde (PFA) for 15 minutes. CellMask™ Deep Red stain (Invitrogen) was used to stain the cell membrane, providing a means to delineate the cell boundary, and DAPI to stain cell nuclei and bacterial DNA.

Confocal microscopy and image analysis

96-well plates were imaged with the microscope Opera Phenix High-Content Screening System (PerkinElmer) using a 40x objective, numerical aperture 1.1, acquiring 20 fields of view per well, and 13 images on the vertical dimension to form a z-stack per each field of view. The image analysis pipeline was developed using Harmony Software of Perkin Elmer (Supplementary Table 5). SVHUC-1 cells were detected by analysing the combined signal of DAPI (nuclei) and CellMask Deep Red (membrane), which allowed quantification of cell confluence. Bacteria were localised and segmented by combining the DAPI and GFP signals. Bacteria that overlapped with the CellMask Deep Red signal of a cell were identified as adherent.

Supplementary material

Supplementary Table 5. *Image analysis pipeline built with Harmony software (Perkin Elmer).*

Building Block	Input	Method	Output	Property prefix
Find nuclei	Channel:DAPI	Method: C	Nuclei	

	ROI: none	Common threshold: 0.41 Area:>30 um^2 Splitting coefficient: 7.0 Individual threshold: 0.39 Contrast:>0.11		
Find Image region	Channel: CellMask Deep Red ROI: none	Method: Common threshold threshold: 0,50 Split into objects: yes	Image region	
Calculate morphology properties	Population: Image region Region: Image region	Method: Standard Area: yes		Image region
Calculate image		Method: By formula Formula: A-300 Channel A: GFP	Calculated image	
Find spots	Channel: Calculated Image ROI: none	Method: A Relative spot intensity: > 0,030 Splitting sensitivity: 1	Spots	
Calculate morphology properties (2)	Population: Spots Region: Spot	Method: Standard Area: yes		Spot
Select	Population:	Method: Filter	Bacteria	

population	Spots	by property Spot area (um^2)> 0.4		
Select population (2)	Population: Bacteria	Method: Select by Mask Region: Spot Mask population: Image Region Mask region: Image Region Select by: Overlap > 50% Use inverted mask: no	Bacteria adherent	
Select population (3)	Population: Bacteria	Method: Select by Mask Region: Spot Mask population: Image Region Mask region: Image Region Select by: Overlap > 50% Use inverted mask: yes	Bacteria non-adherent	

Define Results

Method: List of Outputs

Population: Spots

Number of Objects

Population: Adherent bacteria

Number of Objects

Population: Non-adherent bacteria

Number of Objects

4. Additional research activity: development of mAbs against SARS-COV-2

At the beginning of 2020, in response to the COVID-19 pandemic caused by the severe acute respiratory syndrome coronavirus 2 (SARS-CoV-2), the laboratory where I have pursued my PhD work was involved in the discovery and production of therapeutic mAbs against the virus. 14 COVID-19 survivors were recruited, from which 4,277 spike protein-specific memory B cells were single-cell sorted. From these cells, 453 neutralizing antibodies were identified and 1.4% of them neutralized the virus with a potency of 1-10 ng/mL. The most potent mAb, named J08, was selected and tested in a hamster model for prophylactic and therapeutic efficacy.

I was involved in this research project for approximately 6 months with the aim of implementing a robust pipeline for antibody expression on the high-throughput scale. In details, primers specific for the amplification of the variable regions of the heavy and light chains of the mAbs were designed according to previously published protocols[5] and used in PCR for generating fragments that were subsequently cloned into suitable vectors for heavy and light chain expression. Transfection of the recombinant plasmids into Expi293 cells in the 96-well format allowed generation of a library of mAbs which were tested in the Biosafety Level 3 (BSL3) laboratory against the authentic virus. The cloning pipeline that I contributed to optimize was then used in other research projects in the laboratory, including the one focused on the identification of mAbs against *N. gonorrhoeae*. The work on SARS-CoV-2 was published in Andreano et al, Cell, 2021 (see Publication list).

Conclusions and future perspectives

During my PhD studies I developed tools and two image-based assays to support discovery and development of mAbs against *N. gonorrhoeae.* Rather than relying on traditional assays based on CFU counting, flow cytometry or microplate readers, I exploited the high-throughput and high-content capabilities of the confocal microscope Opera Phenix. First, I engineered *N. gonorrhoeae* strain FA1090 to express sfGFP and, after checking bacterial fitness upon GFP expression, I used the strain in cell-based assays, vOPA and vAIA. These assays investigate the capacity of mAbs to interfere with bacterial pathogenesis, that is, the ability of mAbs to promote phagocytosis (vOPA) or inhibit adhesion of bacteria to cells (vAIA).

Overall, I demonstrated that the confocal microscope Opera Phenix represents a useful tool that can accelerate the evaluation of mAb activity thanks to the high-throughput capability. In particular:

- Opera can quantify the fluorescence of FA1090::sfGFP at the single-cell level and the fluorescence values obtained can be indicators of bacterial fitness. In fact, when bacteria were subjected to conditions that promoted death, fluorescence was drastically reduced.
- Opera can quantify the phagocytic activity of macrophage-like THP-1 cells and help the screening of an array of mAbs for their ability to promote this process.
- Opera can quantify the adhesion of bacteria onto epithelial cells.

In all cases, the high-content features of the microscope provided multiple readouts and metrics that were used for measuring the robustness of the assays that I carried out.

Moreover, I identified some factors which I value as instrumental for the establishment and the optimization of functional assays for anti-bacterial mAbs, especially those based on digital imaging. These are:

- Importance of appropriate positive and negative controls to validate the assay. 2C7 proved to be an excellent positive control for vOPA and allowed to choose the best infection conditions to have a robust assay. vAIA instead, which lacked a valid positive control, was not efficient enough to evaluate the functionality of mAbs.
- Importance of cell models, especially for adhesion assays which imply interaction between bacteria and host cell surface receptors.
- Close cooperation between laboratory scientists and data scientists for image analysis. During my work in Fondazione Toscana Life Sciences, I benefitted

from the interaction with the Data Science for Health Laboratory (DaScH-Lab) whose members provided me with the necessary expertise for proper data mining.

I believe that this work could represent a reference for those who would like to use high-throughput and high-content microscopy to study host-pathogen interactions and define functional assays for the assessment of mAb activity. For instance, the assays that I presented here have been already applied to *Klebsiella pneumoniae* and to *Shigella* spp. by my laboratory colleagues.

In the future, vOPA will be expanded by including more mAbs and a larger panel of strains which may express GFP or other fluorescent proteins or may be stained using commercial fluorescent reagents if not amenable to transformation.
Combinations of anti-*N. gonorrhoeae* mAbs, which can be designed based on the target antigens, could be tested too to assess the impact on bacterial engulfment, survival and replication inside macrophages. One aspect which was not deeply investigated here is the fate of phagocytosed bacteria. This point needs to be explored first by means of standard experiments which rely on CFU counting and then extended to microscope imaging. In the latter case, co-localization of bacteria with early and late phagosome markers could instruct on bacterial survival and replication inside cells.
Finally, another interesting perspective is the combination of commercially available antimicrobials with mAbs in order to favour macrophage-dependent uptake and killing. Targeted delivery of the antimicrobial could be achieved by exploiting the specificity of the mAb in antibody-drug conjugates, such as those designed against *Staphylococcus aureus*[151].

Publication list

1. **Vacca, F**.; Sala, C.; Rappuoli, R. Monoclonal Antibodies for Bacterial Pathogens: Mechanisms of Action and Engineering Approaches for Enhanced Effector Functions. Biomedicines **2022**, *10*,2126.https://doi.org/10.3390/biomedicines10092126
2. **Vacca F**, Cardamone D, Troisi M, Sala C and Rappuoli R (2020) Antimicrobial Resistance: A Tale of Nasty Enemies and Powerful Weapons. Front. Young Minds. 8:554493. doi: 10.3389/frym.2020.554493.
3. Andreano E, Nicastri E, Paciello I, Pileri P, Manganaro N, Piccini G, Manenti A, Pantano E, Kabanova A, Troisi M, **Vacca F**, Cardamone D, De Santi C, Torres JL,Ozorowski G, Benincasa L, Jang H, Di Genova C, Depau L, Brunetti J, Agrati C, Capobianchi MR, Castilletti C, Emiliozzi A, Fabbiani M, Montagnani F, Bracci L, Sautto G, Ross TM, Montomoli E, Temperton N, Ward AB, Sala C, Ippolito G, Rappuoli R. Extremely potent human monoclonal antibodies from COVID-19 convalescent patients. Cell. 2021 Apr 1;184(7):1821-1835.e16. doi: 10.1016/j.cell.2021.02.035.
4. **Vacca F**. et al. Development of a novel visual opsono-phagocytosis screening assay for monoclonal antibodies against *Neisseria gonorrhoeae*. *Manuscript in preparation*.

References

1. Wang XY, Wang B, Wen YM. From therapeutic antibodies to immune complex vaccines. NPJ Vaccines. 2019 Jan 17;4:2. doi: 10.1038/s41541-018-0095-z. PMID: 30675393; PMCID: PMC6336872.
2. Lipman NS, Jackson LR, Trudel LJ, Weis-Garcia F. Monoclonal versus polyclonal antibodies: distinguishing characteristics, applications, and information resources. ILAR J. 2005;46(3):258-68. doi: 10.1093/ilar.46.3.258. PMID: 15953833.
3. Alberts B, Johnson A, Lewis J, et al. Molecular Biology of the Cell. 4th edition. New York: Garland Science; 2002. B Cells and Antibodies. Available from: https://www.ncbi.nlm.nih.gov/books/NBK26884/ ,.
4. Viau M, Zouali M. B-lymphocytes, innate immunity, and autoimmunity. Clin Immunol. 2005 Jan;114(1):17-26. doi: 10.1016/j.clim.2004.08.019. PMID: 15596405.
5. Tiller T, Meffre E, Yurasov S, Tsuiji M, Nussenzweig MC, Wardemann H. Efficient generation of monoclonal antibodies from single human B cells by single cell RT-PCR and expression vector cloning. J Immunol Methods. 2008 Jan 1;329(1-2):112-24. doi: 10.1016/j.jim.2007.09.017. Epub 2007 Oct 31. Erratum in: J Immunol Methods. 2008 May 20;334(1-2):142. PMID: 17996249; PMCID: PMC2243222.
6. Janeway CA Jr, Travers P, Walport M, et al. Immunobiology: The Immune System in Health and Disease. 5th edition. New York: Garland Science; 2001. The distribution and functions of immunoglobulin isotypes. Available from: https://www.ncbi.nlm.nih.gov/books/NBK27162/.
7. Hifumi T, Yamamoto A, Ato M, Sawabe K, Morokuma K, Morine N, Kondo Y, Noda E, Sakai A, Takahashi J, Umezawa K. Clinical Serum Therapy: Benefits, Cautions, and Potential Applications. Keio J Med. 2017 Dec 25;66(4):57-64. doi: 10.2302/kjm.2016-0017-IR. Epub 2017 Apr 28. PMID: 28450682.
8. Wang H, Chen D, Lu H. Anti-bacterial monoclonal antibodies: next generation therapy against superbugs. Appl Microbiol Biotechnol. 2022 Jun;106(11):3957-3972. doi: 10.1007/s00253-022-11989-w. Epub 2022 Jun 1. PMID: 35648146.
9. Chiu ML, Goulet DR, Teplyakov A, Gilliland GL. Antibody Structure and Function: The Basis for Engineering Therapeutics. Antibodies (Basel). 2019 Dec 3;8(4):55. doi: 10.3390/antib8040055. PMID: 31816964; PMCID: PMC6963682.
10. Proetzel G, Roopenian DC. Humanized FcRn mouse models for evaluating pharmacokinetics of human IgG antibodies. Methods. 2014 Jan 1;65(1):148-53.

doi: 10.1016/j.ymeth.2013.07.005. Epub 2013 Jul 16. PMID: 23867339; PMCID: PMC3858440.

11. Vacca F, Sala C, Rappuoli R. Monoclonal Antibodies for Bacterial Pathogens: Mechanisms of Action and Engineering Approaches for Enhanced Effector Functions. Biomedicines. 2022 Aug 30;10(9):2126. doi: 10.3390/biomedicines10092126. PMID: 36140226; PMCID: PMC9496014.
12. Lu LL, Suscovich TJ, Fortune SM, Alter G. Beyond binding: antibody effector functions in infectious diseases. Nat Rev Immunol. 2018 Jan;18(1):46-61. doi: 10.1038/nri.2017.106. Epub 2017 Oct 24. PMID: 29063907; PMCID: PMC6369690.
13. Boes M. Role of natural and immune IgM antibodies in immune responses. Mol Immunol. 2000 Dec;37(18):1141-9. doi: 10.1016/s0161-5890(01)00025-6. PMID: 11451419.
14. Chen K, Cerutti A. The function and regulation of immunoglobulin D. Curr Opin Immunol. 2011 Jun;23(3):345-52. doi: 10.1016/j.coi.2011.01.006. Epub 2011 Feb 24. PMID: 21353515; PMCID: PMC3109135.
15. Vidarsson G, Dekkers G, Rispens T. IgG subclasses and allotypes: from structure to effector functions. Front Immunol. 2014 Oct 20;5:520. doi: 10.3389/fimmu.2014.00520. PMID: 25368619; PMCID: PMC4202688.
16. Al Qaraghuli MM, Kubiak-Ossowska K, Ferro VA, Mulheran PA. Antibody-protein binding and conformational changes: identifying allosteric signalling pathways to engineer a better effector response. Sci Rep. 2020 Aug 13;10(1):13696. doi: 10.1038/s41598-020-70680-0. PMID: 32792612; PMCID: PMC7426963.
17. Ausserwöger, H., Schneider, M.M., Herling, T.W. et al. Non-specificity as the sticky problem in therapeutic antibody development. Nat Rev Chem (2022). https://doi.org/10.1038/s41570-022-00438-x.
18. Dondelinger M, Filée P, Sauvage E, Quinting B, Muyldermans S, Galleni M, Vandevenne MS. Understanding the Significance and Implications of Antibody Numbering and Antigen-Binding Surface/Residue Definition. Front Immunol. 2018 Oct 16;9:2278. doi: 10.3389/fimmu.2018.02278. PMID: 30386328; PMCID: PMC6198058.
19. Zhao, Jun et al. “Antigen binding allosterically promotes Fc receptor recognition.” mAbs vol. 11,1 (2019): 58-74. doi:10.1080/19420862.2018.1522178.
20. Wang X, Mathieu M, Brezski RJ. IgG Fc engineering to modulate antibody effector functions. Protein Cell. 2018 Jan;9(1):63-73. doi: 10.1007/s13238-017-0473-8. Epub 2017 Oct 6. PMID: 28986820; PMCID: PMC5777978.

21. Auzin A, Spits M, Tacconelli E, Rodríguez-Baño J, Hulscher M, Adang E, Voss A, Wertheim H. What is the evidence base of used aggregated antibiotic resistance percentages to change empiric antibiotic treatment? A scoping review. Clin Microbiol Infect. 2021 Dec 11:S1198-743X(21)00700-X. doi: 10.1016/j.cmi.2021.12.003.
22. Bielicki JA, Cromwell DA, Sharland M. Fifteen-minute consultation: the complexities of empirical antibiotic selection for serious bacterial infections-a practical approach. Arch Dis Child Educ Pract Ed. 2017 Jun;102(3):117-123. doi: 10.1136/archdischild-2016-310527. Epub 2016 Nov 22. PMID: 27879280.
23. Dadgostar P. Antimicrobial Resistance: Implications and Costs. Infect Drug Resist. 2019 Dec 20;12:3903-3910. doi: 10.2147/IDR.S234610. PMID: 31908502; PMCID: PMC6929930..
24. Neto RM, Ansaldi MA Jr, da Costa ME, da Silva SO Jr, Luz VH. A case report of a multi-drug resistant bacterial infection in a diabetic patient treated in northeast Brazil. Diabet Foot Ankle. 2012;3. doi: 10.3402/dfa.v3i0.18656. Epub 2012 Jun 26. PMID: 22745851; PMCID: PMC3384988.
25. Unemo M, Jensen JS. Antimicrobial-resistant sexually transmitted infections: gonorrhoea and Mycoplasma genitalium. Nat Rev Urol. 2017 Mar;14(3):139-152. doi: 10.1038/nrurol.2016.268. Epub 2017 Jan 10. PMID: 28072403.
26. Spits M, Tacconelli E, Rodríguez-Baño J, Hulscher M, Adang E, Voss A, Wertheim H. What is the evidence base of used aggregated antibiotic resistance percentages to change empiric antibiotic treatment? A scoping review. Clin Microbiol Infect. 2021 Dec 11:S1198-743X(21)00700-X. doi: 10.1016/j.cmi.2021.12.003.
27. Aitolo GL, Adeyemi OS, Afolabi BL, Owolabi AO. Neisseria gonorrhoeae Antimicrobial Resistance: Past to Present to Future. Curr Microbiol. 2021 Mar;78(3):867-878. doi: 10.1007/s00284-021-02353-8. Epub 2021 Feb 2. PMID: 33528603.
28. Correia IR. Stability of IgG isotypes in serum. MAbs. 2010 May-Jun;2(3):221-32. doi: 10.4161/mabs.2.3.11788. Epub 2010 May 16. PMID: 20404539; PMCID: PMC2881250.
29. Berry JD, Gaudet RG (2011) Antibodies in infectious diseases: polyclonals, monoclonals and niche biotechnology. New Biotechnol 28(5):489–501. https://doi.org/10.1016/j.nbt.2011.03.018.
30. Luciani M, Lannetti L (2017) Monoclonal antibodies and bacterial virulence. Virulence 8(6):635–636. https://doi.org/10.1080/21505594.2017.1292199.

31. Martín-Galiano AJ, McConnell MJ. Using Omics Technologies and Systems Biology to Identify Epitope Targets for the Development of Monoclonal Antibodies Against Antibiotic-Resistant Bacteria. Front Immunol. 2019 Dec 10;10:2841. doi: 10.3389/fimmu.2019.02841. PMID: 31921119; PMCID: PMC6914692.
32. LiverTox: Clinical and Research Information on Drug-Induced Liver Injury [Internet]. Bethesda (MD): National Institute of Diabetes and Digestive and Kidney Diseases; 2012–. Monoclonal Antibodies. 2022 Jul 12. PMID: 31644151.
33. Wagner EK, Maynard JA (2018) Engineering therapeutic antibodies to combat infectious diseases. Curr Opin Chem Eng 19:131–141. https://doi.org/10.1016/j.coche.2018.01.007.
34. Mazumdar S. Raxibacumab. MAbs. 2009 Nov-Dec;1(6):531-8. doi: 10.4161/mabs.1.6.10195. Epub 2009 Nov 29. PMID: 20068396; PMCID: PMC2791309.
35. Greig SL. Obiltoxaximab: First Global Approval. Drugs. 2016 May;76(7):823-30. doi: 10.1007/s40265-016-0577-0. PMID: 27085536.
36. Navalkele BD, Chopra T. Bezlotoxumab: an emerging monoclonal antibody therapy for prevention of recurrent Clostridium difficile infection. Biologics. 2018 Jan 18;12:11-21. doi: 10.2147/BTT.S127099. PMID: 29403263; PMCID: PMC5779312.
37. Pelfrene E, Mura M, Cavaleiro Sanches A, Cavaleri M. Monoclonal antibodies as anti-infective products: a promising future? Clin Microbiol Infect. 2019 Jan;25(1):60-64. doi: 10.1016/j.cmi.2018.04.024. Epub 2018 Apr 30. PMID: 29715552; PMCID: PMC7128139.
38. Zurawski DV, McLendon MK. Monoclonal Antibodies as an Antibacterial Approach Against Bacterial Pathogens. Antibiotics (Basel). 2020 Apr 1;9(4):155. doi: 10.3390/antibiotics9040155. PMID: 32244733; PMCID: PMC7235762.
39. Liu B, Park S, Thompson CD, Li X, Lee JC. Antibodies to Staphylococcus aureus capsular polysaccharides 5 and 8 perform similarly in vitro but are functionally distinct in vivo. Virulence. 2017 Aug 18;8(6):859-874. doi: 10.1080/21505594.2016.1270494. Epub 2016 Dec 9. PMID: 27936346; PMCID: PMC5626342.
40. Sause WE, Buckley PT, Strohl WR, Lynch AS, Torres VJ. Antibody-Based Biologics and Their Promise to Combat Staphylococcus aureus Infections. Trends Pharmacol Sci. 2016 Mar;37(3):231-241. doi: 10.1016/j.tips.2015.11.008. Epub 2015 Dec 22. PMID: 26719219; PMCID: PMC4764385.

41. Pelegrin M, Naranjo-Gomez M, Piechaczyk M. Antiviral Monoclonal Antibodies: Can They Be More Than Simple Neutralizing Agents? Trends Microbiol. 2015 Oct;23(10):653-665. doi: 10.1016/j.tim.2015.07.005. PMID: 26433697; PMCID: PMC7127033.
42. DiLillo DJ, Ravetch JV. Fc-Receptor Interactions Regulate Both Cytotoxic and Immunomodulatory Therapeutic Antibody Effector Functions. Cancer Immunol Res. 2015 Jul;3(7):704-13. doi: 10.1158/2326-6066.CIR-15-0120. PMID: 26138698.
43. Mitra S, Tomar PC. Hybridoma technology; advancements, clinical significance, and future aspects. J Genet Eng Biotechnol. 2021 Oct 18;19(1):159. doi: 10.1186/s43141-021-00264-6. PMID: 34661773; PMCID: PMC8521504.
44. Lanzavecchia A, Frühwirth A, Perez L, Corti D. Antibody-guided vaccine design: identification of protective epitopes. Curr Opin Immunol. 2016 Aug;41:62-67. doi: 10.1016/j.coi.2016.06.001. Epub 2016 Jun 22. PMID: 27343848.
45. Malito E, Carfi A, Bottomley MJ. Protein Crystallography in Vaccine Research and Development. Int J Mol Sci. 2015 Jun 9;16(6):13106-40. doi: 10.3390/ijms160613106. PMID: 26068237; PMCID: PMC4490488..
46. Rappuoli R, Bottomley MJ, D'Oro U, Finco O, De Gregorio E. Reverse vaccinology 2.0: Human immunology instructs vaccine antigen design. J Exp Med. 2016 Apr 4;213(4):469-81. doi: 10.1084/jem.20151960. Epub 2016 Mar 28. PMID: 27022144; PMCID: PMC4821650.
47. Mora M, Veggi D, Santini L, Pizza M, Rappuoli R. Reverse vaccinology. Drug Discov Today. 2003 May 15;8(10):459-64. doi: 10.1016/s1359-6446(03)02689-8. PMID: 12801798.
48. Chesson HW, Mayaud P, Aral SO. Sexually Transmitted Infections: Impact and Cost-Effectiveness of Prevention. In: Holmes KK, Bertozzi S, Bloom BR, et al., editors. Major Infectious Diseases. 3rd edition. Washington (DC): The International Bank for Reconstruction and Development / The World Bank; 2017 Nov 3. Chapter 10. Available from: https://www.ncbi.nlm.nih.gov/books/NBK525195/ doi: 10.1596/978-1-4648-0524-0_ch10.
49. Leone PA. Epidemiology, pathogenesis and clinical manifestations of Neisseria gonorrhoeae infection. April 2013. Available: www.uptodate.com/contents/epidemiology-pathogenesis-and-clinical-manifestations-of-neisseria-gonorrhoeae-infection?source=see_link#H4 (accessed Nov. 8, 2013.

50. Jose PP, Vivekanandan V, Sobhanakumari K. Gonorrhea: Historical outlook. J Skin Sex Transm Dis 2020;2(2):110-4.
51. Springer C, Salen P. Gonorrhea. [Updated 2022 Apr 21]. In: StatPearls [Internet]. Treasure Island (FL): StatPearls Publishing; 2022 Jan-. Available from: https://www.ncbi.nlm.nih.gov/books/NBK558903/.
52. www.who.int/news-room/fact-sheets/detail/multi-drug-resistant-gonorrhoea.
53. National Overview-Sexually Transmitted Disease Surveillance. [(accessed on 10 September 2021)];2019 Available online: https://www.cdc.gov/std/statistics/2019/overview.htm.
54. European Centre for Disease Prevention and Control. Gonorrhoea. In: ECDC. Annual epidemiological report for 2018. Stockholm: ECDC; 2020.
55. Mendes, Ana Clara et al. "Epithelial Haven and Autophagy Breakout in Gonococci Infection." Frontiers in cell and developmental biology vol. 8 439. 9 Jun. 2020, doi:10.3389/fcell.2020.00439.
56. Walker, Cheryl K, and Richard L Sweet. "Gonorrhea infection in women: prevalence, effects, screening, and management." International journal of women's health vol. 3 (2011): 197-206. doi:10.2147/IJWH.S13427.
57. Haese, Ethan C et al. "Vaccine Candidates for the Control and Prevention of the Sexually Transmitted Disease Gonorrhea." Vaccines vol. 9,7 804. 20 Jul. 2021, doi:10.3390/vaccines9070804.
58. Seib KL. Gonorrhoea vaccines: a step in the right direction. Lancet. 2017 Sep 30;390(10102):1567-1569. doi: 10.1016/S0140-6736(17)31605-7. Epub 2017 Jul 10. PMID: 28705461.
59. Quillin SJ, Seifert HS. Neisseria gonorrhoeae host adaptation and pathogenesis. Nat Rev Microbiol. 2018 Apr;16(4):226-240. doi: 10.1038/nrmicro.2017.169. Epub 2018 Feb 12. PMID: 29430011; PMCID: PMC6329377.
60. Lenz, Jonathan D, and Joseph P Dillard. "Pathogenesis of Neisseria gonorrhoeae and the Host Defense in Ascending Infections of Human Fallopian Tube." Frontiers in immunology vol. 9 2710. 21 Nov. 2018, doi:10.3389/fimmu.2018.02710.
61. Criss, Alison K et al. "Challenges and Controversies Concerning Neisseria gonorrhoeae-Neutrophil Interactions in Pathogenesis." mBio vol. 12,3 (2021): e0072121. doi:10.1128/mBio.00721-21.
62. Guvenc, Furkan et al. "Intimate Relations: Molecular and Immunologic Interactions Between Neisseria gonorrhoeae and HIV-1." Frontiers in microbiology vol. 11 1299. 3 Jun. 2020, doi:10.3389/fmicb.2020.01299.

63. Unemo M, Seifert HS, Hook EW 3rd, Hawkes S, Ndowa F, Dillon JR. Gonorrhoea. Nat Rev Dis Primers. 2019 Nov 21;5(1):79. doi: 10.1038/s41572-019-0128-6. PMID: 31754194.
64. McSheffrey, G. G., & Gray-Owen, S. D. (2015). Neisseria gonorrhoeae. Molecular Medical Microbiology, 1471–1485. doi:10.1016/b978-0-12-397169-2.00082-2.
65. Dempsey, J A et al. "Physical map of the chromosome of Neisseria gonorrhoeae FA1090 with locations of genetic markers, including opa and pil genes." Journal of bacteriology vol. 173,17 (1991): 5476-86. doi:10.1128/jb.173.17.5476-5486.
66. Mercer, Ryan G et al. "Genetic determinants of heat resistance in Escherichia coli." Frontiers in microbiology vol. 6 932. 9 Sep. 2015, doi:10.3389/fmicb.2015.00932.
67. Giltner, Carmen L et al. "Type IV pilin proteins: versatile molecular modules." Microbiology and molecular biology reviews : MMBR vol. 76,4 (2012): 740-72. doi:10.1128/MMBR.00035-12.
68. Kolappan, Subramania et al. "Structure of the Neisseria meningitidis Type IV pilus." Nature communications vol. 7 13015. 4 Oct. 2016, doi:10.1038/ncomms13015.
69. Ribet D, Cossart P. How bacterial pathogens colonize their hosts and invade deeper tissues. Microbes Infect. 2015 Mar;17(3):173-83. doi: 10.1016/j.micinf.2015.01.004. Epub 2015 Jan 29. PMID: 25637951.
70. Plant, Laura J, and Ann-Beth Jonsson. "Type IV pili of Neisseria gonorrhoeae influence the activation of human CD4+ T cells." Infection and immunity vol. 74,1 (2006): 442-8. doi:10.1128/IAI.74.1.442-448.2006.
71. Manish Sadarangani, Andrew J. Pollard, Scott D. Gray-Owen, Opa proteins and CEACAMs: pathways of immune engagement for pathogenic Neisseria, FEMS Microbiology Reviews, Volume 35, Issue 3, May 2011, Pages 498–514.
72. James JF, Swanson J. Studies on gonococcus infection. XIII. Occurrence of color/opacity colonial variants in clinical cultures. Infect Immun. 1978 Jan;19(1):332-40. doi: 10.1128/iai.19.1.332-340.1978. PMID: 415007; PMCID: PMC414084.
73. Bos MP, Hogan D, Belland RJ. Selection of Opa+ Neisseria gonorrhoeae by limited availability of normal human serum. Infect Immun. 1997 Feb;65(2):645-50. doi: 10.1128/iai.65.2.645-650.1997. PMID: 9009326; PMCID: PMC176109.
74. Nassif X. Gonococcal lipooligosaccharide: an adhesin for bacterial dissemination? Trends Microbiol. 2000 Dec;8(12):539-40. doi: 10.1016/s0966-842x(00)01879-5. PMID: 1111574).
75. Ram S, Shaughnessy J, de Oliveira RB, Lewis LA, Gulati S, Rice PA. Gonococcal lipooligosaccharide sialylation: virulence factor and target for novel

immunotherapeutics. Pathog Dis. 2017 Jun 1;75(4):ftx049. doi: 10.1093/femspd/ftx049. PMID: 28460033; PMCID: PMC5449626.

76. Gulati S, McQuillen DP, Mandrell RE, Jani DB, Rice PA. Immunogenicity of Neisseria gonorrhoeae lipooligosaccharide epitope 2C7, widely expressed in vivo with no immunochemical similarity to human glycosphingolipids. J Infect Dis. 1996 Dec;174(6):1223-37. doi: 10.1093/infdis/174.6.1223. Erratum in: J Infect Dis 1997 Apr;175(4):1027. PMID: 8940213.
77. Russell, Michael W et al. "Progress Toward a Gonococcal Vaccine: The Way Forward." Frontiers in immunology vol. 10 2417. 15 Oct. 2019, doi:10.3389/fimmu.2019.02417).
78. Ayala, Patricia et al. "Neisseria gonorrhoeae porin P1.B induces endosome exocytosis and a redistribution of Lamp1 to the plasma membrane." Infection and immunity vol. 70,11 (2002): 5965-71. doi:10.1128/IAI.70.11.5965-5971.2002.
79. Hill, Stuart A, and John K Davies. "Pilin gene variation in Neisseria gonorrhoeae: reassessing the old paradigms." FEMS microbiology reviews vol. 33,3 (2009): 521-30. doi:10.1111/j.1574-6976.2009.00171.
80. Zelewska, Marta A et al. "Phase variable DNA repeats in Neisseria gonorrhoeae influence transcription, translation, and protein sequence variation." Microbial genomics vol. 2,8 e000078. 25 Aug. 2016, doi:10.1099/mgen.0.000078.
81. Mayer LW (1982) Rates in vitro changes of gonococcal colony opacity phenotypes. Infect Immun 37: 481–485.).
82. Virji M. Pathogenic neisseriae: surface modulation, pathogenesis and infection control. Nat Rev Microbiol. 2009 Apr;7(4):274-86. doi: 10.1038/nrmicro2097. PMID: 19287450.
83. Jerse AE, Cohen MS, Drown PM, Whicker LG, Isbey SF, Seifert HS, et al. Multiple gonococcal opacity proteins are expressed during experimental urethral infection in the male. J Exp Med 1994;179:911_20.
84. Lu, P., Wang, S., Lu, Y., Neculai, D., Sun, Q., and Van Der Veen, S. (2019). A subpopulation of intracellular Neisseria gonorrhoeae escapes autophagymediated killing inside epithelial cells. J. Infect. 219, 133–144. doi: 10.1093/infdis/jiy237.
85. Mavrogiorgos, Nikolaos et al. "Activation of NOD receptors by Neisseria gonorrhoeae modulates the innate immune response." Innate immunity vol. 20,4 (2014): 377-89. doi:10.1177/1753425913493453).
86. Edwards JL, Jennings MP, Seib KL. Neisseria gonorrhoeae vaccine development: hope on the horizon? Curr Opin Infect Dis. 2018 Jun;31(3):246-250. doi: 10.1097/QCO.0000000000000450. PMID: 29601324.

87. Sintsova, Anna et al. “Global analysis of neutrophil responses to Neisseria gonorrhoeae reveals a self-propagating inflammatory program.” PLoS pathogens vol. 10,9 e1004341. 4 Sep. 2014, doi:10.1371/journal.ppat.1004341.
88. Domínguez-Díaz, Carolina et al. “To Trap a Pathogen: Neutrophil Extracellular Traps and Their Role in Mucosal Epithelial and Skin Diseases.” Cells vol. 10,6 1469. 11 Jun. 2021, doi:10.3390/cells10061469.
89. Yunna C, Mengru H, Lei W, Weidong C. Macrophage M1/M2 polarization. Eur J Pharmacol. 2020 Jun 15;877:173090. doi: 10.1016/j.ejphar.2020.173090. Epub 2020 Mar 29. PMID: 32234529.
90. Escobar, Alejandro et al. “Neisseria gonorrhoeae induces a tolerogenic phenotype in macrophages to modulate host immunity.” Mediators of inflammation vol. 2013 (2013): 127017. doi:10.1155/2013/127017.
91. Château, Alice, and H Steven Seifert. “Neisseria gonorrhoeae survives within and modulates apoptosis and inflammatory cytokine production of human macrophages.” Cellular microbiology vol. 18,4 (2016): 546-60. doi:10.1111/cmi.12529.
92. Ritter, Jessica Leigh, and Caroline Attardo Genco. “Neisseria gonorrhoeae-Induced Inflammatory Pyroptosis in Human Macrophages is Dependent on Intracellular Gonococci and Lipooligosaccharide.” Journal of cell death vol. 11 1179066017750902. 3 Jan. 2018, doi:10.1177/1179066017750902.
93. Zhu, Weiyan et al. “Neisseria gonorrhoeae suppresses dendritic cell-induced, antigen-dependent CD4 T cell proliferation.” PloS one vol. 7,7 (2012): e41260. doi:10.1371/journal.pone.0041260.
94. Tapchaisri, P, and S Sirisinha. “Serum and secretory antibody responses to Neisseria gonorrhoeae in patients with gonococcal infections.” The British journal of venereal diseases vol. 52,6 (1976): 374-80. doi:10.1136/sti.52.6.374.
95. Liu, Y et al. “Experimental vaccine induces Th1-driven immune responses and resistance to Neisseria gonorrhoeae infection in a murine model.” Mucosal immunology vol. 10,6 (2017): 1594-1608. doi:10.1038/mi.2017.11.
96. Boulton IC, Gray-Owen SD. Neisserial binding to CEACAM1 arrests the activation and proliferation of CD4+ T lymphocytes. Nat Immunol. 2002 Mar;3(3):229-36. doi: 10.1038/ni769. Epub 2002 Feb 19. PMID: 11850628.
97. So NS, Ostrowski MA, Gray-Owen SD. Vigorous response of human innate functioning IgM memory B cells upon infection by Neisseria gonorrhoeae. J Immunol. 2012 Apr 15;188(8):4008-22. doi: 10.4049/jimmunol.1100718. Epub 2012 Mar 16. PMID: 22427638.

98. Li, Guocai et al. “Antibodies with higher bactericidal activity induced by a Neisseria gonorrhoeae Rmp deletion mutant strain.” PloS one vol. 9,3 e90525. 4 Mar. 2014, doi:10.1371/journal.pone.0090525.
99. Callaghan, Melanie M et al. “Secretion of Chromosomal DNA by the Neisseria gonorrhoeae Type IV Secretion System.” Current topics in microbiology and immunology vol. 413 (2017): 323-345. doi:10.1007/978-3-319-75241-9_13.
100. Chbib, Christiane et al. “Potential Applications of Microparticulate-Based Bacterial Outer Membrane Vesicles (OMVs) Vaccine Platform for Sexually Transmitted Diseases (STDs): Gonorrhea, Chlamydia, and Syphilis.” Vaccines vol. 9,11 1245. 27 Oct. 2021, doi:10.3390/vaccines9111245.
101. Fifer H, Natarajan U, Jones L, Alexander S, Hughes G, Golparian D, Unemo M. Failure of Dual Antimicrobial Therapy in Treatment of Gonorrhea. N Engl J Med. 2016 Jun 23;374(25):2504-6. doi: 10.1056/NEJMc1512757).
102. Magnus Unemo, Monica M Lahra, Martina Escher, Sergey Eremin, Michelle J Cole, Patricia Galarza, Francis Ndowa, Irene Martin, Jo-Anne R Dillon, Marcelo Galas, Pilar Ramon-Pardo, Hillard Weinstock, Teodora Wi, WHO global antimicrobial resistance surveillance for Neisseria gonorrhoeae 2017–18: a retrospective observational study, The Lancet Microbe, Volume 2, Issue 11, 2021, Pages e627-e636, ISSN 2666-5247,DOI: https://doi.org/10.1016/S2666-5247(21)00171-3.
103. Unemo, Magnus, and William M Shafer. “Antimicrobial resistance in Neisseria gonorrhoeae in the 21st century: past, evolution, and future.” Clinical microbiology reviews vol. 27,3 (2014): 587-613. doi:10.1128/CMR.00010-14.
104. Shimuta, Ken et al. “Antimicrobial resistance and molecular typing of Neisseria gonorrhoeae isolates in Kyoto and Osaka, Japan, 2010 to 2012: intensified surveillance after identification of the first strain (H041) with high-level ceftriaxone resistance.” Antimicrobial agents and chemotherapy vol. 57,11 (2013): 5225-32. doi:10.1128/AAC.01295-13.
105. WHO. Global action plan to control the spread and impact of antimicrobial resistance in Neisseria gonorrhoeae. 2012.
106. WHO. Global health sector strategy on Sexually Transmitted Infections, 2016.
107. Chakraborti, Srinjoy et al. “Phase-Variable Heptose I Glycan Extensions Modulate Efficacy of 2C7 Vaccine Antibody Directed against Neisseria gonorrhoeae Lipooligosaccharide.” Journal of immunology (Baltimore, Md. : 1950) vol. 196,11 (2016): 4576-86. doi:10.4049/jimmunol.1600374.
108. Gulati S, Beurskens FJ, de Kreuk BJ, Roza M, Zheng B, DeOliveira RB, Shaughnessy J, Nowak NA, Taylor RP, Botto M, He X, Ingalls RR, Woodruff TM,

Song WC, Schuurman J, Rice PA, Ram S. Complement alone drives efficacy of a chimeric antigonococcal monoclonal antibody. PLoS Biol. 2019 Jun 19;17(6):e3000323. doi: 10.1371/journal.pbio.3000323. PMID: 31216278; PMCID: PMC6602280.

109. de Jong RN, Beurskens FJ, Verploegen S, Strumane K, van Kampen MD, Voorhorst M, Horstman W, Engelberts PJ, Oostindie SC, Wang G, Heck AJ, Schuurman J, Parren PW. A Novel Platform for the Potentiation of Therapeutic Antibodies Based on Antigen-Dependent Formation of IgG Hexamers at the Cell Surface. PLoS Biol. 2016 Jan 6;14(1):e1002344. doi: 10.1371/journal.pbio.1002344. PMID: 26736041; PMCID: PMC4703389.

110. Parzych EM, Gulati S, Zheng B, Bah MA, Elliott STC, Chu JD, Nowak N, Reed GW, Beurskens FJ, Schuurman J, Rice PA, Weiner DB, Ram S. Synthetic DNA Delivery of an Optimized and Engineered Monoclonal Antibody Provides Rapid and Prolonged Protection against Experimental Gonococcal Infection. mBio. 2021 Mar 16;12(2):e00242-21. doi: 10.1128/mBio.00242-21. PMID: 33727348; PMCID: PMC8092225.

111. Leduc, Isabelle et al. “The serogroup B meningococcal outer membrane vesicle-based vaccine 4CMenB induces cross-species protection against Neisseria gonorrhoeae.” PLoS pathogens vol. 16,12 e1008602. 8 Dec. 2020, doi:10.1371/journal.ppat.1008602.

112. Semchenko EA, Day CJ, Seib KL. The Neisseria gonorrhoeae Vaccine Candidate NHBA Elicits Antibodies That Are Bactericidal, Opsonophagocytic and That Reduce Gonococcal Adherence to Epithelial Cells. Vaccines (Basel). 2020 May 13;8(2):219. doi: 10.3390/vaccines8020219. PMID: 32414194; PMCID: PMC7349534.

113. Zielke, Ryszard A et al. “Proteomics-driven Antigen Discovery for Development of Vaccines Against Gonorrhea.” Molecular & cellular proteomics : MCP vol. 15,7 (2016): 2338-55. doi:10.1074/mcp.M116.058800.

114. Gulati, Sunita et al. “Preclinical Efficacy of a Lipooligosaccharide Peptide Mimic Candidate Gonococcal Vaccine.” mBio vol. 10,6 e02552-19. 5 Nov. 2019, doi:10.1128/mBio.02552-19.

115. Petousis-Harris H, Paynter J, Morgan J, Saxton P, McArdle B, Goodyear-Smith F, Black S. Effectiveness of a group B outer membrane vesicle meningococcal vaccine against gonorrhoea in New Zealand: a retrospective case-control study. Lancet. 2017 Sep 30;390(10102):1603-1610. doi: 10.1016/S0140-6736(17)31449-6. Epub 2017 Jul 10. PMID: 28705462.

116. Arnold R, Galloway Y, McNicholas A, O'Hallahan J. Effectiveness of a vaccination programme for an epidemic of meningococcal B in New Zealand. Vaccine 2011; 29: 7100–06.

117. Davenport V, Groves E, Horton RE, Hobbs CG, Guthrie T, et al. (2008) Mucosal immunity in healthy adults after parenteral vaccination with outer-membrane vesicles from Neisseria meningitidis serogroup B. J Infect Dis. 198: 731–740.

118. Tinsley, C R, and X Nassif. "Analysis of the genetic differences between Neisseria meningitidis and Neisseria gonorrhoeae: two closely related bacteria expressing two different pathogenicities." Proceedings of the National Academy of Sciences of the United States of America vol. 93,20 (1996): 11109-14. doi:10.1073/pnas.93.20.11109.

119. Ruiz García Y, Sohn WY, Seib KL, Taha MK, Vázquez JA, de Lemos APS, Vadivelu K, Pizza M, Rappuoli R, Bekkat-Berkani R. Looking beyond meningococcal B with the 4CMenB vaccine: the Neisseria effect. NPJ Vaccines. 2021 Oct 29;6(1):130. doi: 10.1038/s41541-021-00388-3. PMID: 34716336; PMCID: PMC8556335.

120. Wolff M, Wiedenmann J, Nienhaus GU, Valler M, Heilker R. Novel fluorescent proteins for high-content screening. Drug Discov Today. 2006 Dec;11(23-24):1054-60. doi: 10.1016/j.drudis.2006.09.005. Epub 2006 Sep 25. PMID: 17129823.

121. Zanella F, Lorens JB, Link W. High content screening: seeing is believing. Trends Biotechnol. 2010 May;28(5):237-45. doi: 10.1016/j.tibtech.2010.02.005. Epub 2010 Mar 24. PMID: 20346526.

122. Elliott G, McGrath J, Crockett-Torabi E. Green fluorescent protein: A novel viability assay for cryobiological applications. Cryobiology. 2000 Jun;40(4):360-9. doi: 10.1006/cryo.2000.2258. PMID: 10924267.

123. Pédelacq JD, Cabantous S, Tran T, Terwilliger TC, Waldo GS. Engineering and characterization of a superfolder green fluorescent protein. Nat Biotechnol. 2006 Jan;24(1):79-88. doi: 10.1038/nbt1172. Epub 2005 Dec 20. Erratum in: Nat Biotechnol. 2006 Sep;24(9):1170. PMID: 16369541.

124. Leuzzi R, Serino L, Scarselli M, Savino S, Fontana MR, Monaci E, Taddei A, Fischer G, Rappuoli R, Pizza M. Ng-MIP, a surface-exposed lipoprotein of Neisseria gonorrhoeae, has a peptidyl-prolyl cis/trans isomerase (PPIase) activity and is involved in persistence in macrophages. Mol Microbiol. 2005 Nov;58(3):669-81. doi: 10.1111/j.1365-2958.2005.04859.x. PMID: 16238618.

125. Duffin PM, Seifert HS. Genetic transformation of Neisseria gonorrhoeae shows a strand preference. FEMS Microbiol Lett. 2012 Sep;334(1):44-8. doi: 10.1111/j.1574-6968.2012.02612.x. Epub 2012 Jul 3. PMID: 22676068; PMCID: PMC3466376.

126. Biswas GD, Burnstein KL, Sparling PF. Linearization of donor DNA during plasmid transformation in Neisseria gonorrhoeae. J Bacteriol. 1986 Nov;168(2):756-61. doi: 10.1128/jb.168.2.756-761.1986. PMID: 3096959; PMCID: PMC213547.

127. Schlechter RO, Kear EJ, Remus DM, Remus-Emsermann MNP. Fluorescent Protein Expression as a Proxy for Bacterial Fitness in a High-Throughput Assay. Appl Environ Microbiol. 2021 Aug 26;87(18):e0098221. doi: 10.1128/AEM.00982-21. Epub 2021 Aug 26. PMID: 34260309; PMCID: PMC8388834.

128. Yoon SA, Park SY, Cha Y, Gopala L, Lee MH. Strategies of Detecting Bacteria Using Fluorescence-Based Dyes. Front Chem. 2021 Aug 12;9:743923. doi: 10.3389/fchem.2021.743923. PMID: 34458240; PMCID: PMC8397417.

129. Drevets DA, Elliott AM. Fluorescence labeling of bacteria for studies of intracellular pathogenesis. J Immunol Methods. 1995 Nov 16;187(1):69-79. doi: 10.1016/0022-1759(95)00168-a. PMID: 7490459.

130. Zost SJ, Gilchuk P, Case JB, Binshtein E, Chen RE, Nkolola JP, Schäfer A, Reidy JX, Trivette A, Nargi RS, Sutton RE, Suryadevara N, Martinez DR, Williamson LE, Chen EC, Jones T, Day S, Myers L, Hassan AO, Kafai NM, Winkler ES, Fox JM, Shrihari S, Mueller BK, Meiler J, Chandrashekar A, Mercado NB, Steinhardt JJ, Ren K, Loo YM, Kallewaard NL, McCune BT, Keeler SP, Holtzman MJ, Barouch DH, Gralinski LE, Baric RS, Thackray LB, Diamond MS, Carnahan RH, Crowe JE Jr. Potently neutralizing and protective human antibodies against SARS-CoV-2. Nature. 2020 Aug;584(7821):443-449. doi: 10.1038/s41586-020-2548-6. Epub 2020 Jul 15. PMID: 32668443; PMCID: PMC7584396.

131. Andreano E, Nicastri E, Paciello I, Pileri P, Manganaro N, Piccini G, Manenti A, Pantano E, Kabanova A, Troisi M, Vacca F, Cardamone D, De Santi C, Torres JL, Ozorowski G, Benincasa L, Jang H, Di Genova C, Depau L, Brunetti J, Agrati C, Capobianchi MR, Castilletti C, Emiliozzi A, Fabbiani M, Montagnani F, Bracci L, Sautto G, Ross TM, Montomoli E, Temperton N, Ward AB, Sala C, Ippolito G, Rappuoli R. Extremely potent human monoclonal antibodies from COVID-19 convalescent patients. Cell. 2021 Apr 1;184(7):1821-1835.e16. doi:

10.1016/j.cell.2021.02.035. Epub 2021 Feb 23. PMID: 33667349; PMCID: PMC7901298.

132. Motley MP, Banerjee K, Fries BC. Monoclonal antibody-based therapies for bacterial infections. Curr Opin Infect Dis. 2019 Jun;32(3):210-216. doi: 10.1097/QCO.0000000000000539. PMID: 30950853; PMCID: PMC7050834.

133. Kumar SK, Singh P, Sinha S. Naturally produced opsonizing antibodies restrict the survival of Mycobacterium tuberculosis in human macrophages by augmenting phagosome maturation. Open Biol. 2015 Dec;5(12):150171. doi: 10.1098/rsob.150171. PMID: 26674415; PMCID: PMC4703058.

134. Greenberg S, Grinstein S. Phagocytosis and innate immunity. Curr Opin Immunol. 2002 Feb;14(1):136-45. doi: 10.1016/s0952-7915(01)00309-0. PMID: 11790544.

135. Diago-Navarro E., Calatayud-Baselga I., Sun D., Khairallah C., Mann I., Ulacia-Hernando A., Sheridan B., Shi M., Fries B.C. Antibody-Based Immunotherapy To Treat and Prevent Infection with Hypervirulent Klebsiella Pneumoniae. Clin. Vaccine Immunol. 2017;24:e00456-16. doi: 10.1128/CVI.00456-16.

136. Ouisse LH, Gautreau-Rolland L, Devilder MC, Osborn M, Moyon M, Visentin J, Halary F, Bruggemann M, Buelow R, Anegon I, Saulquin X. Antigen-specific single B cell sorting and expression-cloning from immunoglobulin humanized rats: a rapid and versatile method for the generation of high affinity and discriminative human monoclonal antibodies. BMC Biotechnol. 2017 Jan 9;17(1):3. doi: 10.1186/s12896-016-0322-5. PMID: 28081707; PMCID: PMC5234254.

137. Château A, Seifert HS. Neisseria gonorrhoeae survives within and modulates apoptosis and inflammatory cytokine production of human macrophages. Cell Microbiol. 2016 Apr;18(4):546-60. doi: 10.1111/cmi.12529. Epub 2015 Oct 26. PMID: 26426083; PMCID: PMC5240846.

138. Markossian S, Grossman A, Brimacombe K, et al., editors. Assay Guidance Manual [Internet]. Bethesda (MD): Eli Lilly & Company and the National Center for Advancing Translational Sciences; 2004-. Available from: https://www.ncbi.nlm.nih.gov/books/NBK53196/.

139. Gao Q, Wang Z, Liu Z, Li X, Zhang Y, Zhang Z, Cen S. A cell-based high-throughput approach to identify inhibitors of influenza A virus. Acta Pharm Sin B. 2014 Aug;4(4):301-6. doi: 10.1016/j.apsb.2014.06.005. Epub 2014 Jul 14. PMID: 26579399; PMCID: PMC4629080.

140. van Vliet, E., Daneshian, M., Beilmann, M., Davies, A., Fava, E., Fleck, R., Julé, Y., Kansy, M., Kustermann, S., Macko, P., Mundy, W. R., Roth, A., Shah, I., Uteng, M., van de Water, B., Hartung, T. and Leist, M. (2014) "Current approaches and future role of high content imaging in safety sciences and drug discovery", ALTEX - Alternatives to animal experimentation, 31(4), pp. 479–493. doi: 10.14573/altex.1405271.

141. Chen H, Engkvist O, Wang Y, Olivecrona M, Blaschke T. The rise of deep learning in drug discovery. Drug Discov Today. 2018 Jun;23(6):1241-1250. doi: 10.1016/j.drudis.2018.01.039. Epub 2018 Jan 31. PMID: 29366762.

142. Sokolovska A, Becker CE, Stuart LM. Measurement of phagocytosis, phagosome acidification, and intracellular killing of Staphylococcus aureus. Curr Protoc Immunol. 2012 Nov;Chapter 14:Unit14.30. doi: 10.1002/0471142735.im1430s99. PMID: 23129153. Copy.

143. Solger F, Kunz TC, Fink J, Paprotka K, Pfister P, Hagen F, Schumacher F, Kleuser B, Seibel J, Rudel T. A Role of Sphingosine in the Intracellular Survival of Neisseria gonorrhoeae. Front Cell Infect Microbiol. 2020 May 12;10:215. doi: 10.3389/fcimb.2020.00215. PMID: 32477967.

144. Hauck CR, Meyer TF. 'Small' talk: Opa proteins as mediators of Neisseria-host-cell communication. Curr Opin Microbiol. 2003 Feb;6(1):43-9. doi: 10.1016/s1369-5274(03)00004-3. PMID: 12615218.

145. Iona E, Pardini M, Gagliardi MC, Colone M, Stringaro AR, Teloni R, Brunori L, Nisini R, Fattorini L, Giannoni F. Infection of human THP-1 cells with dormant Mycobacterium tuberculosis. Microbes Infect. 2012 Sep;14(11):959-67. doi: 10.1016/j.micinf.2012.04.003. Epub 2012 Apr 14. PMID: 22546526.

146. Ball LM, Criss AK. Constitutively Opa-expressing and Opa-deficient neisseria gonorrhoeae strains differentially stimulate and survive exposure to human neutrophils. J Bacteriol. 2013 Jul;195(13):2982-90. doi: 10.1128/JB.00171-13. Epub 2013 Apr 26. PMID: 23625842; PMCID: PMC3697530.

147. Rotman E, Seifert HS. Neisseria gonorrhoeae MutS affects pilin antigenic variation through mismatch correction and not by pilE guanine quartet binding. J Bacteriol. 2015 May;197(10):1828-38. doi: 10.1128/JB.02594-14. Epub 2015 Mar 16. PMID: 25777677; PMCID: PMC4402387.

148. Li G, Jiao H, Jiang G, Wang J, Zhu L, Xie R, Yan H, Chen H, Ji M. Neisseria gonorrhoeae NspA induces specific bactericidal and opsonic antibodies in mice. Clin Vaccine Immunol. 2011 Nov;18(11):1817-22. doi: 10.1128/CVI.05245-11. Epub 2011 Sep 14. PMID: 21918113; PMCID: PMC3209019.

149. Liang X, Teng A, Braun DM, Felgner J, Wang Y, Baker SI, Chen S, Zelphati O, Felgner PL. Transcriptionally active polymerase chain reaction (TAP): high throughput gene expression using genome sequence data. J Biol Chem. 2002 Feb 1;277(5):3593-8. doi: 10.1074/jbc.M110652200. Epub 2001 Nov 16. PMID: 11713261.

150. Marjuki H, Topaz N, Joseph SJ, Gernert KM, Kersh EN; Antimicrobial-Resistant Neisseria gonorrhoeae Working Group; Wang X. Genetic Similarity of Gonococcal Homologs to Meningococcal Outer Membrane Proteins of Serogroup B Vaccine. mBio. 2019 Sep 10;10(5):e01668-19. doi: 10.1128/mBio.01668-19. PMID: 31506309; PMCID: PMC6737241.

151. Lehar SM, Pillow T, Xu M, Staben L, Kajihara KK, Vandlen R, DePalatis L, Raab H, Hazenbos WL, Morisaki JH, Kim J, Park S, Darwish M, Lee BC, Hernandez H, Loyet KM, Lupardus P, Fong R, Yan D, Chalouni C, Luis E, Khalfin Y, Plise E, Cheong J, Lyssikatos JP, Strandh M, Koefoed K, Andersen PS, Flygare JA, Wah Tan M, Brown EJ, Mariathasan S. Novel antibody-antibiotic conjugate eliminates intracellular S. aureus. Nature. 2015 Nov 19;527(7578):323-8. doi: 10.1038/nature16057. Epub 2015 Nov 4. PMID: 26536114.